TERTIARY AND QUATERNARY SEDIMENTS OF THE ONTONG JAVA PLATEAU AREA

A DISSERTATION SUBMITTED TO THE GRADUATE DIVISION OF THE UNIVERSITY OF HAWAII IN PARTIAL FULFILLMENT OF THE REQUIREMENTS FOR THE DEGREE OF

DOCTOR OF PHILOSOPHY

IN OCEANOGRAPHY

DECEMBER 1972

By

Mark John Valencia

Dissertation Committee:

James E. Andrews, Chairman
S. A. Cattell
S. A. Margolis
Johanna Resig
H. H. Veeh

We certify that we have read this dissertation and that in our opinion it is satisfactory in scope and quality as a dissertation for the degree of Doctor of Philosophy in Oceanography.

DISSERTATION COMMITTEE

Chairman

ABSTRACT

Forty-seven free-fall, trigger-weight and piston-core tops from an area in the western equatorial Pacific (155°E-175°E, 10°N-10°S) were separated into three size-fractions (<44, 44-246, >246 μ) and the calcium carbonate content of the total sample and of each fraction determined. Subaerial volcanic dilution from the direction of the Solomon Islands prompted exclusion of some samples from calcium carbonate and size-fraction profiles. The initial abrupt decrease in calcium carbonate content in the western equatorial Pacific occurs at 3500 m, whereas the compensation depth is found at 5250 meters. Comparisons of previous work and examination of the present data prompt the assertion that under specified conditions, the sedimentary lysocline may be approximated by the slope break in plots of calcium carbonate versus depth. The less than 44 μ fraction demonstrates a strong positive correlation (0.92,P <.001) with depth, and may be a useful paleosolution indicator as well as a marker of displaced surface sediments in this region.

Paleomagnetic and C^{14} dated correlations of fluctuations in the frequency of the Globorotalia cultrata complex and other faunal and lithologic parameters in seven carbonate cores establish a paleoclimatic stratigraphy for the last 700,000 years in the western equatorial Pacific.

The parameter oscillations are interpreted as being due to variations in surface productivity which are linked to waxing and waning of upwelling intensity. The western equatorial Pacific stratigraphy exhibits eight upwelling-intensity cycles in the Brunhes normal polarity series, preceded by an abrupt climatic change recognizable across the entire equatorial Pacific.

Published chronostratigraphies from the southeastern, eastern, and north Pacific show approximate synchroneity with the cycles in the western equatorial Pacific. The Southern Ocean record exhibits fewer and consistently older climatic variations. Arctic climatic change also consistently preceded that at lower latitudes prior to approximately 250×10^3 yrs. B.P.

Map and statistical interpretation of the distribution of collected pre-Quaternary microfossils from the western equatorial Pacific add support to the concept of stability of the equatorial current system during the Cenozoic Era.

TABLE OF CONTENTS

TABLE OF CONTENTS (Continued)

LIST OF TABLES

LIST OF TABLES (Continued)

LIST OF FIGURES

LIST OF FIGURES (Continued)

LIST OF FIGURES (Continued)

INTRODUCTION

For the prepared investigator, pelagic sediments provide an immense storehouse of information concerning the history of earth systems. Controlling parameters for recent and, presumably, past marine sediment properties include oceanic surface and deep circulation, depth and seafloor morphology, volcanism, tectonism, geographic location and proximity to land, and climate. Time variations in these environmental conditions produce concomitant alterations of the sediment parameters resulting in a marine lithostratigraphy. Interpretations of these lithologic variations provide information on past developments in earth systems (Table 1). This work focuses on surface sediment variations with water depth, Pleistocene climatic lithostratigraphy, and the general Cenozoic sedimentary history in the western equatorial Pacific.

This research was supported financially by the Office of Naval Research under contract N00014-70-A-0016-0001, Dr. George Sutton, principal investigator, and by the National Science Foundation under grant GA-11412, Dr. J. Resig, principal investigator.

Lysocline and compensation depth

Murray and Renard (1891) first noted the negative relationship between pelagic sediment calcium carbonate content and water depth. It has since been more

Table 1

Paleoenvironmental Information Extractable
from Pelagic Sediments

History of:

A. Biological

1. evolutionary developments of pelagic and benthic microorganisms
2. ecological adaptations of pelagic microfauna and flora
3. surface production rate and distribution

B. Physical

1. surface and deep paleocirculation patterns and rates

C. Chemical

1. geochemical balance
2. water-column chemistry
3. diagenesis

D. Geological and Geonomical

1. direction and rate of crustal plate movement
2. local tectonism
3. volcanism
4. climatic change and distribution
5. depositional environment stability
6. earth's paleomagnetic field strength and polarity
7. earth's orbital parameters
8. extraterrestrial developments

specifically documented and discussed by Revelle (1944), Bramlette (1961), Turekian (1964; 1965), Lisitzin (1970), and others. Recent investigations of water column calcium carbonate solution profiles (Peterson, 1966; Berger, 1967) and detailed analyses of solution effects on the foraminiferal component of pelagic sediments (Ruddiman and Heezen, 1967; Berger, 1968; 1970; Kennett, 1966), together with reevaluation of previous results (Heath and Culberson, 1970; Broecker et al., 1968; Broecker, 1971), have led to the definition of five important conceptual horizons in profiles of calcium carbonate distribution with depth in the ocean. These horizons are the calcium carbonate compensation depth, the foraminiferal compensation depth, the critical depth, the lysocline, and the depth of calcium carbonate saturation (Table 2).

This work establishes for the western equatorial Pacific, the approximate depth of the initial abrupt decrease in sediment calcium carbonate content and of calcium carbonate compensation for the total sediment and for three size fractions (less than 44 μ, 44-246 μ, and greater than 246 μ). In addition, the relationships between size fraction, calcium carbonate content, foraminiferal solution indices (Berger, 1968) and water depth are explored.

Table 2

Various Concepts of Calcium Carbonate Depth-Solution Boundaries and the Depth of Occurrence in the Equatorial Pacific

Horizon	Definition	Depth: Equatorial Pacific (Km)	Depth: Western Equatorial Pacific (Km)
compensation depth	depth at which the rate of calcite supply equals the rate of dissolution (Bramlette, 1961)	4.7 (ibid.)	--
planktonic foraminiferal compensation depth	depth at which whole tests of planktonic foraminifera are absent (Parker and Berger, 1971)	5.0 (ibid., Fig. 14a)	--
critical depth	depth at which the sediment contains 10 percent calcium carbonate by weight (Lisitzin, 1970)	5.5 (ibid., Fig. 17)	5.0-5.25 (ibid., Fig. 20)
lysocline	depth of maximum rate of change in Berger's (1968) solution index	3.8 (Parker and Berger, 1971, Fig. 14a)	3.75-4.0 (ibid., Fig. 15)

Table 2. (Continued) Various Concepts of Calcium Carbonate Depth-Solution Boundaries and the Depth of Occurrence in the Equatorial Pacific

Horizon	Definition	Depth: Equatorial Pacific (Km)	Depth: Western Equatorial Pacific (Km)
depth of calcium carbonate saturation in water column	depth at which the ratio of the ion product Ca^{++} CO_3^{--} and the concentration product of solubility equals 1 (Lyakhin, 1968)	0.5 (ibid., Figs. 6-4, 5)	0.5; 1.0-2.5 (ibid., Fig. 6-4b)

Pacific Pleistocene paleoclimatic correlations

Marine Pleistocene paleoclimatic correlations have been impeded in the past by resolution differences in the techniques of various workers, dissimilar working definitions of the Plio-Pleistocene boundary (Funnell, 1970), time transgression of some faunal boundaries (Kennett, 1968) and, possibly, by geographically restricted effects of minor climatic fluctuations originating at latitudinal extremes (Kennett, 1970). Berger (1971b) has criticized the inherent bias in core correlations lacking independent dates, and has devised a statistical method for testing the validity of such "date-free" correlations. In addition, undetected discontinuous deposition and reworking, as well as sampling disturbances, have hampered attempts at definite correlation.

The advent of routine paleomagnetic stratigraphic analysis of pelagic sediment cores is fast removing many correlation difficulties and may prove as significant an advance in marine Pleistocene paleoclimatic studies as that of the piston corer (Kullenberg, 1947) and the C^{14} dating method.

The Pacific has not received as much attention from Pleistocene stratigraphers as have the Caribbean and the Atlantic. Nevertheless, somewhat conflicting but comparable paleoclimatic stratigraphies have been advanced for the Southern Ocean (Kennett, 1970), the southeast Pacific

(Blackman and Somayajulu, 1966), the eastern equatorial Pacific (Arrhenius, 1952, 1963; Hays et al., 1969), the central north Pacific (Kent et al., 1971) and the Arctic (Herman, 1970). The present work contributes a Pleistocene paleoclimatic stratigraphy from the western equatorial Pacific and attempts Pacific-wide correlations of previously published chronostratigraphies.

Pre-Quaternary equatorial sediment distributions

The possibility of geographic shifts in the extent and location of the equatorial high-productivity belt during the Cenozoic is controversial. Several workers have described a significant south to southeasterly shift of the northern boundary of the Countercurrent during the Cenozoic Era (Arrhenius, 1952; 1963; Riedel and Funnell, 1964; Hays et al., 1969; Heezen, 1971; Nesterhoff and von der Borch, 1971). Some of these interpretations neglect the effect of sea-floor spreading which, according to results from DSDP Legs 17 and 20 (Scientific staff, 1971; 1972), moved the thick biogenous sediment belt generally to the north of the present equator throughout Cretaceous and Cenozoic time.

Other researchers conclude that the pattern of sediment thickness and age indicates little Cenozoic change in the location or extent of the equatorial high-productivity zone (Riedel, 1971; Ewing et al., 1968).

General aspects of environmental and diagenetic changes with time can be discerned by comparing physical and faunal parameters of carbonate sediment of different ages from similar environments. Heath (1969) reported that nannoplankton dominate early and middle Tertiary equatorial sediments, whereas foraminifera are more important in late Cenozoic deposits. Recent carbonate sediments have been reworked and sorted, whereas older deposits exhibit little evidence of reworking. Heath also contends from an analysis of water depth, calcium carbonate content and sediment age, that the equatorial calcium carbonate compensation depth was depressed 600 m in Oligocene and early Miocene time.

The present investigation includes an evaluation of western equatorial Pacific pre-Quaternary sediment age distribution as well as a comparison of physical parameters of Eocene through Quaternary sediment.

Oceanography of the investigation area

This sediment investigation concentrates on the Ontong Java Plateau (Figure 1) but includes samples and data to the north and east of the Solomon Islands between 154°E and 180°E Longitude and 10°N to 10°S Latitude.

Pacific Equatorial Water and Western South Pacific Central Water comprise the surface water masses over the research area, exhibiting temperatures between 27 and 30°C

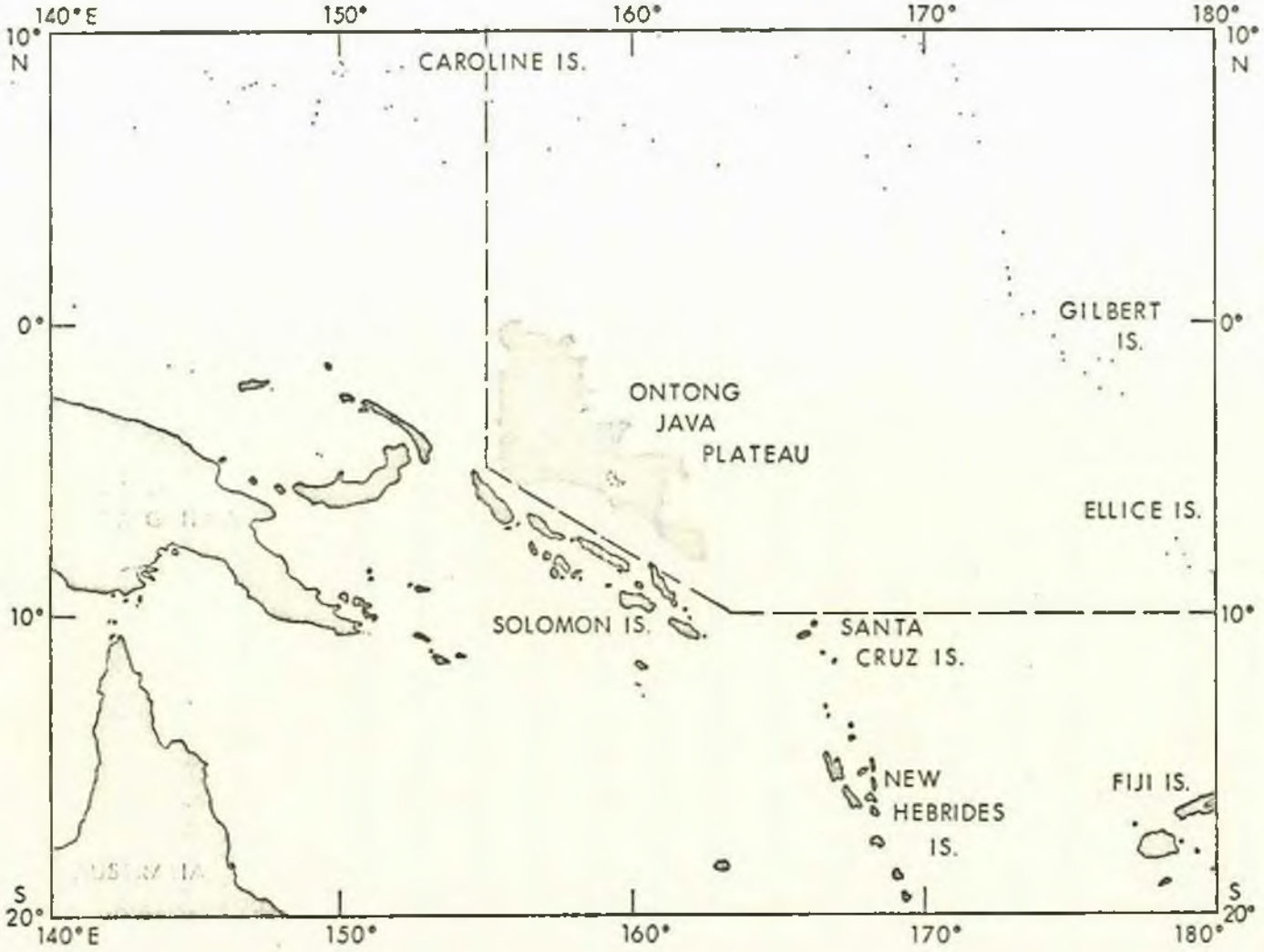

Figure 1. Area of investigation. Dashed line denotes area of samples and data north and east of the Solomon Islands.

and salinities between 34 and 35 °/oo (Sverdrup et al., 1947; Hisard et al., 1969). The depth to the thermocline increases from less than 50 m in the eastern Pacific to nearly 200 m west of 180°.

The meandering easterly Equatorial Countercurrent, generally present at the surface between 3° and 8°N, is enclosed by the westerly North and South Equatorial Currents (Tsuchiya, 1961; Hisard et al., 1969). The easterly Undercurrent extends latitudinally from 3°N to 3°S at 200 to 400 m depth and is vertically continuous with the Countercurrent where the two overlap geographically. At the surface, the Countercurrent exhibits seasonal variations in strength and location, being weaker and several degrees more northerly in April. Occasionally, the Countercurrent crosses the equator and the South Equatorial Current is then entirely in the Southern hemisphere. No evidence exists for an extension of the South Equatorial Countercurrent into the western Pacific.

Equatorial upwelling is ephemeral west of 180° due to velocity instability of the trade wind systems (Stroup, 1972, pers. commun.). No persistent equatorial surface temperature or salinity minimum was observed in the western equatorial Pacific by Tsuchiya (1961).

Wyrtki (1962) has delineated the subsurface water mass structure in the western south Pacific (Table 3). The main abyssal transport in the Pacific is north along the western

Table 3

Subsurface Water Masses in the Western South Pacific Ocean
(from Wyrtki, 1962, Table 1)

Water Mass	Characteristic	Range of Properties in this Area			Depth Range (m)
		Temperature (°C)	Salinity (0/00)	Oxygen (ml/l.)	
Subtropical Lower Water	salinity maximum				
northern component		21-24	30·60-35·95	3·0-4·0	125-250
southern component		18-25	35·50-35·95	4·4-5·4	0-125
Upper oxygen minimum	oxygen minimum	12-24	34·9-35·9	2·7-4·6	150-500
Subantarctic Intermediate Water	oxygen maximum	8-14	34·6-35·2	4·4-6·1	200-500
Antarctic Intermediate Water	oxygen maximum	5·4-9·5	34·4-34·8	3·5-4·9	400-1000
	salinity minimum	4·2-6·0	34·37-34·53	3·5-4·7	700-1100
Deep oxygen minimum	oxygen minimum	1·9-3·9	34·58-34·65	2·76-3·94	1200-2400
Deep Water	salinity maximum	1·4-1·9	34·74	4·0-4·4	2500-3000
Bottom Water	lowest potential		<34·70	3·4-4·6	below 3000

*The low oxygen values, quoted for the Bottom Water, refer to the deep sea basins.

boundary, with indications of eastward spreading at the equator (Knauss, 1962). Velocities probably average 0.05 to 0.1 cm/sec although Warren and Voorhis (1970) have measured near bottom velocities of 5 to 15 cm/sec in a central south Pacific interbasinal constriction at 9°S. Abyssal water decreases in dissolved oxygen content and increases in in situ temperature from south to north in the South Pacific (Wooster and Volkmann, 1960).

An increased density of suspended particles at the surface straddling 10°N between 160°E to 162°E may reflect a divergence, although only a slight indication of a similar association is present at the equator (Lisitzin, 1970, Fig. 11c). Numbers of coccospheres in the surface water along 142°E increase abruptly at the equator, although this peak may only indicate nutrient enrichment by runoff from New Guinea (Okada and Honjo, 1970). Values of inorganic phosphate-phosphorous at the sea surface in the investigation region are between 0.25 and 0.50 mg-at./ℓ. However, at 100 m the phosphate-phosphorous values are between 0.50 and 0.75 mg-at./ℓ, reflecting the shallow pycnocline associated with the equatorward boundaries of the westward currents (Reid, 1962). Zooplankton volumes in the upper 105 m west of 180° are equal to or higher than those sampled in the eastern equatorial Pacific. Primary productivity is generally less than 0.50 $gC/m^2/yr.$ to the east of 180° along the equator (Fleming, 1957; Lisitzin, 1970, Fig. 6;

Koblentz-Mishke et al., 1970, Fig. 1). However, total water column production, i.e., $gC/m^3/yr.$, may be nearly equal for the two regions due to the much greater thermocline depth in the western equatorial Pacific.

Geology of the investigation area

In the western equatorial Pacific, pelagic sediment type and thickness are controlled primarily by water depth. With the exception of the area adjacent to the Gilbert-Marshall Islands, sediment thickness decreases and water depth increases eastward from the Ontong Java Plateau (Ewing et al., 1968; Figure 2). Along the equator, a maximum of 0.8 km of highly stratified, calcareous Cenozoic sediment thins and decreases in carbonate content becoming less than 0.2 km of lutite between 170°E and 170°W (Ewing et al., 1968; Kroenke, 1972). This central region has apparently been below the carbonate compensation depth during its entire sedimentary history.

Structurally, the investigation area is dominated by the Ontong Java Plateau (Figures 1, 5), a northwest-southeast striking platform 800 km wide and 1600 km long, with depths as shallow as 1.7 kilometers. Sediment thickness reaches a maximum of 1 km at about 2°S, 158°E, and decreases bilatitudinally from this area (Figures 3a and 3b) as the carbonate content decreases. These relationships may reflect the continuation of the belt of thick

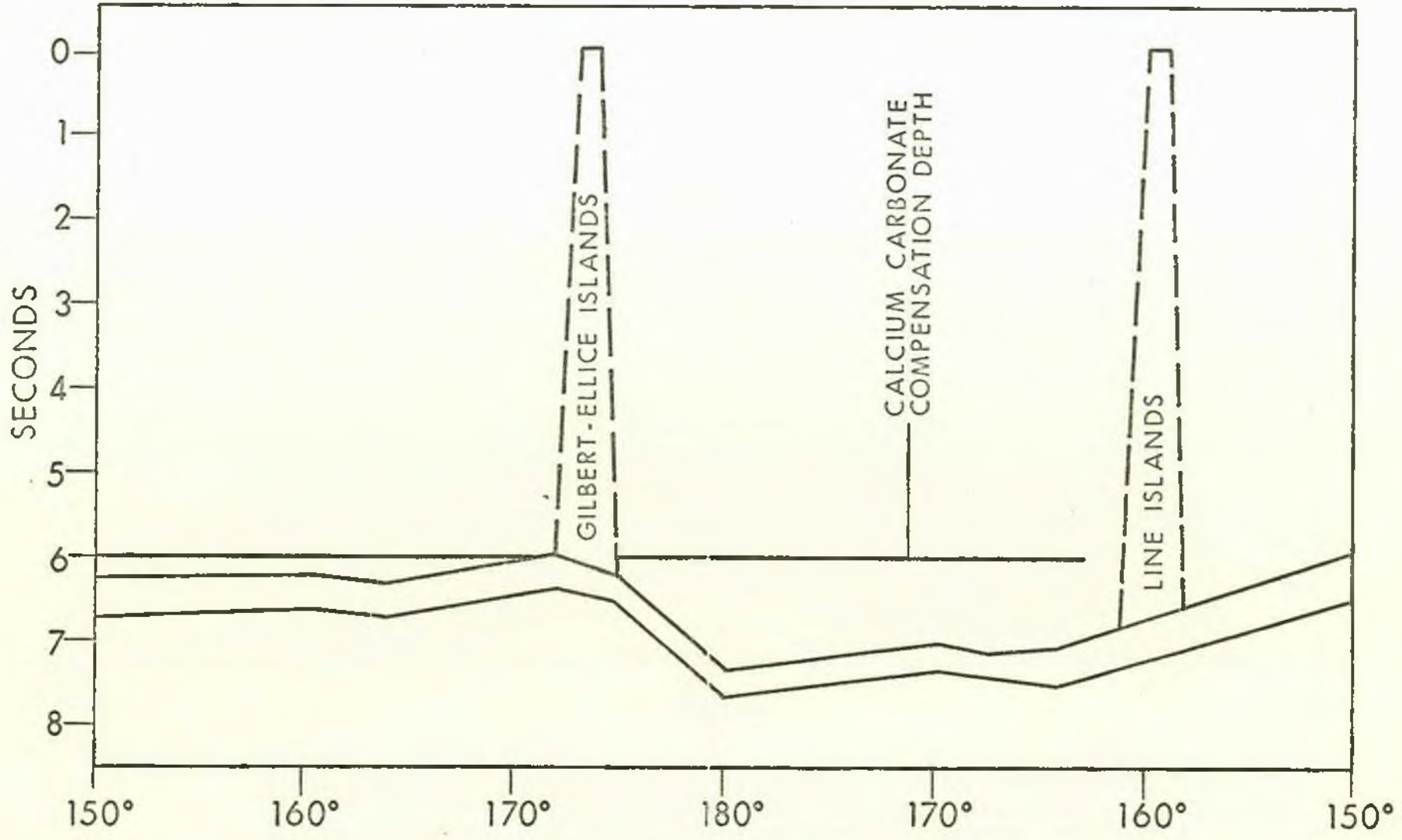

Figure 2. Pacific equatorial sediment thickness section (after Ewing et al., 1968, Fig. 10 (Middle)).

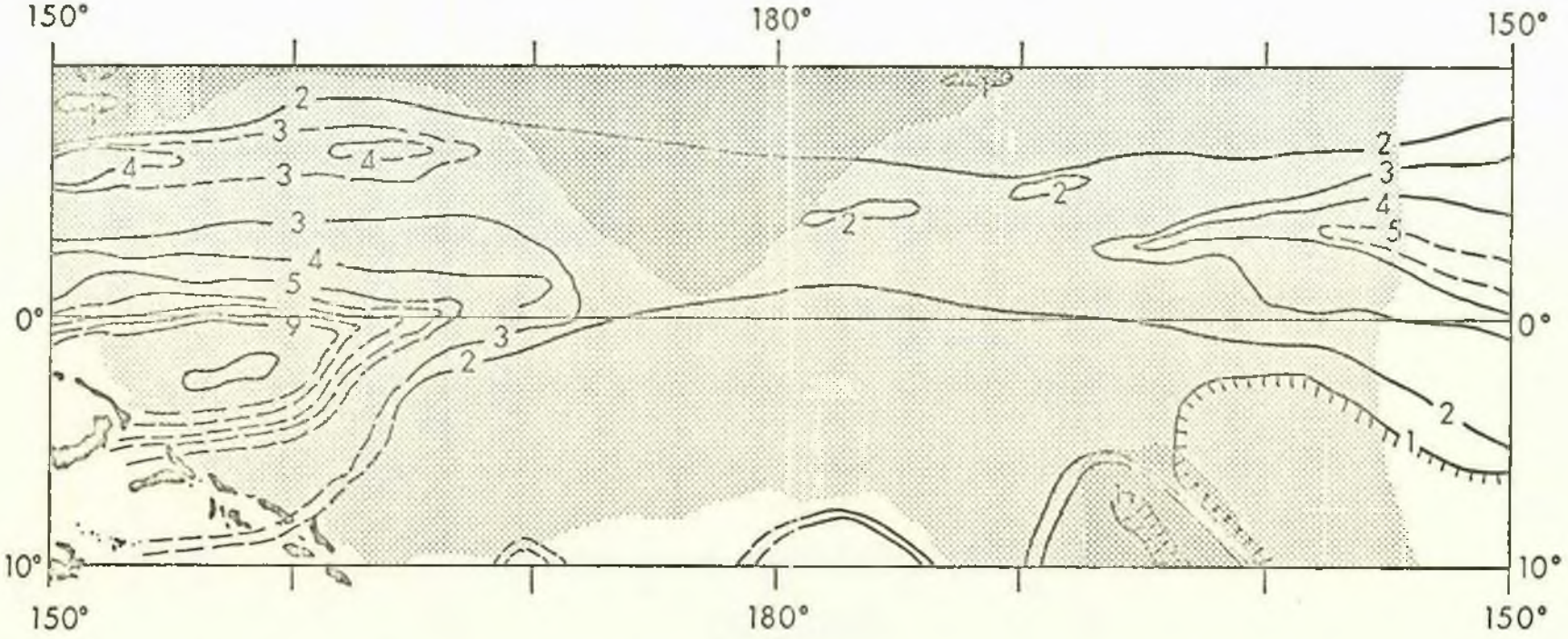

Figure 3a. Map of sediment thickness in the equatorial Pacific (after Ewing et al., 1968, Fig. 2). Contours show thickness of upper transparent layer in 0.1 seconds of reflection time; each contour represents approximately 100 meters. Stipled areas show thickness of opaque plus lower transparent layers; heavy pattern: 200-300 m; light pattern: 20-200 meters.

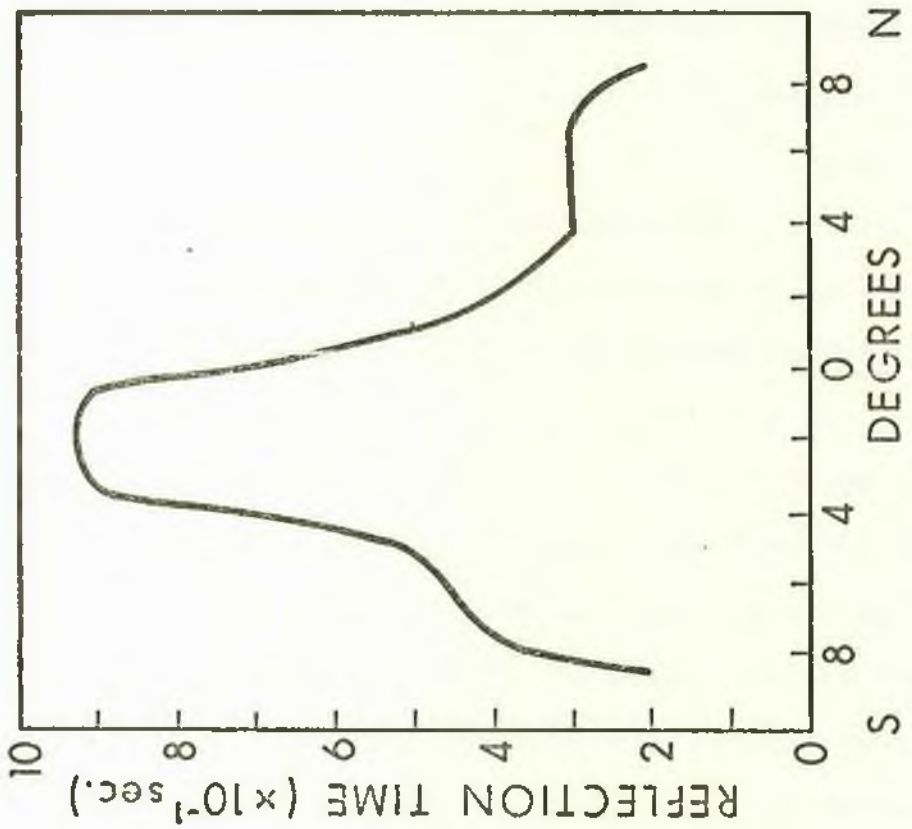

Figure 3b. Cross section of equatorial sediment thickness along 160°E (from Figure 3a).

pelagic sediment associated with high organic productivity in the equatorial upwelling zone.

Site 64 of the Joides Deep Sea Drilling Project was situated on the central Plateau at 1°44.5'S, 158°36.5'E. The 983 m section bottomed in late middle Eocene cherty limestone after penetrating an uninterrupted sequence of calcareous pelagic ooze (Winterer, 1971). More specifically, 400 m of early middle Miocene to Recent foraminiferal and nannofossil chalk ooze overlie 300 m of alternating nannofossil chalk and chalk ooze of late Oligocene to early middle Miocene age (Bronnimann and Resig, 1971). The bottom 283 m consist of late middle Eocene to late Oligocene friable nannofossil and foraminiferal-nannofossil chalk alternating with indurated limestone.

Kroenke (1972) has correlated this section with a structurally deformed discontinuous sedimentary sequence on the island of Malaita (Solomon Islands) which he believes to be an uplifted portion of the Plateau. On the basis of this correlation and additional seismic evidence, the late middle Eocene to Recent calcareous pelagic ooze is considered to be underlain by an unusually thick sequence of late Cretaceous and older flood basalts.

The submarine geomorphology of the Plateau margins is complex, exhibiting frequent sediment thickness variations due to erosion, volcanism, and deformation (Kroenke, 1972). Near-surface erosional unconformities on the frequently

deformed margins provide opportunities to sample the older Cenozoic column with piston cores. Conversely, undisturbed Pleistocene sequences are available on the relatively stable Plateau proper. In addition, the wide range of depths and constant areal productivity values permit an investigation of the relationship of pelagic carbonate sediment parameters with water depth.

The Plateau originated as extensive pre-Tertiary submarine flood basalts in the eastern Pacific (Kroenke, 1972). From late Eocene to late Miocene time, this enormous accumulation moved westward on the migrating lithospheric plate with pelagic sedimentation keeping pace with sinking. At the end of the Miocene, the Plateau crust collided with the Australian plate resulting in intense deformation on the southwest margin, including the uplift of Malaita. Faulting and igneous intrusion produced extensive slumping which denuded portions of the Plateau margins. Subduction ceased in late Miocene time, perhaps due to a coincidental directional change in Pacific plate motion. Tectonic adjustments within and marginal to the Plateau continue in response to present plate interaction.

Buyannanonth (1971) has analyzed the microfossils in seven cores of nannofossil and nannofossil-foraminiferal ooze (Table 4) from the Ontong Java Plateau region. The paleontologic evidence of frequent reworking and hiatuses supports the seismic interpretation of post-depositional

sediment movement on the Plateau's eastern, southern, and southwestern margins. No significant variations in carbonate content were found in the Pleistocene section. However, severe solution at the bottom of cores 68PC 11, 21, and 23 was indicated by low foraminiferal percentages and partially dissolved tests. Pliocene to Recent foraminiferal assemblages imply a constant tropical environment during this time (Equatorial West Central Assemblage of Bradshaw (1959). Nannofossils predominate over foraminifera and Radiolaria in late Eocene to Pliocene sediments and vice versa in Pleistocene sediments. The Pleistocene-Recent boundary was delineated in cores 68PC 21 and 23 by abruptly increased Radiolarian content. Most of the cores studied by Buyannanonth are situated south of the main zone of potential equatorial upwelling.

Pleistocene theory

Although cooling may have commenced in early Eocene time (Margolis and Kennett, 1970), the outstanding characteristic of the Pleistocene Epoch is the waxing and waning of glaciation. The causes of Tertiary climatic deterioration and of the periodic fluctuations extending into the Quaternary are unknown. Numerous theories have been collected, criticized, and reviewed several times (Emiliani and Geiss, 1959; UNESCO, 1963; Mitchell, 1965; 1968), of which the most recent evaluation is that of

Crowell and Frakes (1970; Figure 4). Theories of climatic change can be separated into two categories: those that attempt to explain the occurrence of major glacial ages and those that specialize in the temperature oscillations of the Pleistocene.

In the latter category, the astronomical theory of glaciation has received the most attention. According to this theory, quasi-periodic variations of summer insolation in northern latitudes at intervals of about 40×10^3 yrs. result from the chronological interaction of the earth's orbital parameters (tilt, 40×10^3 yrs. period, precession of the equinoxes, 21×10^3 yr. period, and eccentricity of earth's orbit, 96×10^3 yr. period). This theory is based on the works of Milankovitch (1938), Koppen and Wegener (1924), and Flint (1947), and is supported by paleotemperature determinations in deep-sea cores (Emiliani and Geiss, 1959). Broecker (1966), Mesolella et al. (1969) and Broecker et al. (1968) contend that uplifted reef terrace chronologies in Barbados support a modified "Milankovitch" theory. In this modification, the precession component is given more emphasis than tilt and the concept of fluctuations about a mean climate has been altered by assuming two stable stages of earth climate--glacial and interglacial. Transitions are triggered only by the larger insolation amplitudes, and minor fluctuations around a stable state result from insolation variations insufficient to cause mode transitions (Broecker, 1966).

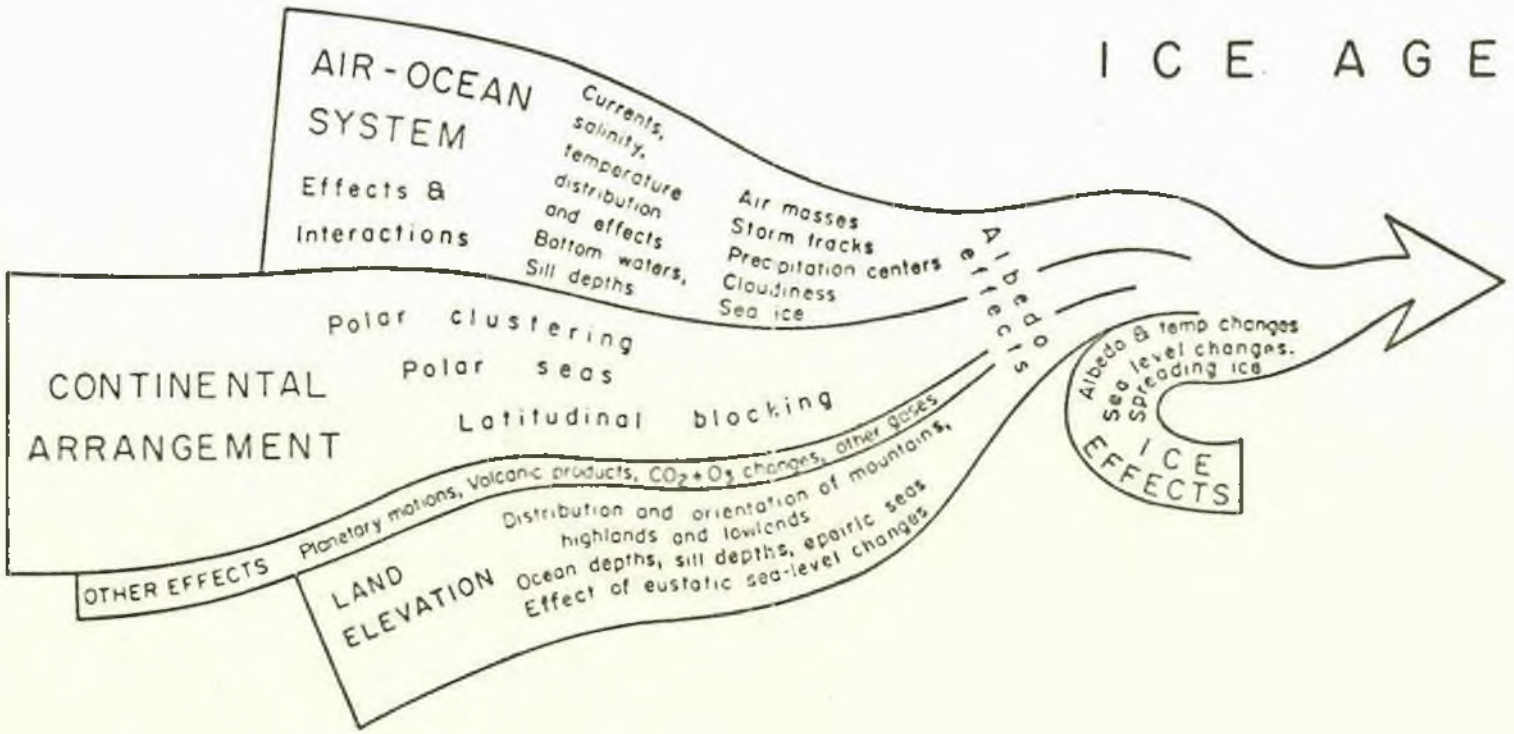

Figure 4. Possible factors that interact to cause an ice age (from Frakes and Crowell, 1970, Fig. 7).

Worldwide synchroneity of Pleistocene paleoclimatic events is an important but open question for theories of glacial fluctuations. Correlation of absolute chronologies from oceans to continents is hampered by the poor resolution and few available dates in continental deposits, although the meager data agree rather closely with the marine chronology over the last several hundred thousand years (Emiliani, 1966b; Hays et al., 1969). More information is available on the synchroneity of changes in oceanic surface water temperature and circulation. Although resolution differences and other complications have produced considerable controversy between the faunal and the isotopically determined climatic record in the Atlantic, the synchronism within each method is established for broad geographic areas (Ericson and Wollin, 1968; Emiliani, 1966b).

Synchroneity between the Pacific and Atlantic records is controversial. Southeastern (Blackman and Somayajulu, 1966) and equatorial Pacific (Hays et al., 1969) chronostratigraphies agree with those of Ericson and Wollin (1968) for the equatorial Atlantic. However, Ericson and Wollin (1970) concluded from chronologically opposing trends of the Globorotalia cultrata complex frequency in southeastern Pacific and Atlantic cores that the Pleistocene record in the Pacific varies geographically. This conclusion contradicts the "Milankovitch" theory and supports a modified version of Simpson's (1940) hypothesis which points

out that accumulation of ice on the continents implies copious precipitation. Increased evaporation at low latitudes provided the precipitation necessary for glacier formation in high latitudes (Ericson and Wollin, 1970). Thus, while North Atlantic surface water was cooled by adjacent ice sheets during glacial stages, increased insolation may have raised the surface temperatures of the equatorial Pacific. However, Ericson and Wollin's conclusions have been severely criticized due to the correlations between different water masses on the basis of a single species (Morin et al., 1970).

Herman (1970) has suggested that Quaternary climatic oscillations in the Arctic Ocean were not in phase with those at lower latitudes. Increased insolation enhanced glacial melting in high latitudes as well as the rise in surface water temperature in low latitudes. Consequently, a time lag may have been introduced between surface water temperature variations in high and low latitudes.

Equatorial surface circulation

The effects of glacial advances on atmospheric and, ultimately, oceanic surface circulation have received little attention. The information can be separated into meteorological theory and sedimentary evidence although the former has been heavily influenced by the latter.

Paleoatmospheric circulation changes have been theorized by extrapolating from observations over the past 600 years (Lamb and Woodroffe, 1970; Lamb, 1971). For example, for the North America-Atlantic sector, the center of the circumpolar vortex and surface polar anticyclone were displaced during glacials to more easterly and lower latitudes with an accompanying tendency for any progressive systems to pass in very low latitudes. Also, there was less seasonal change in the vigor of the mean circulation. If these variations can be extrapolated on a bipolar basis to the Pacific sector, the effect would be to increase average velocity in the oceanic anticyclonic gyres and thus, ultimately, upwelling and productivity at the equator.

Quinn (1971) has theorized that a persistent zone of equatorial upwelling extended across the entire Pacific during glacial stages. When atmospheric pressure is low in the Malay-Indonesia region, it is high in the sub-tropical southeast Pacific and the pressure gradient strengthens the atmospheric and, consequently, the oceanic circulation. The South Equatorial Current is accelerated as is equatorial upwelling, and sea-surface temperatures decline. An important attendant development is the longitudinal extension of the equatorial dry zone. Surface waters reaching the Malay-Indonesian area are thus cooler than normal, producing an increase in atmospheric pressure. A reversal of relative pressure values from the Malay-Indonesian region

to the southeast Pacific produces a decrease in atmospheric and oceanic circulation with concomitant reduced upwelling intensity and increased surface water temperature. Again the cycle is completed by a decrease in atmospheric pressure in the Indonesia-Malay region due to the warmer waters arriving from the east.

This cycle was interrupted by the drop in sea level in glacial stages. The emergent areas between West Malaysia and Indonesia-East Malaysia and between New Guinea and Australia prevented the cooler waters from entering the Malay-Indonesia region, thus preventing a gradual geographic pressure reversal. The Indonesian equatorial low and South Pacific sub-tropical high persisted, accompanied by intense and longitudinally extensive equatorial upwelling. As sea level rose in interglacial stages, conditions returned to those of the present.

This theory is supported by historical observations of an extensive dry zone extending westward past Kapingamarangi Atoll (1°04'N, 154°45'E) and associated with the previously discussed atmospheric pressure increase. Extrapolation of this theory to the Pleistocene is supported by two types of geologic evidence.(Quinn, 1971). Phosphate deposits are found on several western equatorial Pacific islands (Purdy, Nauru, Ocean) which presently lack the large bird colonies and permanent dry climate necessary for the source material and phosphate rock preservation. Strong upwelling in the

western equatorial Pacific during the last glacial stage would have produced the higher productivity and lower rainfall necessary for phosphate rock development in this region.

Eastern Equatorial Pacific deep-sea cores indicate the existence of an equatorial upwelling zone throughout the Quaternary, with fluctuations in its intensity and accompanying planktonic productivity (Arrhenius, 1950; 1963; Hays et al., 1969). However, these authors ascribed upwelling intensity cycles to an alternating compression and expansion of the trade wind belts due to waxing and waning of continental ice sheets. Evidence from the Timor Sea (van Andel et al., 1967) and Africa (Fairbridge, 1964; 1965) supports the theory of climatic zone compression at low latitudes.

Abyssal circulation

Speculations by physical oceanographers on changes of abyssal circulation during glacial stages are rare. One theory considers the overall amplitude of abyssal circulation as dependent on the depth of the thermocline (Stommel, 1958; Stommel and Arons, 1960). The existence of a thermocline and the maintenance of low, deep-water temperature infer a balance of downward diffusion of heat from warm surface layers and a slow upward component of velocity in the deep water. The thermocline thus acts as a

pumping mechanism drawing up deep water which, by continuity, is replaced by abyssal flow. Unless the thermocline depth is altered, the overall amplitude of deep flow is constant, despite creation of significant new sinks such as those in the North Pacific or in the Ross Sea.

However, if expansion of continental ice sheets produced a compression of the sub-tropical gyres and a deepening of the thermocline over extensive areas, the amplitude of abyssal transport would decrease. This is, of course, contrary to the usual contention that the magnitude of abyssal circulation is dependent on winter cooling at the poles. However, climatic change might alter the relative importance of deep-water sources. Stommel and Arons (1960) do state that a warming at the poles could result in a rise of deep-water temperature and a change of oxygen distribution. The former parameter variation would tend to reduce carbonate solution at depth.

MATERIALS AND METHODS

Surface sediment analysis

Surface sediment samples were extracted from the tops of free-fall, trigger weight and piston cores obtained by Hawaii Institute of Geophysics personnel on cruises of the R/V MAHI over a three year period (Figure 5). The core tops were all Quaternary (J. Resig and V. Buyannanonth, pers. commun.); although the few top centimeters or more may not have been collected.

Samples were separated by U. S. standard sieves (#60, 246 μ; #325, 44 μ) into three size-fractions and the weight of each fraction recorded. Weight percent calcium carbonate was determined for the total sample and for each of the three size-fractions by Hulsemann's (1966) rapid gas volumetric technique. In addition, foraminiferal species counts were made on at least 300 specimens for each sample and Berger's (1968) solution indices calculated. Computer correlation analysis using the University of Hawaii's IBM 360 enabled the delineation of significant relationships between water depth, size fraction, calcium carbonate content, and solution indices.

Core analysis

Table 4 summarizes the data compiled or collected from the piston cores used in this study. The major portion of 2 to 5 gm paleomagnetic and porosity samples collected at

Table 4

Cores and Parameters Investigated

Core	Length (cm)	Oldest Sediment	GS	PP	CO_3	CO_361	P	F	PM	MP	Des
68PC10	413	L. Pliocene	X		X					X	X
11	1111	M. Pliocene	X		X		X		X	X	X
12	991	Quaternary	X	X	X	X	X	X	X	X	X
15	767	Quaternary	X	X	X	X		X	X	X	X
16	782	Quaternary	X	X	X	X	X	X		X	X
20	394	L. Pliocene	X						X	X	X
21	744	U. Eocene	X						X	X	X
22	888	Quaternary	X						X	X	X
23	679	L. Miocene	X		X				X	X	X
27	817	Pliocene	X		X		X			X	X
70PC62		Pliocene						X	X	X	X
64		Quaternary						X	X	X	X
71PC35		Pliocene						X	X	X	X

Key: GS: grain size; PP: physical properties; CO_3: total percent calcium carbonate; CO_361: percent calcium carbonate greater than 61 μ; P: phosphorus; F: selected species frequencies; PM: paleomagnetic analysis; MP: micropaleontologic analysis; Des: megascopic and smear slide description; L, M, U: lower, middle, upper.

Figure 5. Sample locations and general bathymetry of the Ontong Java Plateau area. ● = 70, piston core; △ = 68, piston core; ■ = 70, free-fall core; ○ = 68, free-fall core; ▲ = 67 free-fall core; □ = 68 trigger core; bathymetric contour interval: 1 km; solid line is line of section of Figure 14.

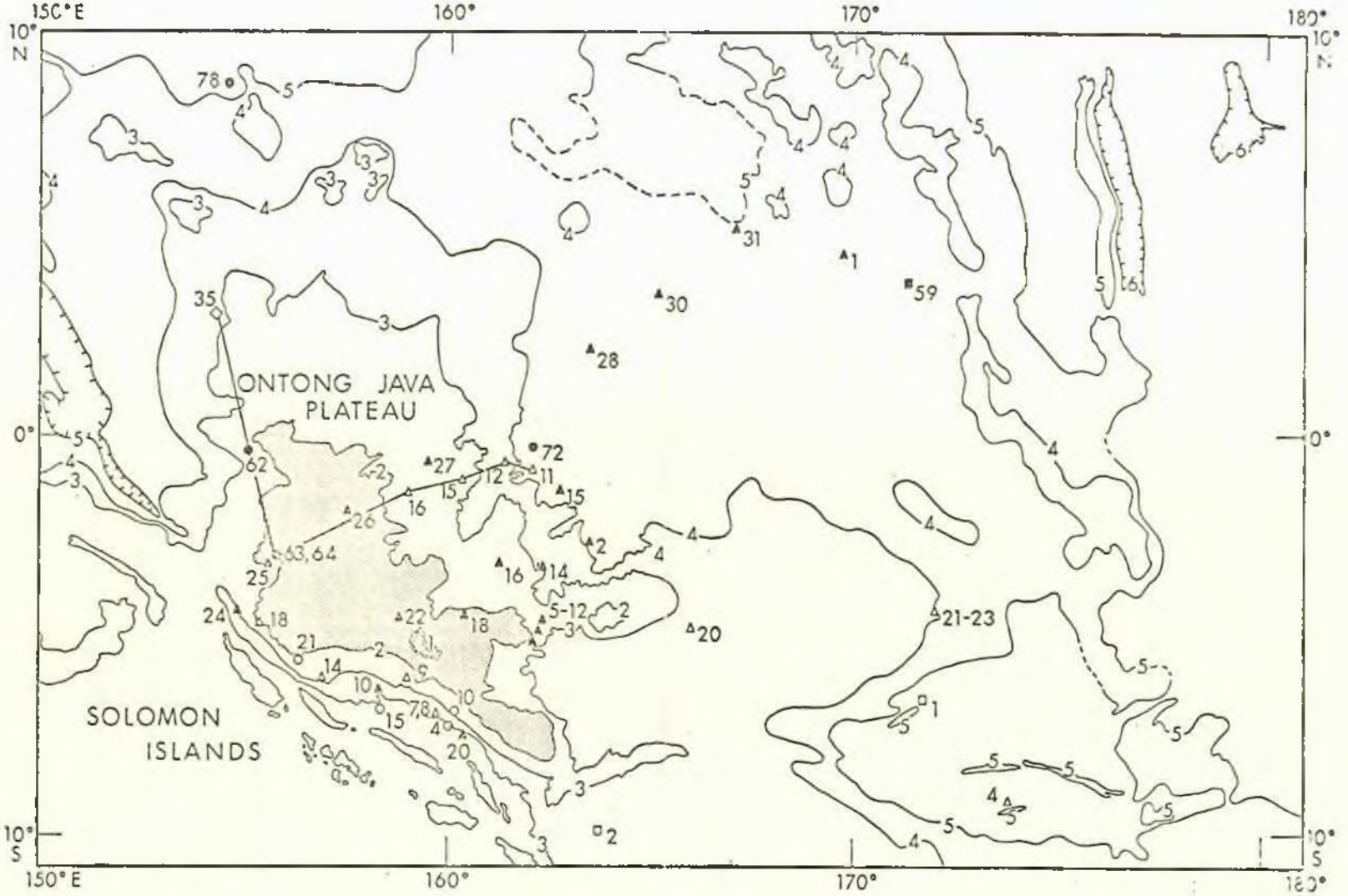
150°E
160°
170°
180°
10° N
0°
10° S
ONTONG JAVA PLATEAU
SOLOMON ISLANDS

20-cm intervals throughout the cores were washed through a 246 μ, 124 μ, 61 μ and 44 μ 3-inch diameter sieve series. Each fraction was then dried, weighed, and recorded. Calcium carbonate weight percent for the total sample and, in some cores, for the greater than 61 μ fraction was determined by Hulsemann's (1966) technique.

Phosphate was determined colorometrically as phosphomolybdenum blue on a Technicon analyzer after extraction with a mixture of equal proportions of 1N HCl and 0.5 N H_2SO_4 containing 3 gm of $(NH)_2SO_4$ per liter (H. Y. Young, 1971, pers. commun.).

Routine megascopic and smear slide descriptions were carried out by core laboratory personnel with the assistance and supervision of the author. For detailed description of core laboratory procedures see Southworth (1971) and Andrews et al. (1970). The raw data were submitted to a series of FORTRAN programs which calculated, correlated, and plotted the final core parameters.

Chronology

Previous foraminiferal and nannofossil information on age and continuity (Buyannanonth, 1971; Resig, 1971, pers. commun.; Landmesser, 1971) were supplemented, altered, or confirmed by the paleomagnetic stratigraphies interpreted by S. Hammond (1972, pers. commun.). Average Brunhes sedimentation rates were determined for continuous cores

assuming a contemporaneous surface and an age of 7×10^5 yrs. B.P. for the Brunhes-Matuyama boundary. Chronologies of specific paleoclimatic events were approximated by extrapolating these sedimentation rates throughout the Brunhes series. Four samples of 10 to 20 gm from a 2 to 3-cm span in the interior of the archive core half were submitted to Buddemeier and Hufen (in press) for C^{14} dating. Ages are based on a conventional half-life of 5560 years and are uncorrected for isotopic fractionation. The C^{14} ages revealed that very little near-surface sediment was lost during collection of the cores.

Foraminiferal paleoclimatic analysis

Counts of foraminiferal species (always exceeding 300 individuals) were made on known weights of the greater than 246 μ fraction every 20 cm in selected piston cores (Table 4). According to the paleomagnetic, micro-paleontologic, site topography, and station log data, these cores were most likely to represent continuous Pleistocene sections (Appendix B). The frequency of the species per gram of dry sediment greater than 246 μ was determined following the frequency-to-weight-ratio method of Ericson and Wollin (1968). Considering that the sedimentation rates in the selected cores are between 1 and 2 cm per thousand years, a 20-cm sampling interval should have provided at least two data points per 40 to 50 $\times 10^3$ yrs. climatic

half-cycle (Hays et al., 1969). A comparison of preliminary results using both a 10 and 20-cm sampling interval revealed no significant informational advantage of the closer sampling interval.

The species counted were the Globorotalia cultrata (d'Orbigny) complex in which G. tumida (Brady) was included, Globorotalia truncatulinoides (d'Orbigny), Globigerinoides sacculifer (Brady), and Globigerina conglomerata (Schwager). These species were chosen as potential paleoclimatic indicators due to their conflicting and/or restricted geographic ranges and wide differences in relative susceptibility to solution (Table 5). In addition to individual frequency-to-weight ratios, species to species ratios were designed to detect and separate sea-surface temperature and dissolution intensity fluctuations. The variation of the ratio of two species exhibiting similar geographic ranges but widely disparate resistance to solution, i.e., the G. cultrata complex and G. sacculifer or G. sacculifer and G. conglomerata, should indicate fluctuations in dissolution intensity. Conversely, the ratio trends of two species with similar solution characteristics but conflicting or exclusive geographic ranges, i.e., G. truncatulinoides and the G. cultrata complex or G. truncatulinoides and G. conglomerata, should provide insight into the surface water temperature variations which affect the species' ranges. It should be noted that if

Table 5*

Environmental and Solution Characteristics of Foraminiferal Species Counted

Species	Principal Geographic Range (Parker and Berger, 1971, Table 2; Bradshaw, 1959)	Temperature Range (and Preference) (Bradshaw, 1959)	Solution Rank (Parker and Berger, 1971)
GLOBOROTALIA CULTRATA (plus G. tumida)	40°N-25°S (20°N-20°S) both extend to 35°S	16-33 (19-31) (28-29, (29-31.5))	30 (36)**
GLOBOROTALIA TRUNCATULINOIDES	20° -40°N 20° -60°S occasional low frequencies at depth in equatorial region	13-27 (26-27)	27
GLOBIGERINOIDES SACCULIFER	20°N-30°S (extends to 40°S)	16-33 (26-27)	8
GLOBIGERINA CONGLOMERATA	20°N-12°S (extends to 30°S)	22-31 (27-28.5)	25

*Distribution data for the southern hemisphere is from tests in surface sediment and may reflect in part previous ranges during the Wisconsin.

**A high value indicates high resistance to solution.

temperature variations are severe enough to cause changes in the ranges of both species, the climatic record will be difficult to interpret. Also, proportional increases or decreases of production of one species relative to another could invalidate both the "climatic" and "solution" indices.

RESULTS

Surface sediment

Calcium carbonate

A contour map of percent calcium carbonate in the sediments superimposed on a bathymetric map of the area (Figure 6) reveals that the percent calcium carbonate values decrease markedly off the Plateau into deeper water due to solution of the calcium carbonate. The marked decrease in the direction of the Solomon Islands is anomalous, however, as the percent calcium carbonate values in these samples are much too low for the depth of water.

In the plot of surface sediment calcium carbonate versus depth (Figure 7), the sample values in the hatched area marked "Dilution" are all from the area between the Plateau and the Islands. Microscopic examination of the anomalous samples revealed significant amounts of volcanic ash and traces of pumice incorporated in rounded calcareous pellets coarser than 246 microns. These observations suggest dilution by volcanic material in this area and prompted the exclusion from the calcium carbonate and size fraction profiles of 17 samples situated southwest of the 80 percent carbonate contour.

Figure 8 presents plots of surface sediment calcium carbonate content versus sample depth for the total sediment (a) and for the three size fractions (b). Noteworthy

Figure 6. Contours of percent calcium carbonate in the surface sediment superimposed on the bathymetry of the area. Carbonate contour interval: 10 percent; bathymetric contour interval: 1 kilometer.

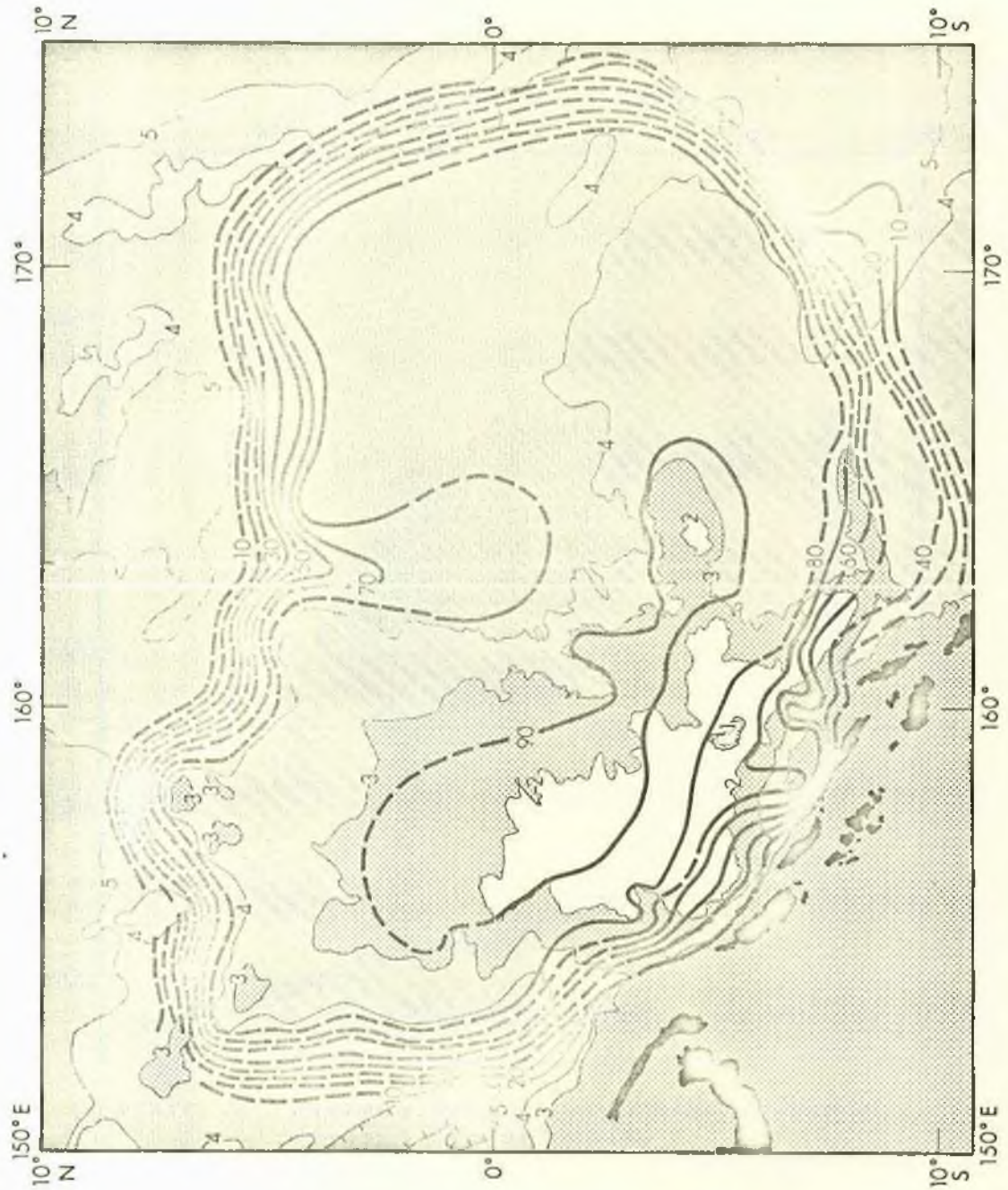
10° N
0°
10° S
170°
160°
150° E

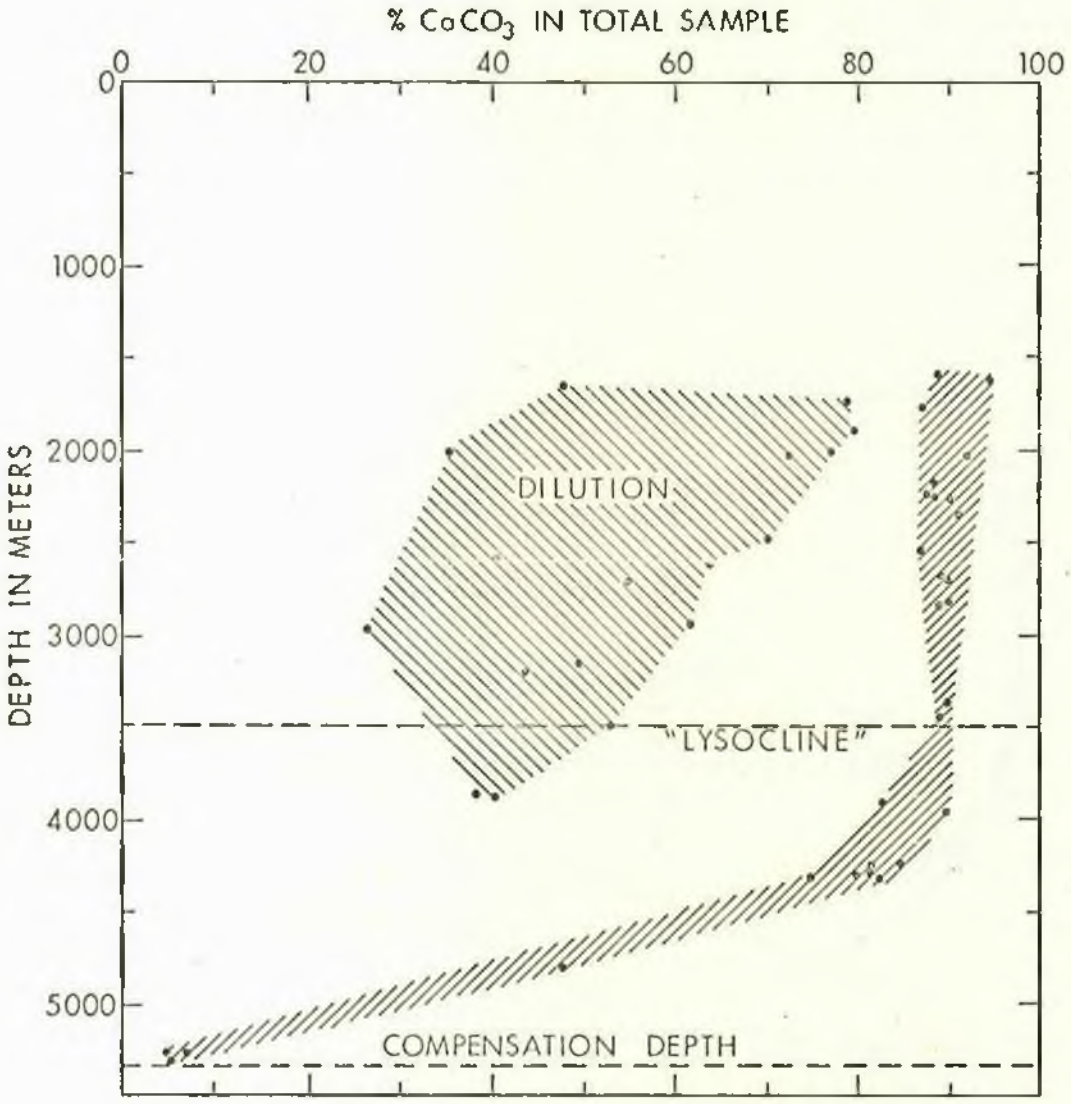

Figure 7. Surface sediment calcium carbonate percent versus depth.

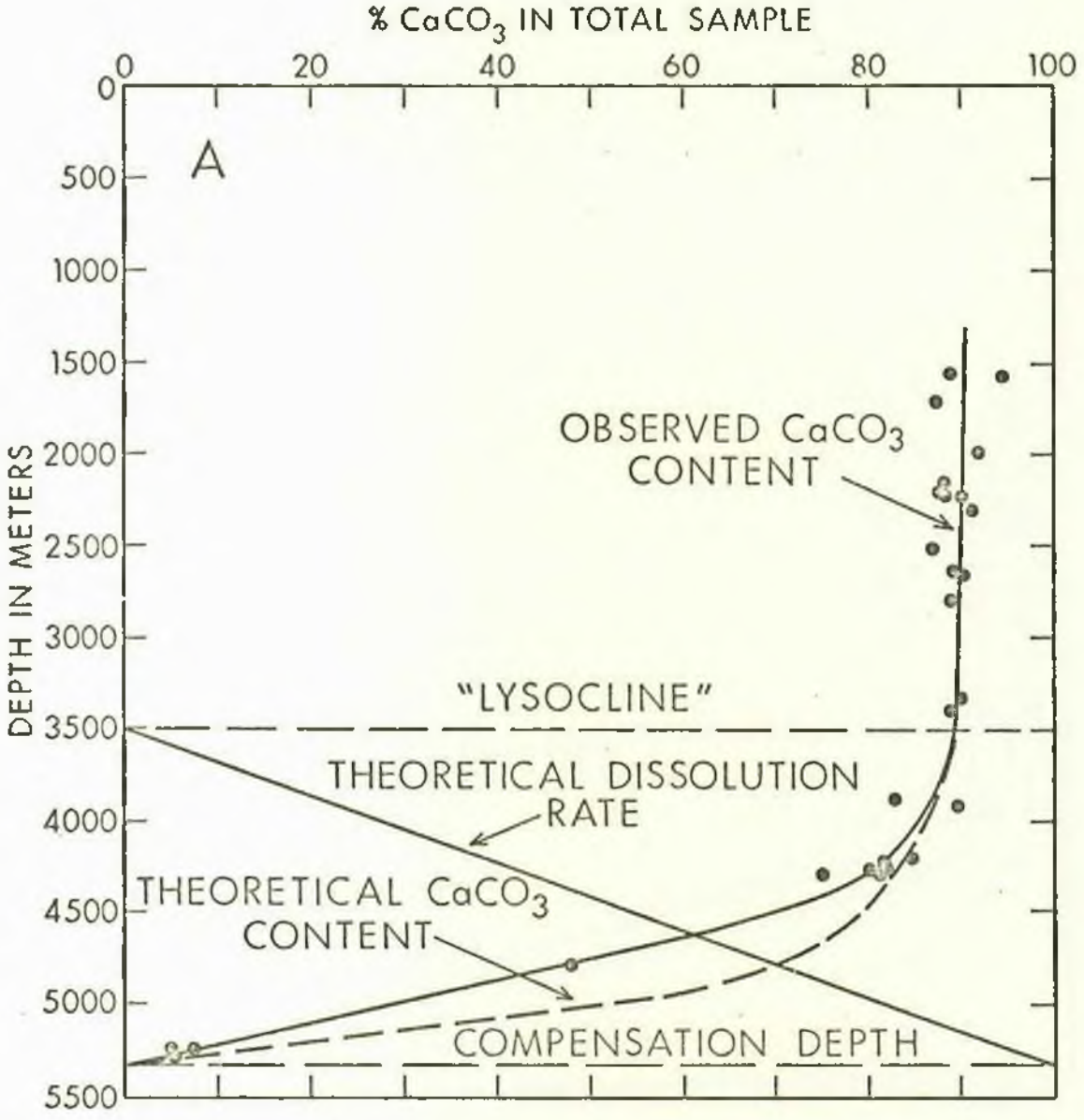

Figure 8a. Comparison of observed and theoretical curves of percent calcium carbonate with depth (total sample).

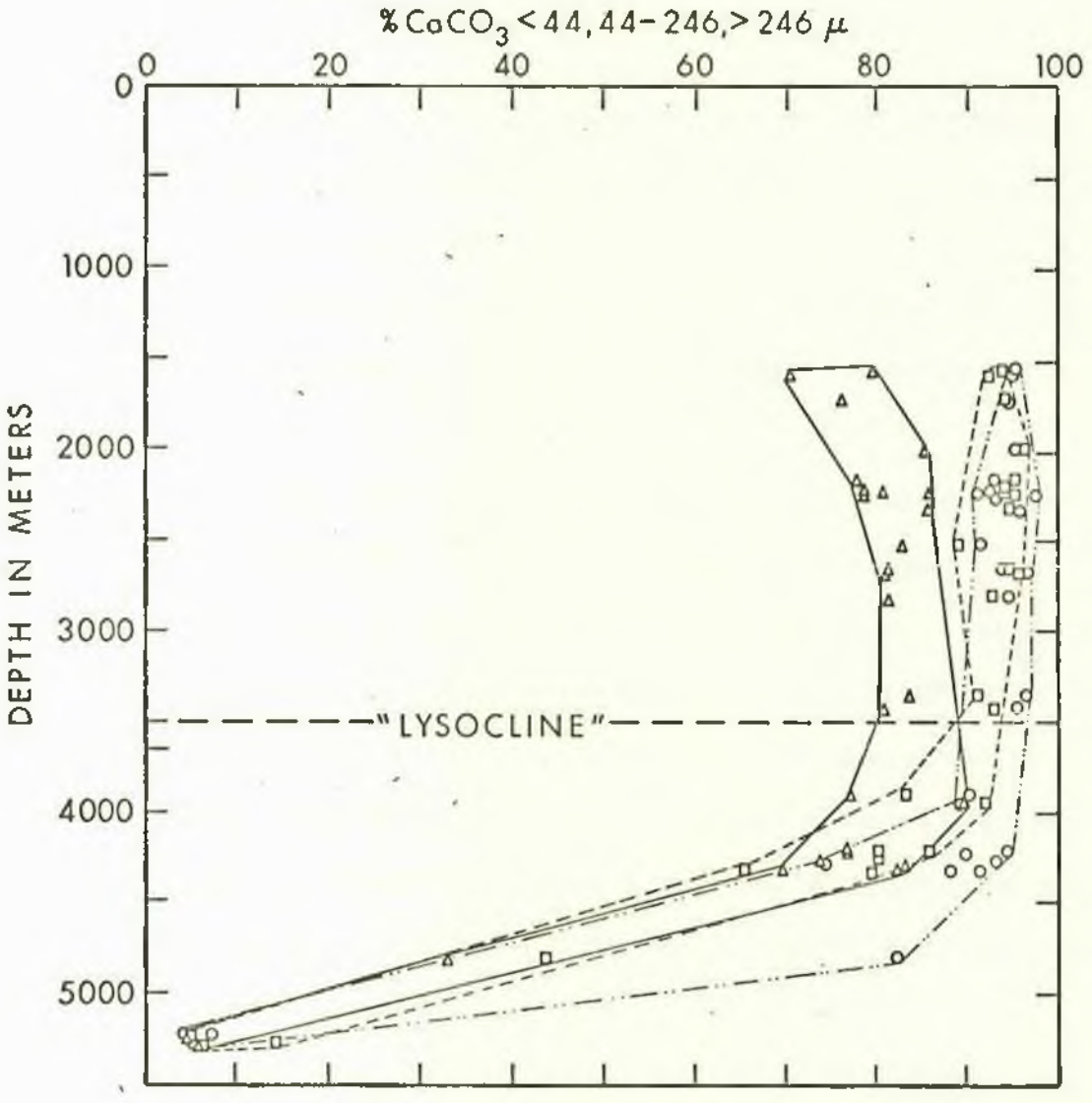

Figure 8b. Variation of percent calcium carbonate with depth, each size fraction: △ = <44 μ; □ = 44-246 μ; O = >246 μ.

observations based on these profiles are:

1. For all profiles, an abrupt decrease in calcium carbonate content occurs in the vicinity of 3500 m whereas the compensation depth is at about 5250 m;
2. Above 4000 m, the less than 44 μ fraction contains less weight percent calcium carbonate than the other size fractions;
3. The less than 44 μ fraction exhibits a maximum calcium carbonate percentage between 2500 and 3500 m;
4. All calcium carbonate profiles except that of the greater than 246 μ fraction display a linear relationship with depth below 4250 meters. Since the 44-246 μ and the greater than 246 μ fractions comprise nearly equal proportions of the total sediment and also have equal weight percentages of calcium carbonate above 4250 m, the attenuation of the greater than 246 μ profile is particularly striking.

Assuming that the rate of dissolution of calcium carbonate is zero above the saturation level, that it is slow in the interval of slight undersaturation between the saturation level and the lysocline, and that this rate increases linearly with depth below the lysocline, sediment calcium carbonate profiles may be mathematically generated

from estimations of the original calcareous content of the settling sediment and the lysocline and compensation depths (see Table 2 for horizon definitions) (Heath and Culberson, 1970). A comparison of a theoretical profile with that of the observed total sediment calcium carbonate is presented in Figure 8a (see Table 6 for calculations). The observed carbonate content appears to decrease more rapidly with depth than predicted by Heath and Culberson's model, although additional data below 4500 m would strengthen this conclusion.

A profile of the weight percent calcium carbonate contribution of each size fraction to the total percent carbonate is presented in Figure 9. Above 2500 m there is considerable scatter, but below this depth, the calcium carbonate less than 44 μ clearly predominates, reaching a maximum at about 4000 meters. The calcareous contribution of the other size fractions exhibits a relatively consistent decrease below 2500 meters.

Size fractions

Weight percent less than 44 μ correlates remarkably well with sample depth ($r = 0.92$, $P < .001$), especially between 2500 and 4500 m (Figure 10a). This size fraction approaches a constant 90 percent at about 4750 meters. Weight percent greater than 246 μ shows a high negative correlation with water depth ($r = -0.93$, $P < .001$). The weight percent of the 44-246 μ and greater than 246 μ

Table 6

Calculation of Theoretical $CaCO_3$ Content with Depth

L = lysocline depth = 3500 m, D_o = compensation depth = 5250 m, d = a depth at or between L and D_o in meters, R = rate of solution expressed as a percentage of the rate of supply; $R = d - L/D_o - L \cdot 100$; C^o = carbonate content of undissolved sediment, N = non-carbonate content of undissolved sediment, C = calcite content of sediment = $[(1 - R/100) \cdot C^o \cdot 100]/[(1 - R/100) \cdot C^o + N]$

d	d - L	R	C
3500	0	0	*90
3750	250	14.3	88.6
4000	500	28.6	86.5
4250	750	42.9	83.7
4500	1000	57.1	79.5
4750	1250	71.4	72.3
5000	1500	85.7	55.8
5250	1750	100.0	0

*Observed average carbonate content above 3500 meters.

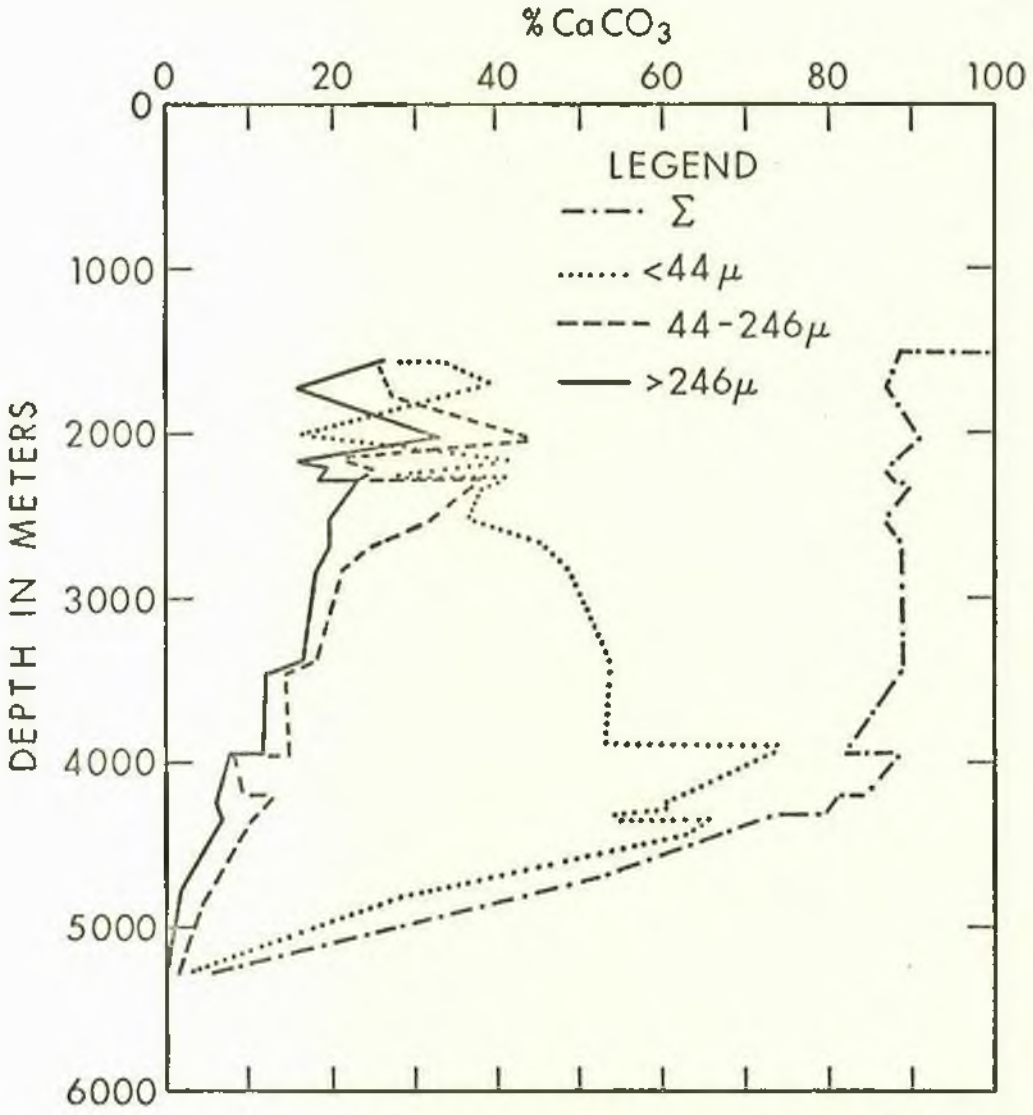

Figure 9. Weight percent calcium carbonate contribution of each size fraction ($\%CaCO_3$ x wt. % size fraction).

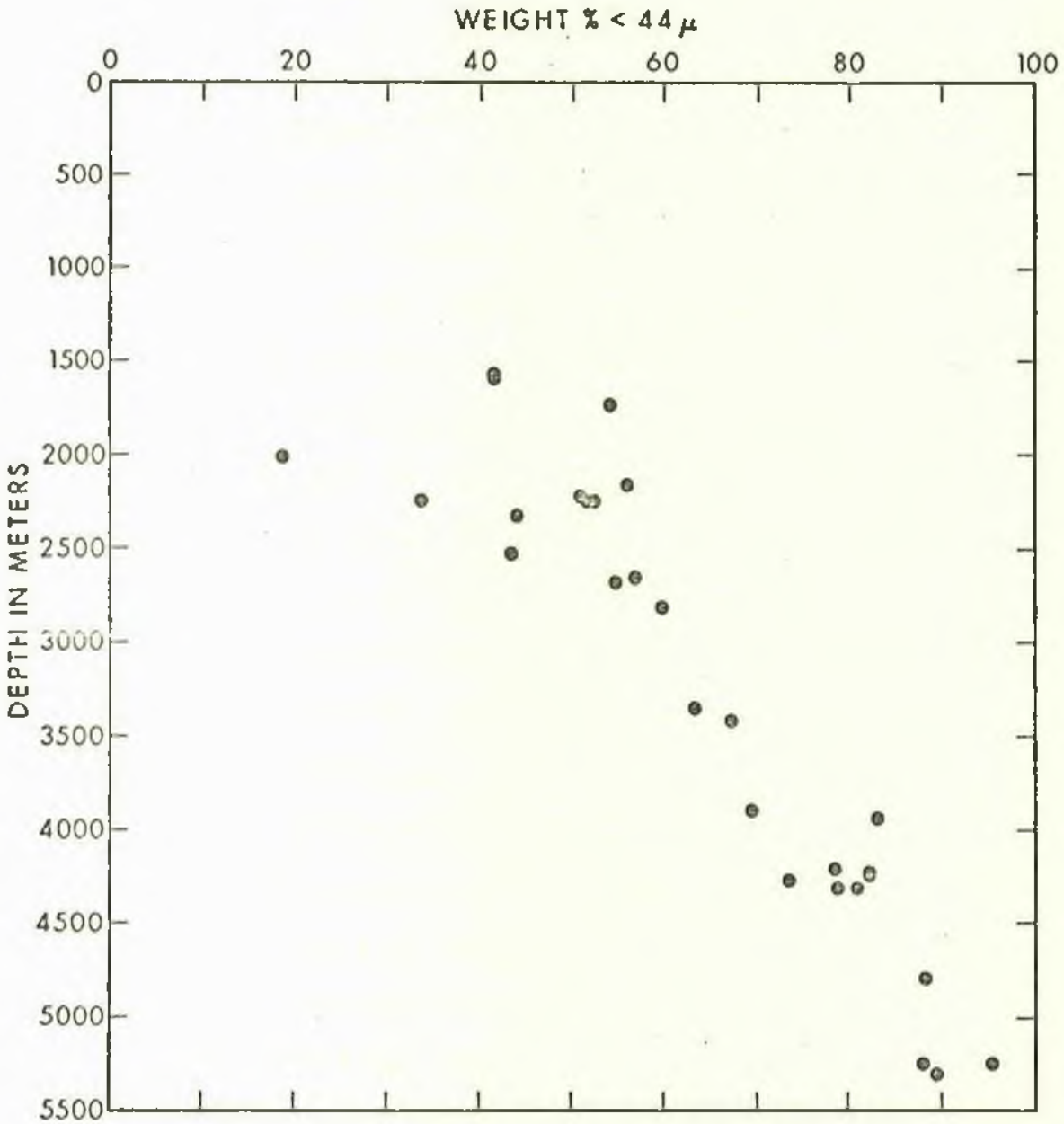

Figure 10a. · Weight percent less than 44 μ versus depth.

fractions approaches a constant 10 to 15 percent at 3900 m and 2 to 3 percent at 4750 m, respectively (Figures 10b and 10c).

Faunal parameters

Parker and Berger (1971, Fig. 14a) indicate a lysocline depth of 3800 m for the entire equatorial Pacific region. Solution indice profiles for my data (Figure 11a) and for data extracted from Parker and Berger (1971, Appendix A) for the region 10°N to 10°S, 150°-180°E (Figure 11b) delineate a lysocline at about 3500 meters. This depth disagrees with the 3750-4250 m range depicted in Parker and Berger's Fig. 15. Data from Parker and Berger (1971, Appendix A) for the eastern equatorial Pacific (Figure 11c) agrees with their entire equatorial Pacific figure of 3800 m for the lysocline. Thus the lysocline depth is greater in the eastern than in the western equatorial Pacific, and combining data from these two regions of disparate productivities masks this difference.

Plots of foraminiferal species frequencies and of selected ratios of these species with surface sediment collection depth permit the delineation of potential paleoclimatic and paleosolution indices. For example, of the potential paleoclimatic indices, the ratio of G. truncatulinoides to G. conglomerata (Figure 12) is not appreciably affected by increasing water depth in the

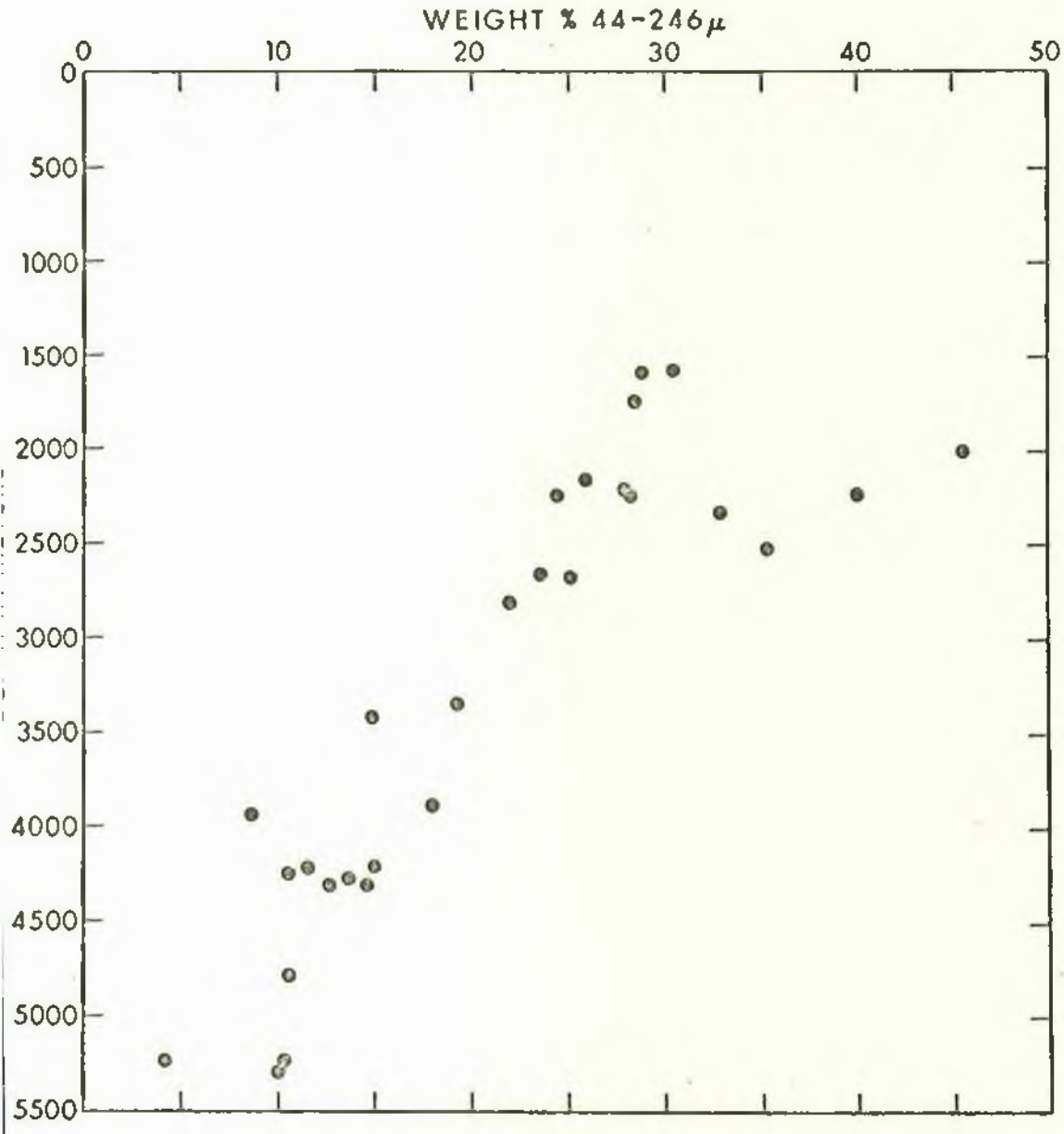

Figure 10b. Weight percent 44-246 μ versus depth.

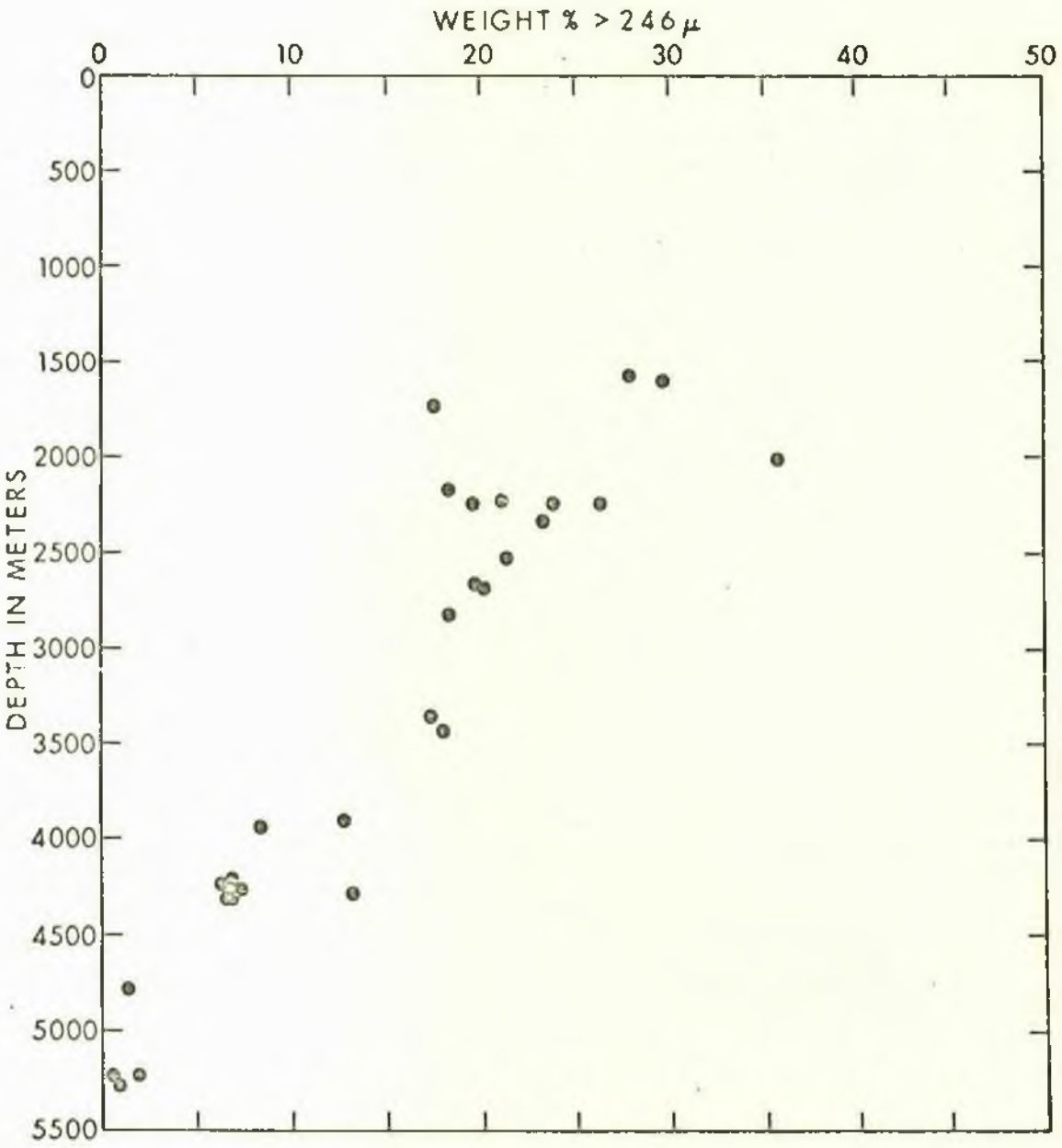

Figure 10c. Weight percent greater than 246 μ versus depth.

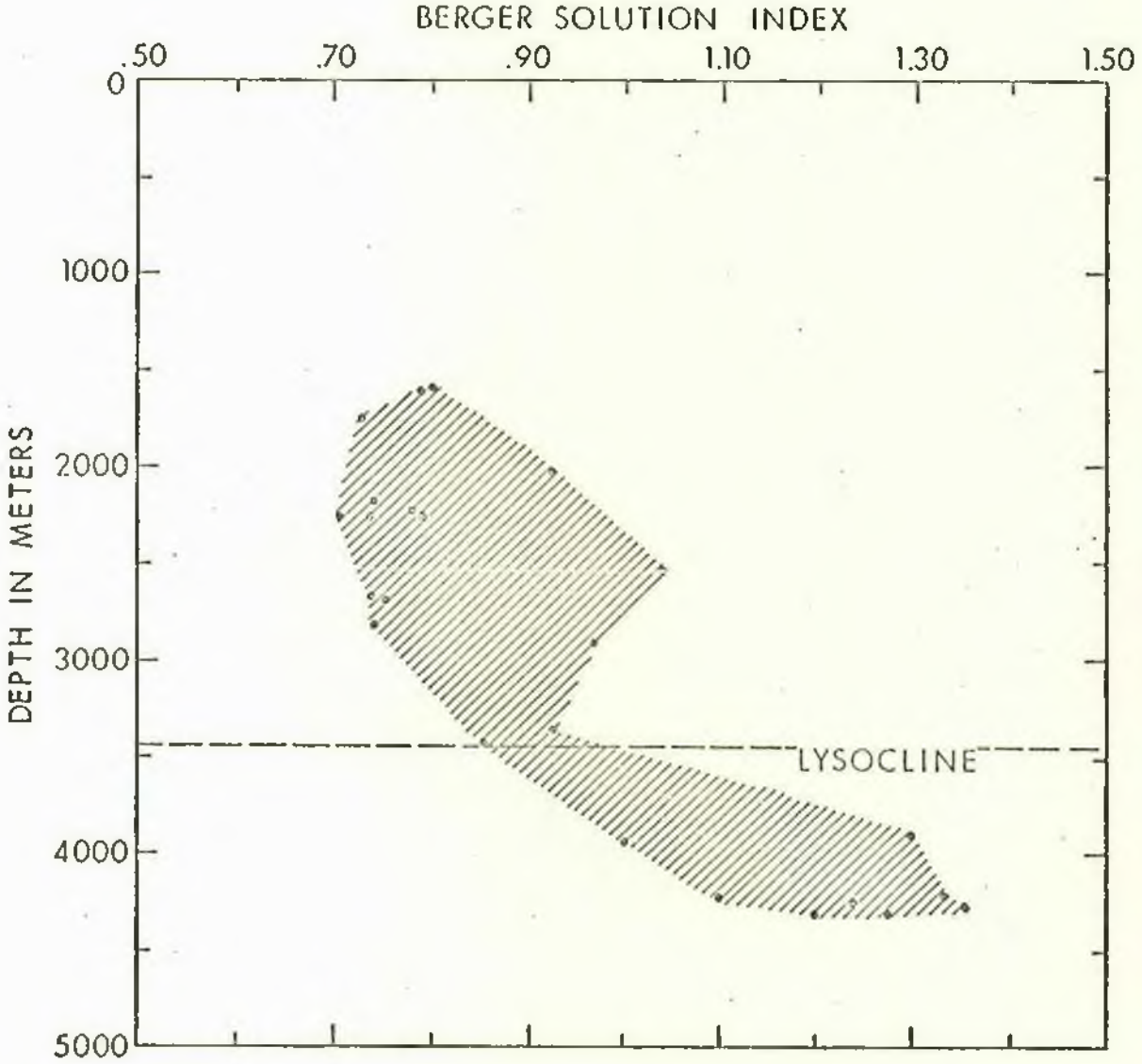

Figure 11a. Berger solution index profile for the western equatorial Pacific (data from this work).

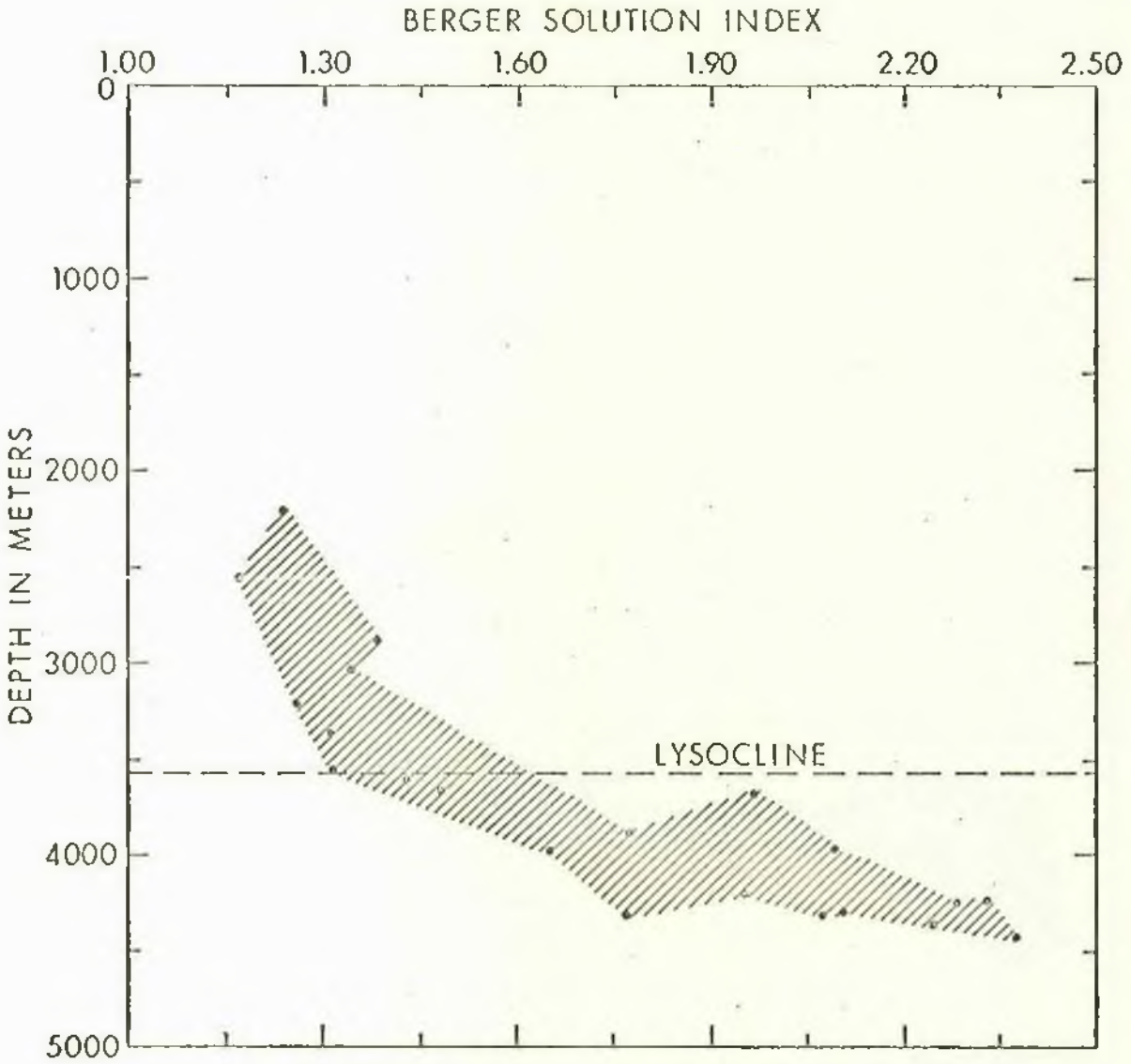

Figure 11b. Berger solution index profile for the western equatorial Pacific (data from Parker and Berger, 1971, Appendix A).

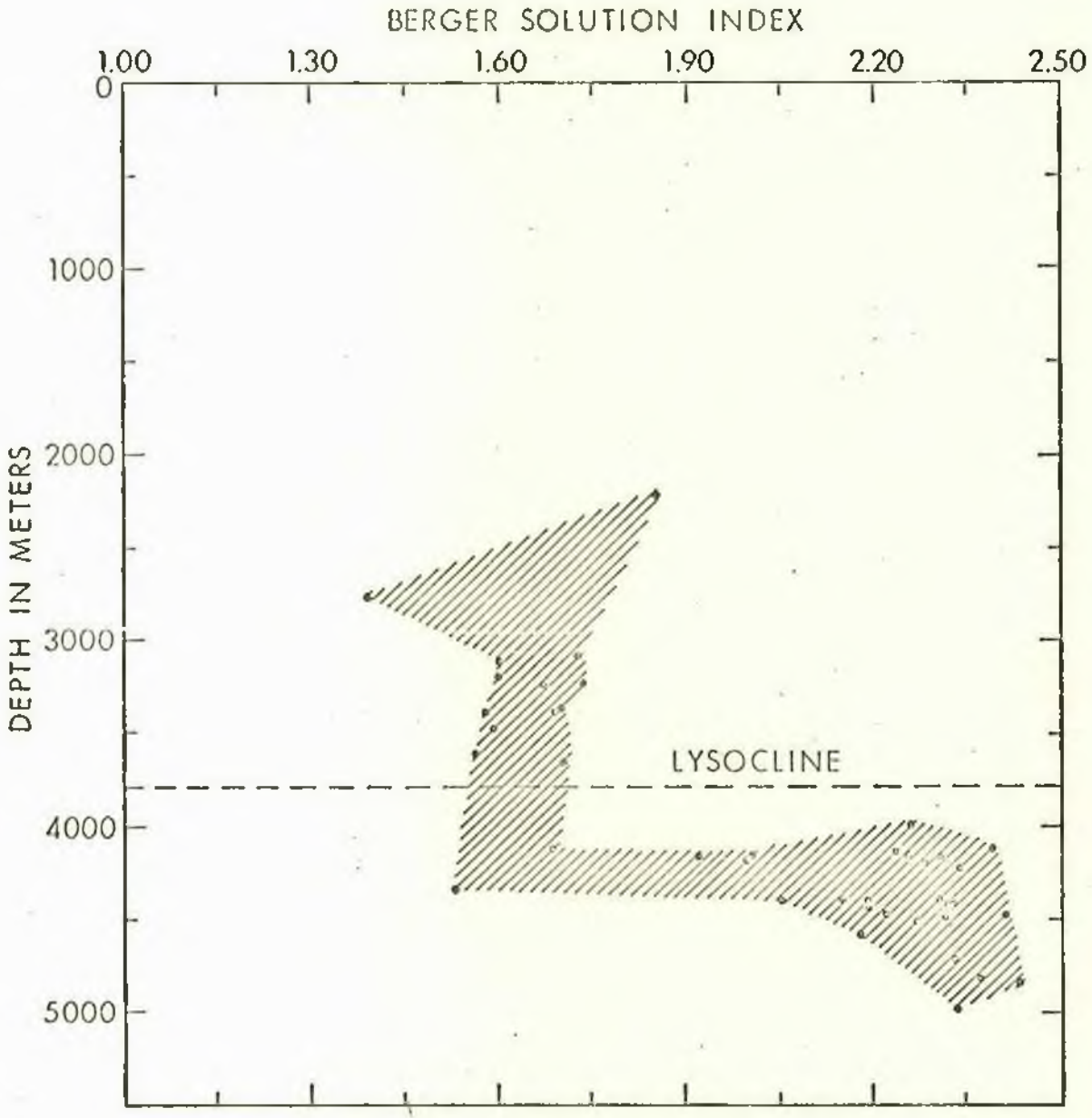

Figure 11c. Berger solution index profile for the eastern equatorial Pacific (data from Parker and Berger, 1971, Appendix A).

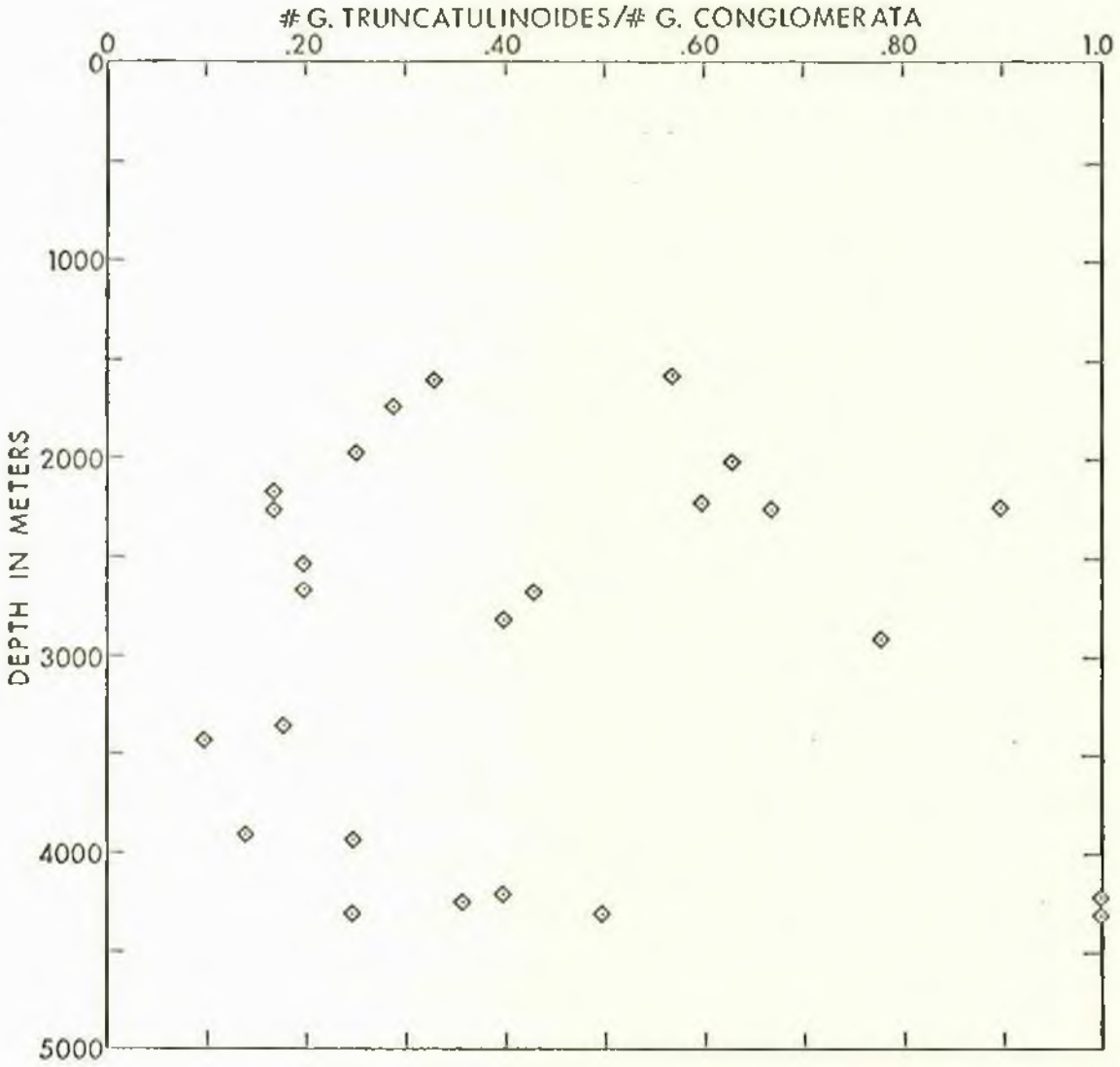

Figure 12. Frequency ratio of G. truncatulinoides to G. conglomerata versus depth.

investigation area. Past oscillations of this faunal parameter should only be attributable to changes in the geographic distribution or relative production of the species at the surface. Conversely, the frequency of G. sacculifer exhibits a negative linear trend with increasing water depth (Figure 13a). The variation of the ratio of G. cultrata complex and G. sacculifer with depth (Figure 13b) resembles the solution indice profile (Figure 11a), although the inflection point of the former curve is 200 m deeper than that of the latter plot. These indices may be useful in determining past fluctuations in solution intensity.

Pleistocene core analysis

Parameter oscillations and correlations

In any paleoclimatic study based on fluctuations of lithologic or faunal parameters in cores, it is necessary to understand the reasons for the parameter variation. No significant variation in non-biogenic debris, i.e., micro-manganese nodules or aeolian silt was noticed during the core analyses. Upwelling at the equator in the western equatorial Pacific during glacial stages would simultaneously lower the surface water temperature and increase biogenic productivity. Water column and surface sediment dissolution might also increase with the greater rate of supply of oxidizable organics. To separate the

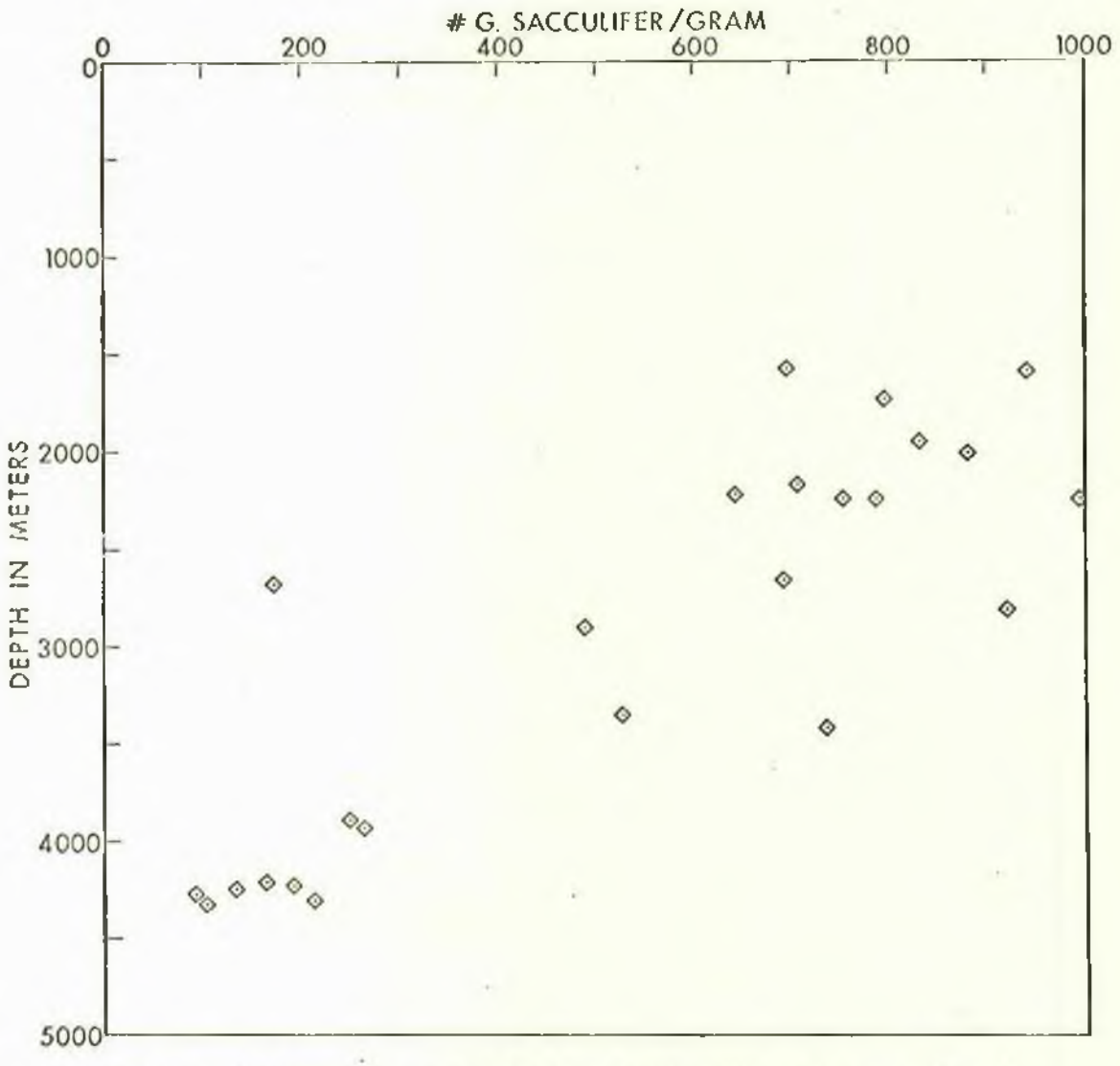

Figure 13a. G. sacculifer frequency versus depth.

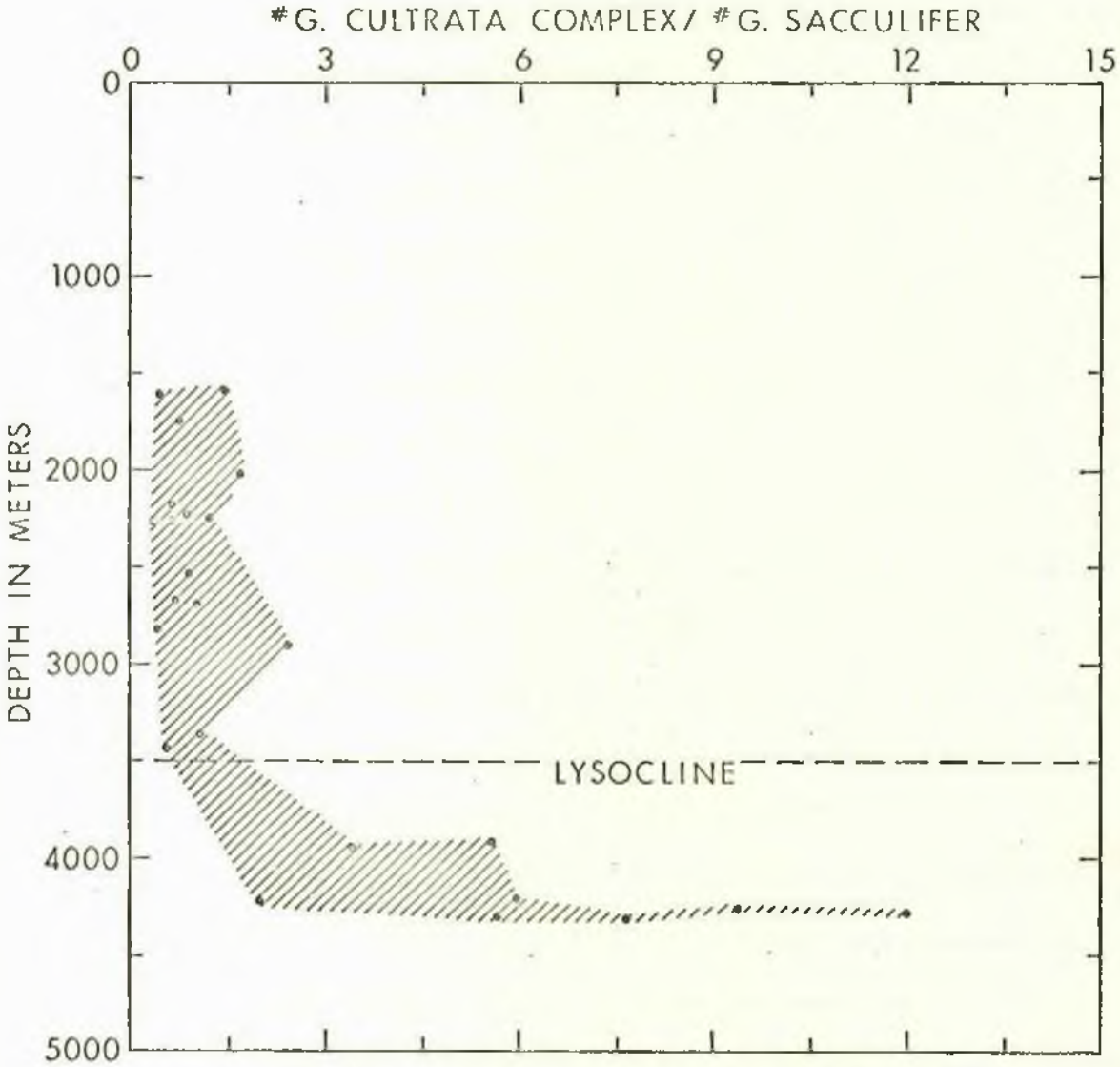

Figure 13b. Ratio of G. cultrata complex to G. sacculifer frequencies versus depth.

influence of these factors on the final sediment components is not an easy task. Ideally, one could examine the surface value of a variable and draw conclusions as to its variation with climate. However, surface sediment values from piston cores are sometimes unreliable due to sampling distortions (Ross and Riedel, 1967) or vertical mixing (Berger and Heath, 1968). Therefore, C^{14} dating and correlation with known climatic chronologies must suffice.

The C^{14} dates link peaks of the G. cultrata complex with glacial stages. The marine record of the last glacial (Wisconsin-Wurm) is generally reported as lasting from about 80×10^3 yrs. B.P. to $11\text{-}12 \times 10^3$ yrs. B.P. (Hays et al., 1969; Kent et al., 1971). In core 70PC64, whole sediment taken from near the top of the first significant peak yielded a C^{14} age of $23{,}590\ ^{+965}_{-860}$ yrs. B.P. (Figures 20 and 23). Sediment from the first, although subdued, peak in core 68PC12 was $30{,}660\ ^{+3080}_{-2220}$ C^{14} years old (Figures 16 and 23). The C^{14} activities from core 68PC15 (8780 ± 150 C^{14} years, Figures 17 and 23) and core 68PC16 ($17{,}440 \pm 430$ C^{14} years, Figures 18 and 23) were measured on samples taken in a transition zone between an older G. cultrata complex frequency low and a surface high. These dates and the surface frequency values are considered less reliable than the former data. Extrapolated paleomagnetically determined sedimentation rate chronologies for core 68PC16 support a correlation of the first G. cultrata

complex peak with the last glacial stage. Paired, group and total mean t-tests revealed significant differences between peaks and troughs of the G. cultrata complex frequency in all cores.

The data reviewed above imply a relationship between cooler climates and high frequencies of the G. cultrata complex in sediments from the western equatorial Pacific. This relationship may be due to a proportionally greater concentration of this resistant species with the increase of both production and solution in glacials as postulated for the eastern equatorial Pacific by Arrhenius (1952; 1963). The average peak-to-trough ratio of frequencies is 2:1. If the increase is due to production alone, productivity values would have been about equal to those of the present eastern equatorial Pacific (100 g $C/m^2/yr.$). However, Olausson (1971) suggests that Globorotalia species frequencies in the eastern equatorial Pacific cores are controlled by selective solution and are low in glacials due to the more rapid sedimentation rates. The resolution of these conflicting hypotheses may lie in the disparate depths of the collection sites (the cores examined by Olausson are all sublysoclinal), but confirmation awaits quantitative analysis of the production-solution problem.

In the Pleistocene cores examined, G. cultrata peaks are directly correlated with frequencies of G. truncatulinoides (cores 68PC15, 16; 70PC62, 64),

G. sacculifer (cores 68PC16, 70PC62), fine fraction (less than 44 μ) cores 68PC12, 15, 16) and the ratio of G. truncatulinoides to G. conglomerata (cores 68PC16; 70PC64) (Table 7). Although G. truncatulinoides is generally present in relatively small frequencies, the increase of this species in respect to the nearly equally resistant G. conglomerata indicates lowered surface water temperatures which enabled the penetration of the former species into the western equatorial region. Because G. conglomerata is commonly associated with high temperatures, upwelling may have curtailed its production by lowering surface water temperatures. According to Olausson (1971), Globigerinoides species frequencies should increase during glacials due to higher production. The positive correlation of G. sacculifer frequency and the cool-water index, G. truncatulinoides/G. cultrata complex in core 68PC12 supports this conclusion.

Some authors use the sand-silt division (61 or 62 μ) as a "coarse-fine" break, whereas the smallest mesh sieve available--44 μ--was used in this work. In pelagic calcareous ooze the separation of whole tests of foraminifera and coccoliths is not significantly affected by this division difference and the results of other authors can be compared to my data. The weight percent greater than 62 μ is directly proportional to, and the finer fraction inversely related to, paleotemperature in the Atlantic

Table 7

Correlations of Parameters in Pleistocene Cores

Parameter	Sign	% Sig. Level	Core						
			68PC11	68PC12	68PC15	68PC16	70PC62	70PC64	71PC35
DPT	+	1	P	GT, GS/GC GT, GC WP1, PC	GCC, GT GC, WP1 XPC	P, GT GT/GC	GCC/GS	GT, GC GT/GS GT/GCC	GCC GCC/GS
		5	WP3 R1, PC			WP1, R1			
	-	1		WP2, C44	WP3 WP4, WP5 C44, C61 C124, R2		GC, GS		
		5			GS/GC	GCC/GT WP4, C44 C61, C124			GS

Table 7. (Continued) Correlations of Parameters in Pleistocene Cores

Parameter	Sign	% Sig. Level	Core						
			68PC11	68PC12	68PC15	68PC16	70PC62	70PC64	71PC35
		1		R1	DPT, GT GC, WP1 R1	GT, WP1		GT GT/GS	DPT
	+	5		WP1		GS, GT/GC R1	GT, GS	GT/GC	
GCC									
		1			WP4, WP5 C44, C61 C124, R2	C44, C61			
	-	5		WP2, C44	GS/GC WP3	WP2, WP4 WP5, C124			

Table 7. (Continued) Correlations of Parameters in Pleistocene Cores

Parameter	Sign	% Sig. Level	Core						
			68PC11	68PC12	68PC15	68PC16	70PC62	70PC64	71PC35
		1		DPT	DPT, GCG	DPT, GCC		DPT, GCC	
	+			GS/GC					
		5		PC, XPC	GC, GS				
GT									
		1		WP3, P					
	-								
		5					GC		GC
					DPT, GCC				
		1		GS	WP1, R1			DPT	
	+								
		5			GT	GCC/GT			
GC									
					WP3				
					WP4, WP5				
					C44, C61				
		1			C124, R2		DPT		
	-								
		5		WP3			GT		GT/GCC, GT

Table 7. (Continued) Correlations of Parameters in Pleistocene Cores

Parameter	Sign	% Sig. Level	Core						
			68PC11	68PC12	68PC15	68PC16	70PC62	70PC64	71PC35
		1		GC					
	+			DPT					
		5		GT/GCC	GT	GCC	GCC		
GS									
		1					DPT		
	-								
		5							DPT
		1					DPT		
		5				WP1, R1			
GCC/GS									
		1							
	-					WP4			
						C44, C61			
		5				C124, R2			

Table 7. (Continued) Correlations of Parameters in Pleistocene Cores

Parameter	Sign	% Sig. Level	Core						
			68PC11	68PC12	68PC15	68PC16	70PC62	70PC64	71PC35
	+	1							DPT
		5		P					
GC/GS									
	-	1							
		5		WP2					
	+	1		DPT, WP1 R1, PC		DPT			
		5				GCC		GCC	
GT/GC									
	-	1							
		5		C124, P					

Table 7. (Continued) Correlations of Parameters in Pleistocene Cores

Parameter	Sign	% Sig. Level	Core						
			68PC11	68PC12	68PC15	68PC16	70PC62	70PC64	71PC35
GT/GCC	+	1						DPT	
		5		GS		GC			
	-	1					GC		
		5		P		DPT			GC
GT/GS	+	1						DPT, GCC	
		5							
	-	1							
		5					GC		

Table 7. (Continued) Correlations of Parameters in Pleistocene Cores

Parameter	Sign	% Sig. Level	Core						
			68PC11	68PC12	68PC15	68PC16	70PC62	70PC64	71PC35
		1		DPT GT/GC	DPT GCC, GC	GCC			
	+					DPT			
		5		GCC, PC		GCC/GS			
WP1									
		1			GS/GC				
	-								
		5							
		1							
	+								
		5							
WP2									
		1		DPT					
	-								
				GCC					
		5		GCC/GS		GCC			

Table 7. (Continued) Correlations of Parameters in Pleistocene Cores

Parameter	Sign	% Sig. Level	Core						
			68PC11	68PC12	68PC15	68PC16	70PC62	70PC64	71PC35
		1							
	+								
		5	DPT						
WP3									
		1		GT	DPT, GC				
	-								
		5		GC	GCC				
		1							
	+								
		5			GS/GCC				
WP4									
					DPT				
		1			GCC, GC				
	-								
						DPT, GCC			
		5		XPC		GCC/GS			

Table 7. (Continued) Correlations of Parameters in Pleistocene Cores

Parameter	Sign	% Sig. Level	Core						
			68PC11	68PC12	68PC15	68PC16	70PC62	70PC64	71PC35
	+	1			GS/GC				
		5							
WP5									
					DPT				
	-	1			GCC, GC				
		5	DPT, P	PC		XPC, GCC			
	+	1			GS/GC				
		5							
C44									
					DPT				
	-	1		DPT	GCC, GC	GCC			
						DPT			
		5		GCC, PC		GCC/GS			

Table 7. (Continued) Correlations of Parameters in Pleistocene Cores

Parameter	Sign	% Sig. Level	Core						
			68PC11	68PC12	68PC15	68PC16	70PC62	70PC64	71PC35
		1			GS/GC				
	+								
		5							
C61									
					DPT				
		1			GCC, GC	GCC			
	-								
						DPT			
		5		PC		GCC/GS			
		1			GS/GC				
	+								
		5							
C124									
					DPT				
		1			GCC, GC				
	-								
		5	DPT		GT/GC				

Table 7. (Continued) Correlations of Parameters in Pleistocene Cores

Parameter	Sign	% Sig. Level	Core						
			68PC11	68PC12	68PC15	68PC16	70PC62	70PC64	71PC35
R1	+	1		GCC GT/GC	DPT GCC, GC				
		5	DPT	DPT, PC					
	-	1			GS/GC				
		5							
R2	+	1			GS/GC				
		5							
	-	1			DPT GCC, GC				
		5							

Table 7. (Continued) Correlations of Parameters in Pleistocene Cores

Parameter	Sign	% Sig. Level	Core						
			68PC11	68PC12	68PC15	68PC16	70PC62	70PC64	71PC35
				DPT					
		1		GT/GC					
	+								
				GT					
		5	DPT	WP1, R1	GS/GC				
PC									
		1							
	-								
				WP5					
		5		C44, C61					
		1			DPT				
	+								
		5		GT					
XPC									
		1		P					
	-								
		5		WP4		WP5, R2			

Table 7. (Continued) Correlations of Parameters in Pleistocene Cores

Parameter	Sign	% Sig. Level	Core						
			'68PC11	68PC12	68PC15	68PC16	70PC62	70PC64	71PC35
		1	DPT			DPT			
	+								
		5		GCC/GS					
P									
		1		XPC, GT					
	-								
				GS/GC					
		5	WP5	GT/GC					

Key:

DPT: depth in core
GCC: G. cultrata complex
GT : G. truncatulinoides
GC : G. conglomerata
GS : G. sacculifer
WP1, 2, 3, 4, 5: <44, 44-61, 61-124, 124-246, >246 μ, weight percent coarser
R1 : weight percent <44/>246 μ
R2 : weight percent </24 μ />/24 μ
PC : weight percent calcium carbonate total
XPC: weight percent calcium carbonate >6/μ
P : phosphorus in ppm

(Emiliani and Flint, 1963). These relationships are explained by a decrease of coarse and fine carbonate as well as non-carbonate sedimentation rates from glacials to interglacials with the coarse carbonate exhibiting the least decrease (Broecker et al., 1958). The relatively greater reduction of fine fraction is probably due to the more rapid adaptation of the autotrophic coccolithophores to climatic change (Broecker et al., 1958), a contention supported by the positive correlation of fine fraction percent carbonate and G. truncatulinoides/G. conglomerata in core 68PC12. However, Berger (1967) suggests that the increase of the finer fractions (less than 177 μ) is among other variables, a reliable indicator of solution. This alternative is supported by a direct relation of fine fraction (less than 44 μ) and G. cultrata complex/G. sacculifer in core 68PC16. The fine fraction does not show a detectable difference in foraminifer fragment content between peaks and troughs. If fine fraction variation is governed by solution, then breakdown of foraminifera fragments keeps pace with their production as the fine fraction is proportionately increased. The fact that coccoliths are generally more resistant to solution than tests of foraminifera may also contribute to the increase of fine fraction in glacial stages. Thus fine fraction increase in glacials may be a combined result of increased

solution and increased production of coccoliths relative to foraminifera tests.

Other pertinent correlations include a positive association of G. truncatulinoides frequency with calcium carbonate weight percent total and greater than 61 μ (core 68PC12) and with G. sacculifer frequency (core 68PC15). Relations of G. truncatulinoides frequency are also inverse with phosphorous (core 68PC12). Basin-basin element fractionation stimulated by climatic change resulted in a net transfer of calcium carbonate and other nutrients from the Atlantic to the Pacific during glacials (Olausson, 1967; 1971). Increased depositional rates of calcium carbonate have been linked with glacial stages in the eastern equatorial Pacific (Arrhenius, 1950; 1952; 1963). In core 68PC12, percent carbonate is directly related to the "climatic" index G. truncatulinoides/G. conglomerata, supporting this association. Berger (1971a) has shown, however, that for calcareous ooze, as much as half of the carbonate may be lost without a significant decrease in carbonate percentage. Thus, increased solution is not ruled out by higher carbonate percentages associated with glacials although the glacial increase of G. sacculifer certainly indicates that production outstripped solution.

Because the percent carbonate greater than 61 μ represents the foraminiferal component, this value is an approximation of the foraminifera/radiolarian ratio used by

Duncan et al. (1970) and Buyannanonth (1971) to delineate climatic variations. High percent of carbonate greater than 61 μ may indicate cooler periods in this region (Buyannanonth, 1971). The G. sacculifer - G. truncatulinoides positive correlation confirms the inferred association of cooler surface waters and higher production.

The climatic implications of phosphorous fluctuations are problematical. Arrhenius (1952; 1971, pers. commun.) used concentrations of this element to delineate past variations in primary productivity, assuming that phosphate debris (apatite) from bathypelagic fish is less sensitive to solution than calcium carbonate. Olausson (1971) contends that apatite is slightly more soluble than calcium carbonate and that phosphorous content may decrease relative to calcium carbonate with increasing solution. The relationships exhibited in the Hawaii Institute of Geophysics cores indicate that phosphorous is either diluted by high carbonate production during glacials or concentrated by solution during interglacials. For example, in core 68PC12, phosphorous concentration is positively correlated with the two "solution" ratios, G. cultrata complex/G. sacculifer and G. conglomerata/G. sacculifer and is inversely related to the "climatic" index G. truncatulinoides/G. conglomerata.

G. conglomerata frequencies exhibit conflicting trends (e.g., with G. truncatulinoides frequency in core 68PC15

and core 70PC62) and are therefore considered unreliable.

In summary, the correlations indicate the influence of production, solution, and surface water temperature variations on the sedimentary parameters. Since all the cores except core 68PC11 are situated above the lysocline (Figure 14), solution was probably not a dominant factor, although the lysocline may have been somewhat shallower with an increased supply of organics in periods of upwelling. At most, increases of the G. cultrata complex and the fine fraction were aided by increased water column dissolution in glacials (Heath and Culberson, 1970). Surface water temperature was probably no lower than that of the present area of most intensive upwelling in the eastern equatorial Pacific, i.e., 20°C. This temperature reduction enabled G. truncatulinoides to expand from its patchy distribution in the Peru current (Bradshaw, 1959) along the equator to the western equatorial Pacific and also possibly decreased G. conglomerata production. Any temperature variation had no detectable effect on the geographic ranges of the other species examined.

Initiation of upwelling in a glacial stage increased production resulting in higher frequencies of G. cultrata complex and G. sacculifer as well as coccoliths (fine fraction). The sedimentation rate of calcium carbonate increased and phosphorous concentrations decreased due to dilution. Thus a dominant production control dependent on

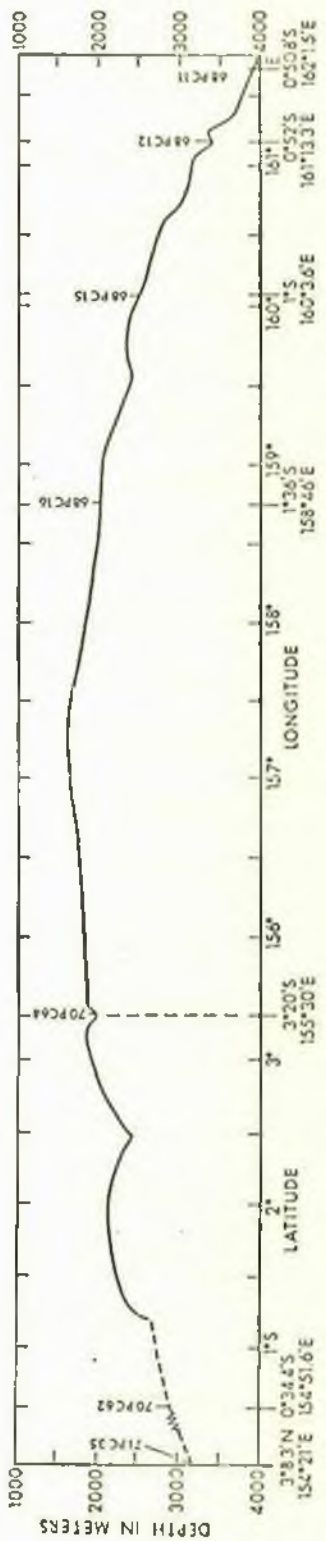

Figure 14. Bathymetric cross section of Pleistocene core locations. Line of section is 11-35 in Figure 6.

climatic change generally explains the parameter relationships in these cores.

Correlation with depth in cores

Having explored the climatic import of the variables investigated, the parameter relationships with depth throughout the cores (Table 7), or with increasing age, can now be examined for paleoclimatic significance. An increase with depth of G. truncatulinoides frequency, by itself in cores 68PC12, 15, 16 and 70PC64, and in respect to G. conglomerata (cores 68PC12, 16) and the G. cultrata complex (cores 68PC16, 70PC64) certainly indicates cooler surface waters in the past. Greater past production is inferred from the increase with depth of total percent calcium carbonate (cores 68PC11, 12) and percent carbonate greater than 61 μ (core 68PC15). However, some component relationships also seem to point to greater dissolution in the past. For example, phosphorous content (cores 68PC11, 16) and the ratio of G. cultrata complex to G. sacculifer (cores 70PC62, 71PC35) increase with depth, possibly reflecting more intense solution in the past.

Some factor trends could signify either greater past production and/or solution. For example, a fine-fraction increase with depth (cores 68PC12, 15, 16) may be attributed to either greater past coccolith production or to foraminifera fragmentation through greater solution.

Other parameters, e.g., weight percent 61-124 μ, frequency of G. sacculifer and G. conglomerata and the ratio of these species exhibit conflicting trends with depth, and are thus unreliable as indicators of production or solution variations with age.

Individual cores

Appendix B reviews for each core the available descriptive characteristics as follows: location, depth, topography of collection site, smear slide description, lithology, C^{14} and paleomagnetic chronology, micropaleontology, interpretations of core continuity, descriptive statistics of the measured physical, chemical, and faunal properties, and an annotated paleoclimatic chronostratigraphy. Evidence of discontinuities and reworking in the cores, as reviewed in Appendix B and indicated on the figures, has direct bearing on the correlations. Profiles of pertinent potential paleoclimatic parameters are displayed in a summary or "supporting" diagram for each core: 68PC11, Figure 15; 68PC12, Figure 16; 68PC15, Figure 17; 68PC16, Figure 18; 70PC62, Figure 19; 70PC64, Figure 20; 71PC35, Figure 21.

The chronologies are based on sedimentation rates extrapolated from known ages of paleomagnetic boundaries (Figure 22) and are computed for climatic half-cycles between stage transition midpoints. Justification of the

Figure 15 (top). Supporting diagram for core 68PC11.

Figure 16 (center). Supporting diagram for core 68PC12.

Figure 17 (bottom). Supporting diagram for core 68PC15.

Key for Figures 15-21:

GCC = G. cultrata complex; GS = G. sacculifer; GC = G. conglomerata; GT = G. truncatulinoides; GTo = G. tosaensis; P = phosphorus. Stratigraphic nomenclature after Hays et al., 1969; odd numbers denote conditions similar to present.

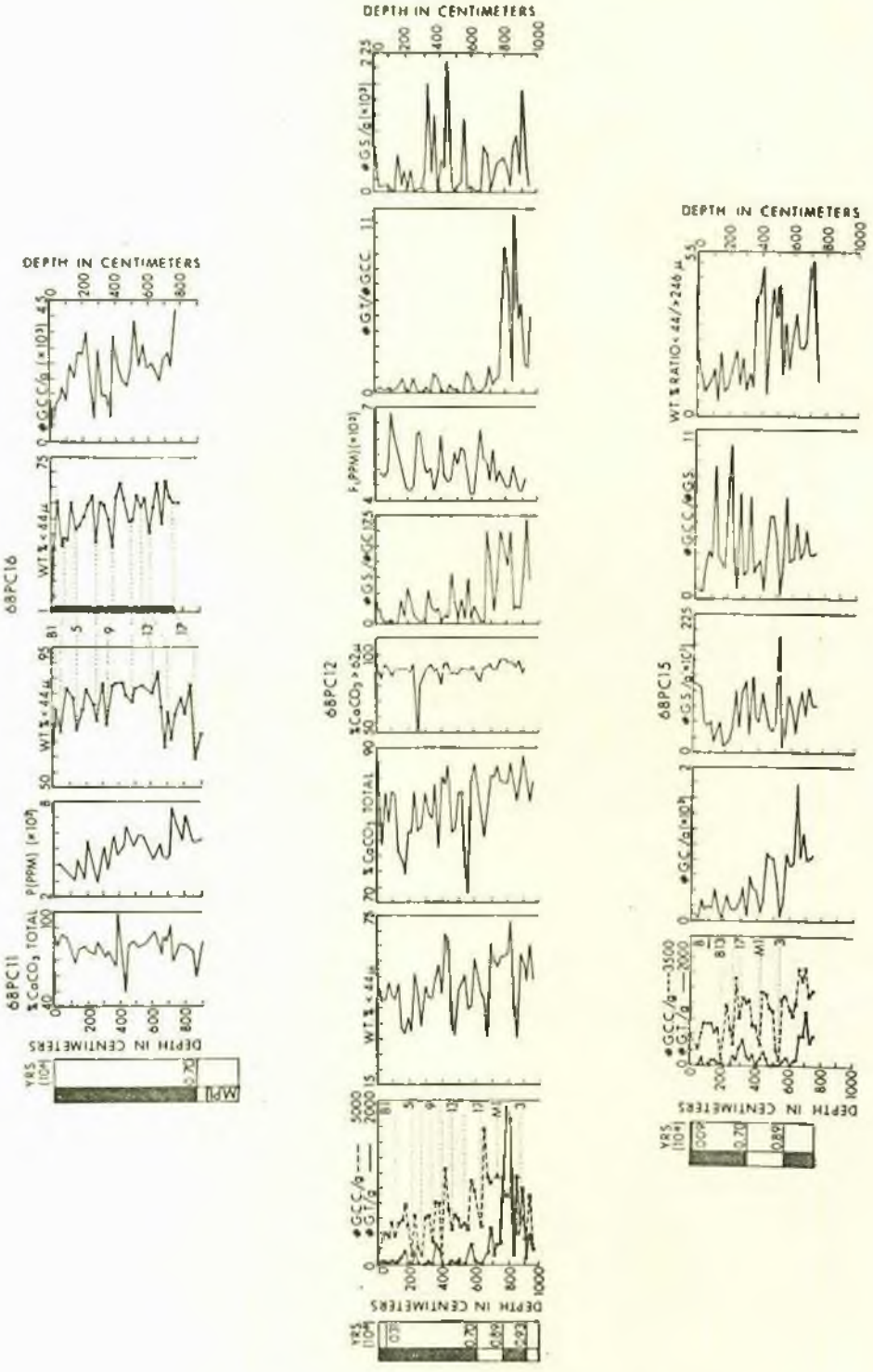
DEPTH IN CENTIMETERS
68PC16
68PC11
68PC12
68PC15
DEPTH IN CENTIMETERS

Figure 18 (top). Supporting diagram for core 68PC16.

Figure 19 (center left). Supporting diagram for core 70PC62.

Figure 20 (bottom). Supporting diagram for core 70PC64.

Figure 21 (center right). Supporting diagram for core 71PC35.

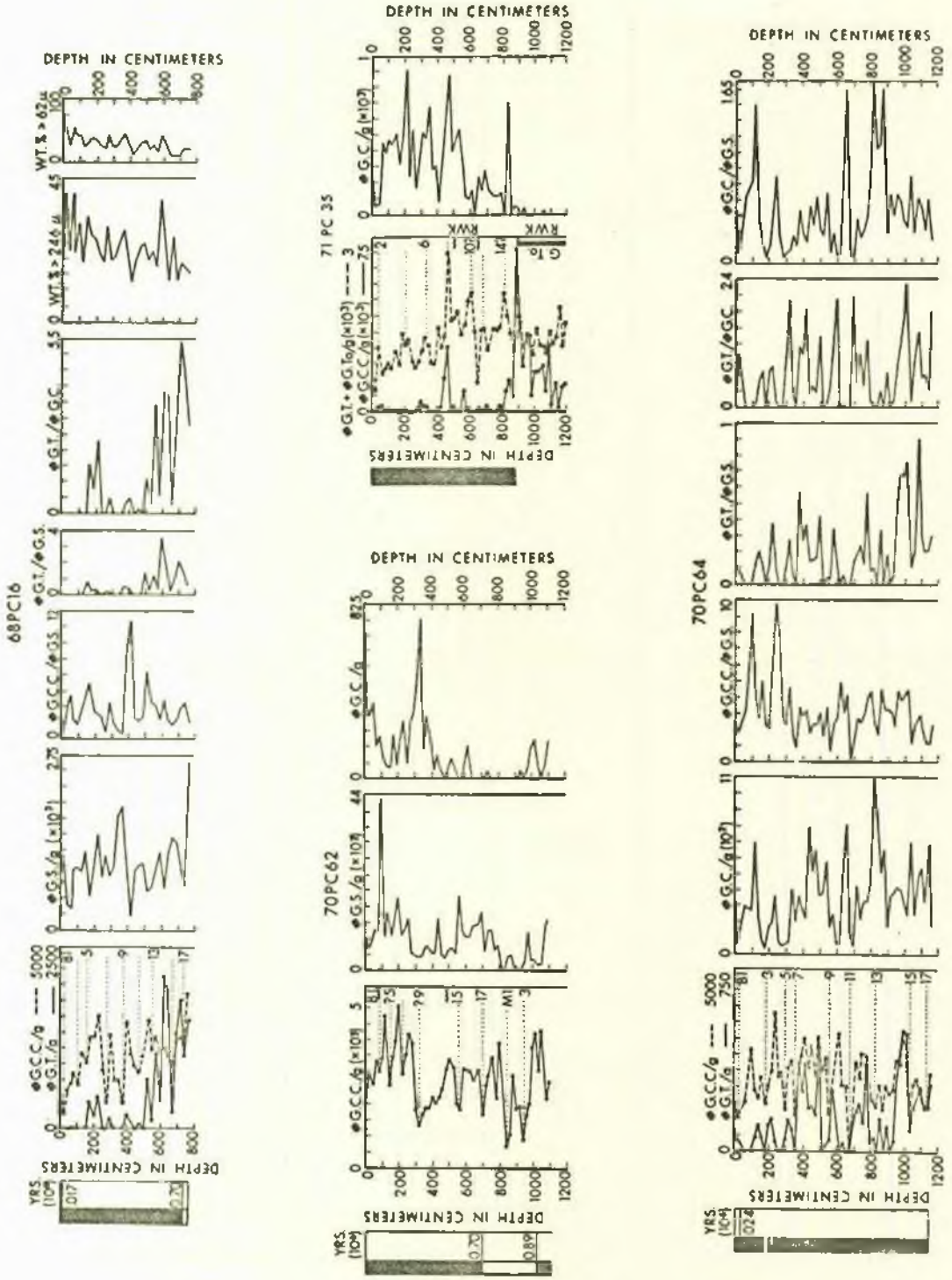
68PC16
DEPTH IN CENTIMETERS
WT.% > 62μ
WT.% > 246 μ
●GT./●GC
●GT./●GS
●GCC./●GS
●GS./g (×10³)
●GCC./g
●GT./g
DEPTH IN CENTIMETERS
YRS (10⁴)
71 PC 35
DEPTH IN CENTIMETERS
●GC./g (×10³)
RWK
●GT+●GTo/g (×10³)
●GCC./g (×10³)
DEPTH IN CENTIMETERS
70PC62
DEPTH IN CENTIMETERS
●GC./g
●GS./g (×10⁴)
●GCC./g (×10⁴)
DEPTH IN CENTIMETERS
YRS (10⁴)
70PC64
DEPTH IN CENTIMETERS
●GC./●GS.
●GT./●GC
●GT./●GS
●GCC./●GS.
●GC./g (10³)
●GCC./g
●GT./g
DEPTH IN CENTIMETERS
YRS (10⁴)

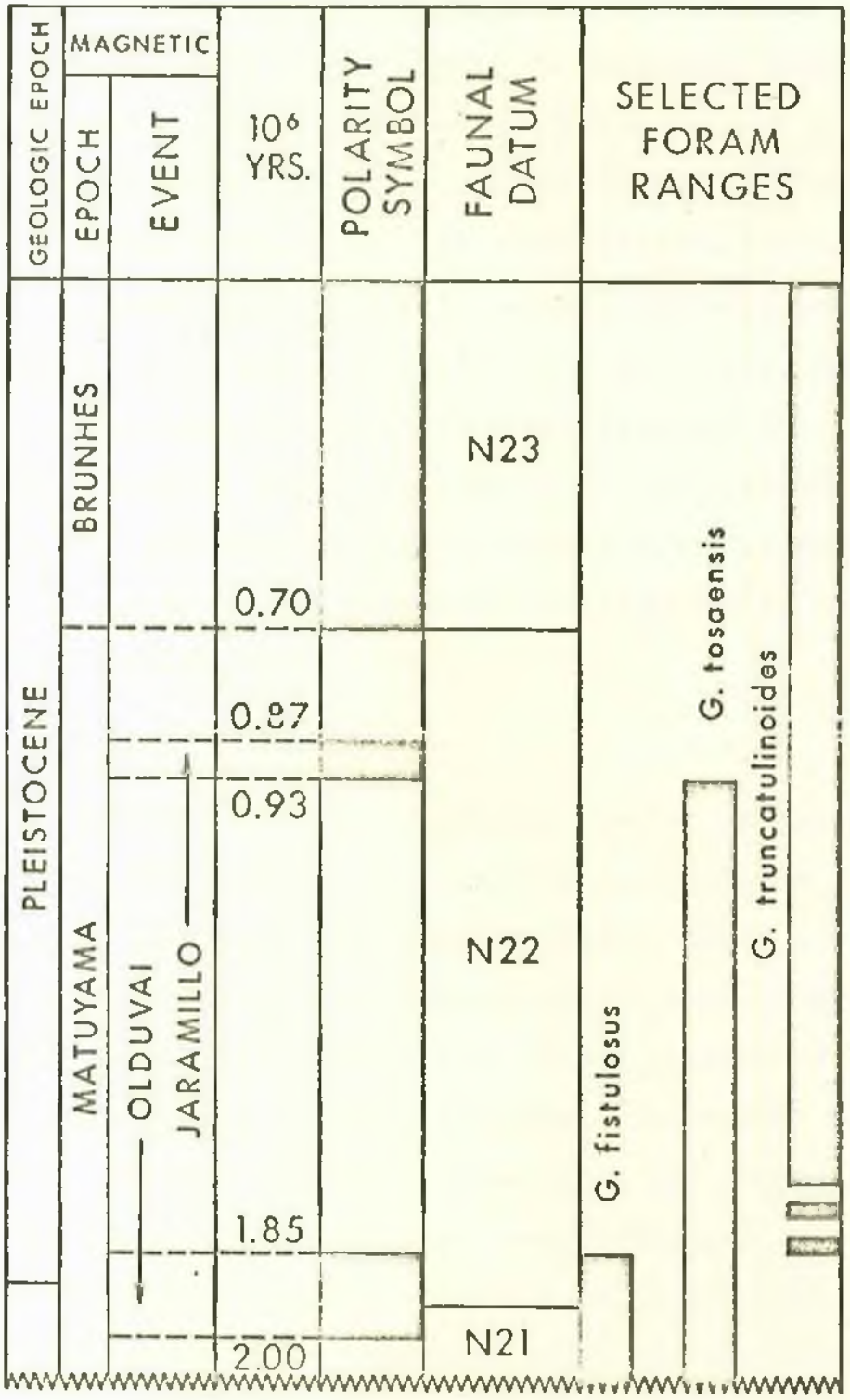

Figure 22. Pleistocene paleomagnetic and faunal chronostratigraphy. Paleomagnetic stratigraphy after Hays et al., 1969; faunal stratigraphy after Banner and Blow, 1965, and Blow, 1969.

use of the eastern equatorial Pacific stratigraphic nomenclature of Hays et al. (1969) is discussed under "Equatorial Pacific Pleistocene Correlations."

The supporting figure for core 68PC11 is different from the summary diagrams of the other Pleistocene cores in that the profiles of potential upwelling indicators for core 68PC11, i.e., phosphorous, calcium carbonate, and fine fraction, are compared to the fine fraction and the G. cultrata complex trends with depth in core 68PC16. The fine fraction variation is significantly and positively related to the G. cultrata complex oscillations in cores 68PC12, 15, and 16.

Intercore correlation

The frequency of the G. cultrata complex per gram greater than 246 μ is the most readily correlatable parameter in the investigated cores (Figure 23). A composite interpretation of these profiles reveals nine periods of negligible upwelling and eight periods of intensive production during the Brunhes, two cycles between the Brunhes and the top of the Jaramillo, and two to three cycles during the Jaramillo. An abrupt climatic amelioration in the vicinity of the Brunhes-Matuyama boundary is indicated in some core profiles, e.g., cores 68PC12 and 15.

A general curve for the Brunhes was created by averaging the midpoints of climatic stages and the stage

Figure 23. Intercore correlation using the frequency of the G. cultrata complex. Stratigraphic nomenclature after Hays et al., 1969; odd numbers denote conditions similar to present.

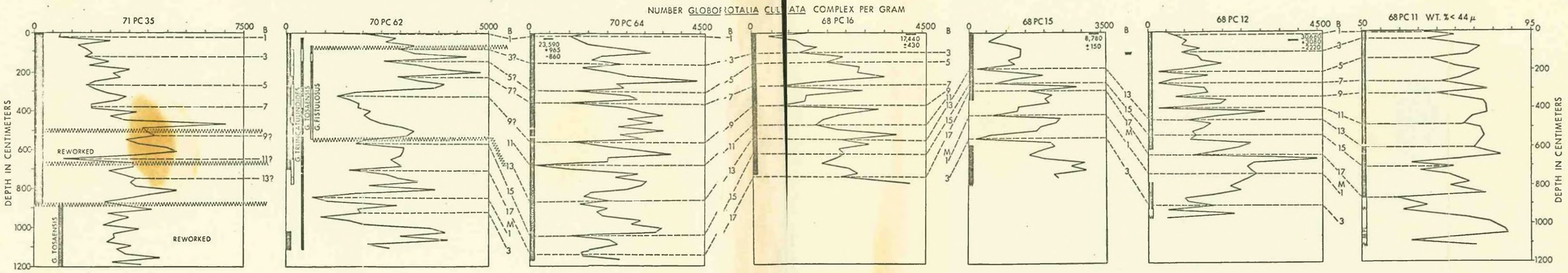
NUMBER GLOBOROTALIA CULTRATA COMPLEX PER GRAM
71 PC 35
70 PC 62
70 PC 64
68 PC 16
68 PC 15
68 PC 12
68 PC 11 WT. % < 44 μ
DEPTH IN CENTIMETERS
REWORKED
REWORKED
G. TOSAENSIS
G. TRUNCATULINOIDES
G. TOSAENSIS
G. FISTULOSUS
23,590 ±965 ±860
17,440 ±430
6,780 ±150

peak G. cultrata complex frequencies for the three continuous cores, 68PC12, 16, and 70PC64 (Figure 26). This graph is intended to present only the relative intensity and chronology of the upwelling cycles and does not include observations of detail. Thus, inconsistencies between relative peak heights and chronologies of the individual cores are smoothed over in this average model. This average chronology is combined in Table 8 with a qualitative summary description of the Brunhes paleoclimatic record compiled from the individual core characteristics with emphasis on the G. cultrata frequency oscillations. Paired, group, and total mean t-tests between interpreted cold and warm durations revealed no significant differences in climatic stage length.

Pre-Quaternary sediment properties and distribution

Ages of the oldest microfossils observed at 84 collection sites in the western equatorial Pacific from 160 to 180°E Longitude and 10°N to 10°S Latitude (Saito et al., 1971; Funnell, 1970; Riedel, 1971; Heath, 1968) have been plotted and contoured (Figure 24). Although the greater portion of the reported ages is based on microfossils that have been reworked into younger sediments, the existence of Oligocene fauna, for example, is evidence of the occurrence of in situ Oligocene sediments in the vicinity of the core (Riedel, 1967).

Table 8

Chronology, Periodicity and Characteristics of Average Brunhes Paleoclimatic Curve in the Western Equatorial Pacific

Unit	$t_1 - t_2$ ($\times 10^3$yrs.)	Midpoint ($\times 10^3$yrs.)	# GCC/g	Half-cycle ($\times 10^3$yrs.)	Whole cycle ($\times 10^3$yrs.)	Remarks*
B 1	0 - 11.5**	---	1124			
2	11.5- 84	48	2138			warmest cold
				56		
3	84 -124	104	1187		96	
				40		
4	124 -163	144	2944			
				37		
5	163 -199	181	1772		72	
				35		
6	199 -234	216	2646			longest cold
				32		
7	234 -261	248	1570		78	
				46		
8	261 -327	294	2696			
				49		
9	327 -348	343	876		83	
				34		
10	348 -396	377	3076			
				39		
11	396 -436	416	693		80	warmest warm
				41		
12	436 -478	457	3358			
				47		

Table 8. (Continued) Chronology, Periodicity and Characteristics of Average Brunhes Paleoclimatic Curve in the Western Equatorial Pacific

Unit	$t_1 - t_2$ ($\times 10^3$ yrs.)	Midpoint ($\times 10^3$ yrs.)	# GCC/g	Half-cycle ($\times 10^3$ yrs.)	Whole cycle ($\times 10^3$ yrs.)	Remarks*
13	478 -529	504	1858		87	least fluctuation
				40		
14	529 -559	544	2777			
				54		
15	559 -627	598	1388		97	
				43		
16	627 -656	641	2646			shortest cold
				31		
17	656 -688	672	1646		79	greatest fluctuation
				48		
18	688 -751	720	3397			coldest cold
			Average	42	84	

*Surface: warming trend surpassed only by B11 and B9. Wisconsin: warmest cold. Cold to warm G. cultrata complex ratio = 2:1.

**Accepted date of end of last glacial.

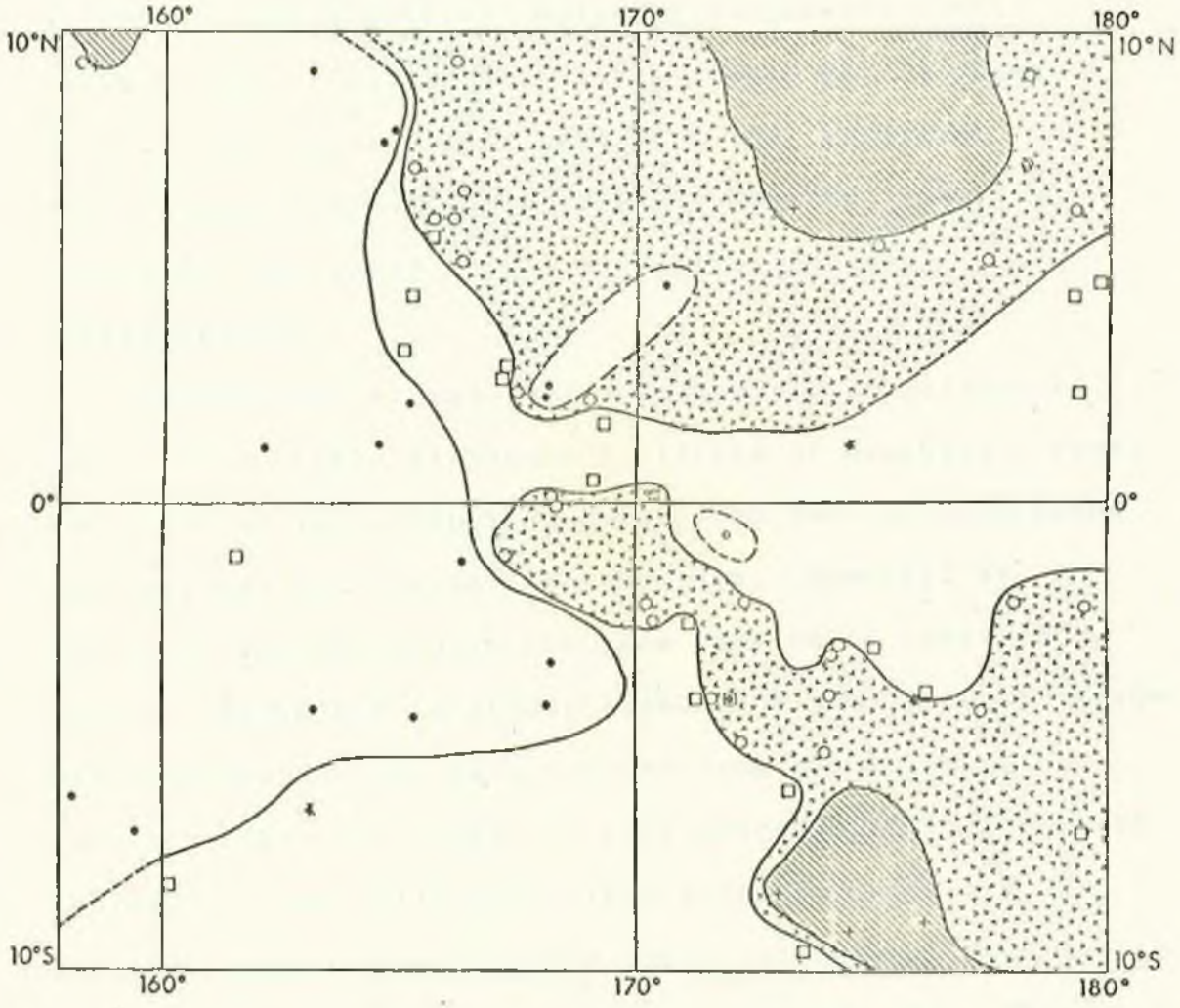

Figure 24. Distribution of oldest pre-Quaternary microfossils in samples collected in the western equatorial Pacific. + = Cretaceous; △ = Paleocene; O = Eocene; ★ = Oligocene; □ = Miocene; ● = Pliocene; patterns and contours serve to differentiate geographic age groupings.

The age pattern generally reflects sediment thinning to the east due to carbonate solution, and to the north and south of the equator due to lower biogenic production (cf. Figures 2, 3, and 5). The faunal ages were assigned numerical approximations following Berggren's (1971) Tertiary chronological boundaries (Table 9). Assigned absolute age shows significant ($P < .01$) positive correlations with distance from the equator, easterly longitude, and water depth, supporting the map interpretation.

Comparisons of physical and chemical properties of Cenozoic sediments in Hawaii Institute of Geophysics cores are necessarily qualitative due to the lack of sufficient measurements for statistical analysis. However, by comparing sediments from the same core or in cores from similar depths and locations (Table 10) some general trends and observations can be extracted from the meager data (see Appendix C for detailed core descriptions). Tertiary sediment is generally finer than that of Quaternary age, and the percent fine fraction tends to increase with age in cores older than the middle Miocene (Figure 25). This tendency of the fine fraction to increase with age is also indicated by a significant positive correlation of depth and fine fraction in core 68PC23. Bramlette (1958) and Heath (1968) have previously documented the predominance of nannofossils in pre-Pliocene sediments. Cores 68PC10, 19,

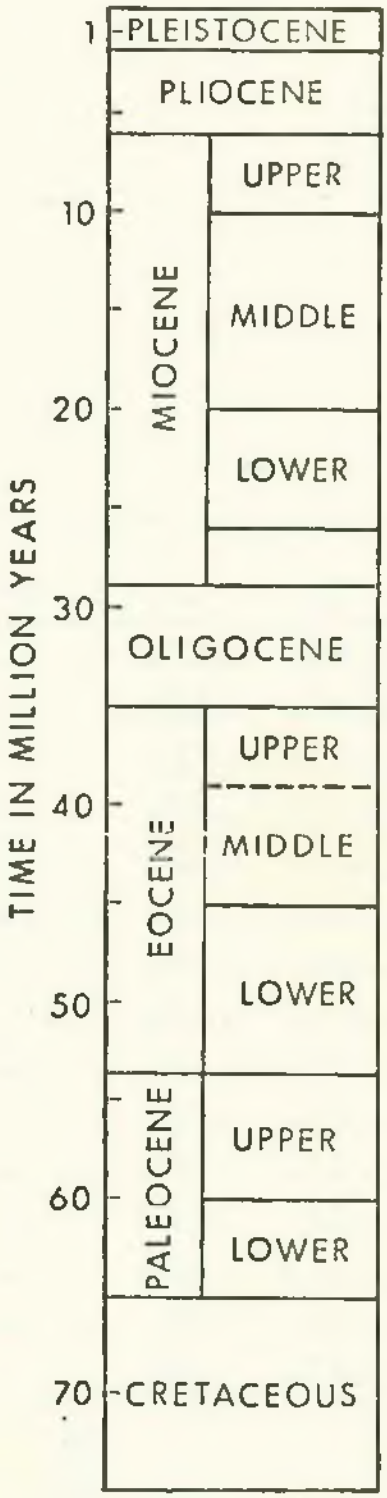

Table 9. Cenozoic chronology (after Berggren, 1971, Table 52.37).

Table 10

Statistical Parameters of Fossil Cores

Core	Depth (m)	Location	Series	No. of Observations	Parameter											
					P1	P2	P3	P4	P5	R1	R2	C44	C61	C124	PC	P
68PC23	3940	4°19.5'S 172° 3.9'E	Quaternary	2	64.0 62.0-66.0	5.1 4.8- 5.4	10.2 8.7-11.7	11.6 9.0-14.2	8.9 2.5-15.3	15.3 2.5- 26.8	0.26 0.20-0.32	35.8 33.8-37.7	30.7 28.4-33.0	20.5 16.7-24.3	93.5 93.0-93.9	
			Pliocene	14	67.6 52.1-80.8	39.0 2.4-13.3	6.8 0.6- 9.5	8.5 5.7-11.7	13.2 4.8-25.8	6.6 2.0- 16.0	0.29 0.11-0.40	32.4 19.2-47.8	28.5 11.8-46.9	21.7 11.7-35.3	93.1	
			Upper Miocene	3	89.4 86.8-93.1	2.0 1.3- 2.6	3.2 2.2- 3.8	3.0 1.9- 3.6	2.4 1.4- 3.3	42.9 26.7- 65.7	0.06 0.03-0.07	10.6 6.9-13.2	8.6 5.5-10.4	5.3 3.3- 6.9	91.8 87.5-93.1	
			Middle Miocene	4	66.0 53.9-73.3	10.2 4.1-21.4	8.6 7.9- 9.1	7.6 4.8-10.8	7.7 3.4-11.5	11.1 6.0- 21.8	0.18 0.09-0.25	34.1 26.7-46.1	23.8 16.3-29.1	15.2 8.3-19.9	90.5 87.6-92.5	
			Lower Miocene	2	73.6 72.7-74.1	4.9 4.1- 5.7	13.5 11.7-15.2	4.6 4.5- 4.7	3.6 1.6- 5.6	28.7 13.1- 44.3	0.09 0.06-0.11	26.6 25.9-27.3	21.7 21.6-21.8	8.3 6.4-10.1	79.4 68.9-90.4	
68PC21	3875	4°19.5'S 172° 3.9'E	Quaternary	14	60.3 45.8-71.4	4.7 1.6- 7.3	9.9 5.2-32.1	8.3 0.4-11.0	16.9 0.8-33.1	9.6 1.4- 81.1	0.36 0.01-0.73	39.7 28.6-54.2	35.1 24.7-49.9	25.1 1.2-42.0		
			Lower Pliocene	5	64.5 55.2-84.2	4.3 3.1- 5.5	9.4 7.5-11.8	10.8 4.8-13.5	10.9 0.1-17.4	56.2 3.2-264.0	0.29 0.05-0.44	35.5 15.8-44.8	31.1 12.7-40.3	21.7 5.1-30.6		
			Upper Eocene	6	82.8 74.0-87.4	2.3 2.9- 2.6	11.3 6.6-20.6	3.2 2.9- 3.5	0.3 0.2- 0.4	263.5 202.8-372.9	0.037 0.03-0.04	17.2 12.6-26.0	14.9 10.6-23.9	3.6 3.3- 3.7		
68PC20	2250	4°19.5'S 165°40.5'E	Quaternary	10	32.0 16.0-45.5	6.6 4.6- 1.2	15.5 9.9-32.6	15.8 12.0-23.9	30.0 22.2-42.1	1.11 0.54- 1.75	0.87 0.61-1.34	68.0 54.5-84.0	61.3 48.2-72.8	45.8 38.0-60.7		
			Lower Pliocene	11	54.8 48.6-60.1	9.0 7.7-10.3	13.6 11.2-16.3	10.4 9.3-12.9	12.1 9.4-14.8	4.6 3.4- 5.66	0.29 0.24-0.37	45.2 39.9-51.4	36.2 31.9-43.6	22.6 19.2-26.8		
68PC11	3900	0°50.8'S 162°01.5'E	Quaternary	31	78.2 59.3-86.9	4.4 1.8-22.6	5.9 3.5-12.9	6.0 3.3-16.4	9.0 3.2-26.4	12.2 2.5- 26.2	0.18 0.07-0.43	24.8 13.1-40.7	20.4 10.1-37.1	14.6 6.6-29.9	79.5 46.0-100.0	512.0 287.3-762.1
			Middle Pliocene	7	77.4 60.7-88.5	3.1 2.4- 3.7	9.0 5.4-14.1	7.9 3.0-21.4	2.6 0.3- 7.1	95.1 8.5-327.5	0.13 0.03-0.34	22.6 11.5-39.3	19.5 9.1-35.6	10.5 3.3-25.1	91.6 89.3- 95.3	573.0 476.4-762.1
63PC10	3350	6°26.0'S 158°17.0'E	Pliocene	19	45.6 37.7-61.7	9.9 6.4-27.1	11.1 8.3-15.4	13.1 6.9-17.2	20.2 13.4-35.9	2.4 1.1- 4.6	0.51 0.28-0.86	54.4 38.3-62.3	44.5 30.6-54.5	33.3 21.6-46.2	79.5 73.0- 87.9	
68PC27	5610	2°15.2'N 166°31.0'W	Pliocene ($CaCO_3$)	22	87.5 80.3-94.5	4.8 2.2-15.7	2.6 1.2- 9.5	1.8 0.9- 9.5	3.3 0.3-24.0	102.5 5.5-262.1	0.06 0.01-0.33	12.5 5.5-39.7	7.6 2.9-27.4	5.1 1.4-24.7	84.9 70.5- 88.7	532.1 322.3-777.6
			Pliocene (SiO_2)	3	69.5 62.1-83.1	7.1 13.0-10.1	9.5 3.9-11.4	9.1 3.7-12.2	2.9 2.2- 6.2	17.3 10.3- 28.2	0.16 0.11-0.22	30.5 16.9-37.9	23.4 13.9-29.6	13.9 10.0-18.2	4.1 3.6- 4.9	1076.6 430.8-1198.0

P1, 2, 3, 4, 5 = weight percent <44 μ, 44-61 μ, 61-124 μ, 124-246 μ, >246 μ
R1 = <44 μ/>246 μ
R2 = <124 μ/>124 μ
C44, 61, 124 = weight percent coarser 44 μ, 61 μ, 124 μ
PC = percent carbonate total
P = phosphorus in ppm

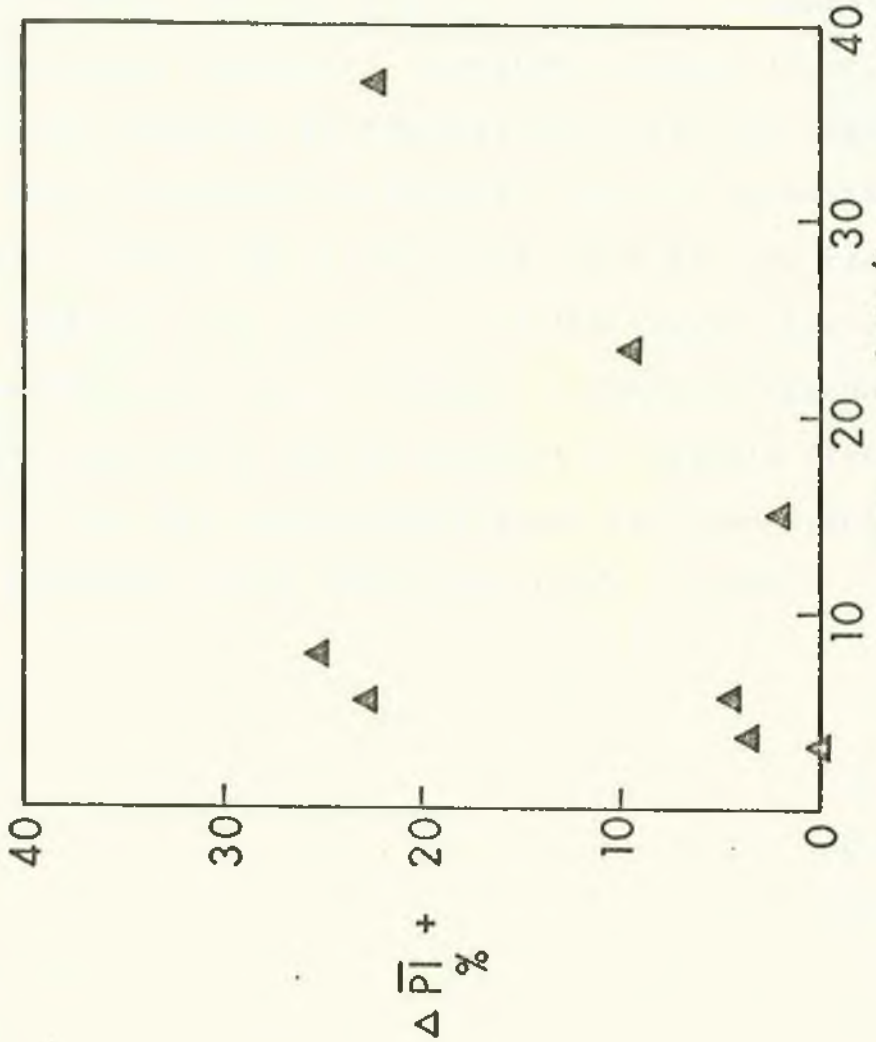

Figure 25. Percentage difference between Quaternary and pre-Quaternary fine fraction versus age.

and 20 contain Pliocene nannofossil ooze despite their positions well above the present foraminiferal compensation depth.

Calcium carbonate percentages of middle and upper Miocene sediments are equal to Quaternary sediments content, whereas lower Miocene sediment carbonate content is lower, and middle Pliocene higher, than that of comparable Quaternary sediments. Phosphate content is also higher in middle Pliocene, as compared to Quaternary sediment. A highly calcareous, apparently normally deposited, Pliocene core, 68PC27 (02° 15.2'N, 166° 31.0'W), was collected from a depth of 5610 m, well below the present carbonate compensation depth. Barring sediment or tectonic movement, this observation is in contrast to Heath's (1968) conclusion that the compensation depth has been within 200 m of its present depth since the middle Miocene.

DISCUSSION

Lysocline and compensation depth

Although the compensation depth is mapped on the basis of sediment calcium carbonate content, the lysocline, according to Berger (1968; 1970) must be defined in sediments by the concentration of resistant species of foraminifera. Depending on the initial composition of the sediment, a sample consisting entirely of calcium carbonate may have undergone more solution than one with a very small calcareous component. However, an examination of the mathematics of lysocline generation leads to the possibility of delineating a depth approximating the lysocline in nature and origin on profiles of sediment calcium carbonate content for a uniform sedimentary regime.

Consider the formula:

$$L = 100\ (1-R_o/R) \qquad \text{(Berger, 1971a)}$$

where L is the loss of sediment necessary to increase the insoluble fraction R_o to R percent. If R_o equals 5% and R equals 10%, loss L equals 50%, i.e., 50% of the sediment dissolved as the carbonate content decreased from 95 to 90%. In comparison, if R_o equals 50% and R equals 60%, loss L equals 17%. As the percentage of insoluble material approaches that of the calcareous component, the same amount of solution loss produces a greater percentage decrease of the soluble fraction. Thus, irrespective of actual solution

rate variations, an abrupt change in slope of calcite versus depth plots would occur where the amount of calcite becomes comparable to the non-calcareous fraction. Minimum dissolution loss in foraminiferal assemblages can be described by the same equation, if resistant forms are considered insoluble (Berger, 1971a). The solution index is formed by multiplying the species percentage by its solution rank, summing the products, and dividing by the average rank number. Because the solution indices are comparisons of resistant and non-resistant species, the lysocline can be thought of as a "compensation depth of easily destroyed species" (Berger, 1971a, p. 350).

The initial composition of the settling foraminiferal assemblage in the South Pacific is no more than 5% resistant species (Berger, 1971a), and the non-calcareous fraction of the shallowest samples in the investigation region also approaches 5%. The initial biogenic calcite rain and deep physico-chemical hydrographic structure are relatively uniform over the western equatorial Pacific. Samples containing anomalous amounts of non-calcareous material or exhibiting evidence of reworking have been excluded from the carbonate profile. Thus, the calcium carbonate and solution indice profiles for this relatively uniform sedimentary environment show a similar abrupt slope change in the vicinity of 3500 m (Figures 8 and 11a, b). The lysocline depth in the southeastern Pacific is also

consistent with the level of abrupt decrease of sediment calcium carbonate content in the equatorial Pacific (Berger, 1971a). Of course, wherever the two initial insoluble fractions are disparate, the profile horizons would not be coincident.

It must be emphasized that the concept of the sedimentary lysocline as a measurable boundary produced by a hydrographic dissolution rate change (hydrographic lysocline) is open to some question. In fact, marked dissolution occurs at depths as shallow as 3000 m in the equatorial Pacific (Berger, 1971a). Tentative associations by Berger (1968) of the sedimentary lysocline and actual levels of water column solution rate increases documented by Peterson (1966) and Berger (1967) remain unsupported.

The extrapolated compensation depth of 5250 m for the western equatorial Pacific is similar to previous reports for the central equatorial Pacific, whereas the lysocline depth of 3500 m is at the shallower end of the range of previous data for the equatorial Pacific. The depth and sharpness of the compensation level depend on the rate of supply of calcium carbonate, the hydrographic lysocline depth, and the slope of the dissolution rate curve below the lysocline (Heath and Culberson, 1970). The general pattern of the lysocline is primarily controlled by the mass balance of calcium carbonate (Broecker et al., 1968), thermodynamics (Sillen, 1967), and deep circulation

(Berger, 1970), but areally variable rates of surface production of organic carbon supposedly alter this general pattern (Heath and Culberson, 1970; Berger, 1970). Increased surface production would both raise the lysocline by supplying more oxidizable organic matter for carbon dioxide formation and depress the compensation depth by supplying more calcareous tests (Heath and Culberson, 1970). However, Kroopnick (1971) reports that oxygen consumption is not limited by a lack of carbon. Most of the dissolved oxygen is probably consumed in the oxidation of organic matter to form carbon dioxide which, in turn, increases the undersaturation of the water with respect to calcium carbonate. If oxygen consumption in the formation of carbon dioxide is limited by kinetics rather than by a lack of carbon, local lysocline depth may not be greatly affected by surface productivity.

Surface production in the area of investigation is less than 100 $mgC/m^2/day$ as compared to a range of 100-250 $mgC/m^2/day$ for the eastern equatorial Pacific (Koblentz-Mishke, 1970, Fig. 1). If the inverse relation of production and these calcium carbonate profile boundaries is also correct, and if surface production is a locally dominant controlling factor, the lysocline should be deeper and the compensation depth shallower in the western equatorial Pacific as compared to the eastern equatorial Pacific. A greater interval between the lysocline and the

compensation depth coupled with lower production in the western equatorial Pacific contradicts this hypothesis. The biological, physical, and chemical processes leading to local hydrographic and sedimentary lysocline depth variations obviously require further elucidation.

A linear dissolution rate increase below the lysocline as postulated by Heath and Culberson (1970) is perhaps inconsistent with the observed percent calcium carbonate profile (Figure 8a). A non-linear dissolution rate increase is also supported by Berger's (1967) findings of successive doublings of foraminiferal ooze weight loss between 2750 and 5250 meters. However, Heath and Culberson's model assumes that all dissolution occurs at the depth of deposition. Actually, the biogenic particles may undergo some dissolution during settling (Peterson, 1966), thus possibly accounting for the discrepancy between the theoretical and observed profiles.

Size fractions

Disregarding slumping and turbidity flows, the grain size of the carbonate fraction of a pelagic sediment is a function of its original biogenic constituents and dissolution history. The less than 44 μ fraction exhibits a high positive correlation with depth, and Figure 9 confirms that a dominant solution effect above 4000 m is the fragmentation of particles coarser than 44 microns.

Berger (1967) has also found that in foraminiferal ooze, preferential fragmentation of larger (greater than 125 μ) specimens tends to increase the finer fraction weight percentage. The calcareous particles greater than 246 μ show greater resistance to solution than the other size fractions (Figure 8b), presumably due to the greater resistance of some species of large foraminifera e.g., P. obliquiloculata.

Since the weight percent of the greater than 246 μ fraction is composed almost entirely of foraminifera, the linear trend with depth of this parameter (Figure 10c) indicates its potential use as a solution index within a particular core, although climatically induced ratio variations in the production of large foraminiferal tests and coccoliths may confuse the interpretation. Similarly, anomalous values for this fraction or for the less than 44 μ fraction in surface sediment for a given depth may indicate Recent tectonic or sediment movements.

Equatorial Pacific correlation

Figure 26 is a correlation diagram for core 68PC12 from this work and published cores from the eastern equatorial Pacific. This correlation is possible with known paleomagnetic stratigraphy for cores V24-58, 59, 62, and RC11-209 (Hays et al., 1969), a previous correlation of cores RC11-209 and SDSE 58 (Hays et al., 1969), Olausson's

Figure 26. Equatorial Pacific core correlations. Stratigraphic nomenclature after Hays et al., 1969. Even numbers denote glacial stages.

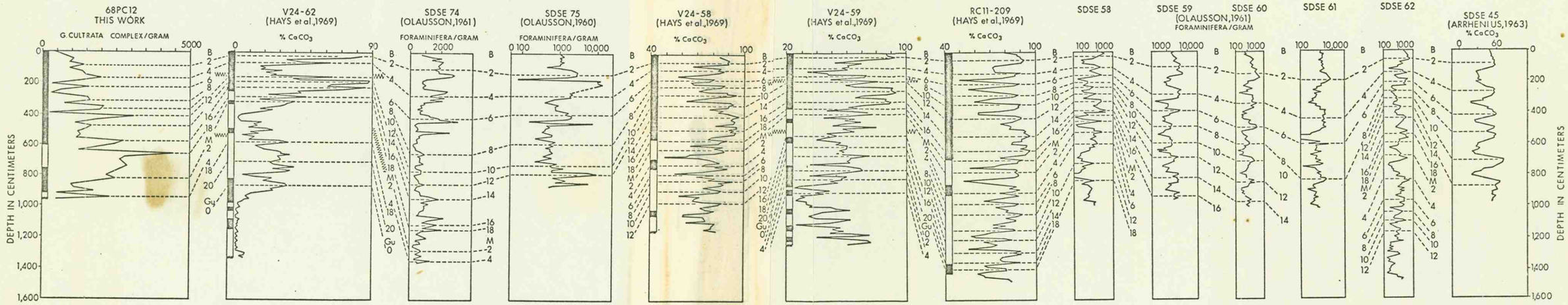
68PC12
THIS WORK
G. CULTRATA COMPLEX/GRAM
0
5000
V24-62
(HAYS et al.,1969)
% CaCO3
0
90
SDSE 74
(OLAUSSON,1961)
FORAMINIFERA/GRAM
0
2000
SDSE 75
(OLAUSSON,1960)
FORAMINIFERA/GRAM
0 100
1000
10,000
V24-58
(HAYS et al.,1969)
% CaCO3
40
100
V24-59
(HAYS et al.,1969)
% CaCO3
20
100
RC11-209
(HAYS et al.,1969)
% CaCO3
40
100
SDSE 58
100 1000
SDSE 59
(OLAUSSON,1961)
FORAMINIFERA/GRAM
1000 10,000
SDSE 60
100 1000
SDSE 61
100 10,000
SDSE 62
100 1000
SDSE 45
(ARRHENIUS,1963)
% CaCO3
0
60
DEPTH IN CENTIMETERS
0
200
400
600
800
1,000
1,200
1,400
1,600
B
M
Gu

(1960; 1961) faunal correlations of cores SDSE74 and 75 and cores SDSE58, 59, 60, 61, 62, and 74, and Arrhenius' (1963) faunal and paleoclimatic comparison of cores SDSE60 and 45 (see Table 11 for core depths and locations).

Hays et al. (1969) compared the paleomagnetically controlled carbonate percentage stratigraphy of V24-58 to RC11-209 and V24-59 to V24-62 in separate illustrations. These authors used an identifying letter for the paleomagnetic polarity epoch and sequential odd numbers to define interglacial stages (low carbonate percentage) within each epoch. I have correlated the four cores on the basis of these illustrations, using the same stratigraphic nomenclature and emphasizing the glacial stages as even numbers.

Hays et al. (1969) also delineated the correlative horizons in RC11-209 and SDSE-58 by comparing the carbonate oscillations and faunal stratigraphy. The abundance of Sphaeroidinella dehiscens decreases abruptly at the Brunhes-Matuyama boundary, as does the calcium carbonate percentage. This level is correlated with the same parameter changes in SDSE58 and 62. A second correlative datum is the disappearance of Pterocanium prismatium just above the top of the Olduvai event.

Equivalent numbers of cycles between the surface and paleomagnetic reversal horizons permit a tentative peak-by-peak correlation of the G. cultrata complex frequency in

Table 11

Equatorial Pacific Core Locations
(Arrhenius, 1952; Hays et al., 1969)

Core	Depth (m)	Latitude	Longitude
SDSE 58	4440	6°44'N	129°28'W
SDSE 59	4370	3°05'N	133°06'W
SDSE 60	4540	1°35'N	134°57'W
SDSE 61	4475	0°06'S	135°58'W
SDSE 62	4510	3°00'S	136°26'W
SDSE 45	3725	7°40'N	106°21'W
RC11 209	4400	3°39'N	140°04'W
V24 58	4490	2°16'N	141°40'W
V24 59	4662	2°34'N	145°32'W
V24 62	4834	3°04'N	153°35'W

core 68PC12 and the carbonate percentages in core RC11-209. Both cores show eight cycles in the Brunhes normal epoch, two between the Brunhes-Matuyama boundary and the top of the Jaramillo event, and one to two during the Jaramillo. Near-surface C^{14} dates in both cores add assurance to the Brunhes correlation. However, the cycles do not exhibit the same sequence of amplitude and durations. This discrepancy may be due to the use of different sedimentary parameters.

Olausson (1960; 1961) correlated the profiles of the number of entire foraminifera per gram greater than 150 μ in cores SDSE74 and 75 and in cores SDSE58, 59, 60, 62, and 74 by delineating equivalent horizons in the size distribution of Coscinodiscus nodulifer and the trends of Globigerina, Globorotalia, Pulleniatina, and Sphaeroidinella species (Table 12). The percentage carbonate curves correspond very well to the distribution of foraminifera number (Olausson, 1961) and permit correlation of core RC11-209 horizons to Olausson's (1961) stratigraphy via core SDSE58. Olausson's (1961) stratigraphic nomenclature corresponds to glacial maxima (high foraminifera number) except for i-1 (an extensive interglacial with minor cold phases) and a-d (faunal horizons totally unrelated to climate).

Arrhenius (1963) has compared cores SDSE60 and 45 mainly by the sequence of carbonate fluctuations. I have matched the carbonate peaks in core SDSE60 with those of

Table 12

Comparison of Equatorial Pacific Pleistocene Stratigraphies

SDSE58

Hays et al. (1969) SDSE58	Arrhenius (according to Hays et aI., 1969) SDSE58	Arrhenius (1963) SDSE60 **	Arrhenius (1952; according to Funnel, 1970) SDSE62	Olausson (1961) SDSE60 **
B 2	2	2.2	2.2	o three peaks in foraminifera content, Globergerina and size of C. nodulifer
4	6	4.2, 4.4		n
6	8	6	4.2	m
			4.4	
8	10	8.2, 8.4,8.6		1 minimum of Globigerina;
10	12	10		k discontinuity of S. dehiscens
			8.3	
12	14	12.2,12.4		i
			8.4	
14	16	14.2		h increase in Pulleniatina
			8.6	
16	18			g peak of Globigerina
18				
			12.2	
			12.4	

Table 12. (Continued) Comparison of Equatorial Pacific Pleistocene Stratigraphies

SDSE58

Hays et al. (1969) SDSE58	Arrhenius (according to Hays et al., 1969) SDSE58	Arrhenius (1963) SDSE60 **	Arrhenius (1952; according to Funnel, 1970) SDSE62	Olausson (1961) SDSE60 **
M 2			(e) f	peak of Globorotalia
4			e	peak of Globigerina
8			*d	maximum of Pulleniatina
12			*c	peak of Globorotalia
16			*b	minimum of Sphaeroidinella
18			*a	peak of Globorotalia

*These horizons are approximately equivalent in stratigraphic position to the Matuyama carbonate peaks in core SDSE58 but do not in themselves identify glacial maxima.

**Arrhenius' and Olausson's horizons are correlated with Hays et al. climatic stratigraphy on the basis of peak definition but are not exactly synchronous.

Olausson's foraminifera frequencies which were previously related above using core SDSE58 (Olausson, 1961) to core RC11-209 (Hays et al., 1969). Thus the Brunhes stratigraphy of Hays et al. (1969) can be extended to core SDSE45. Hays et al.'s (1969) correlation of Arrhenius' stratigraphic nomenclature and their own for core SDSE58 is incorrect according to this comparison of Olausson's (1961) and Arrenhius' (1963) labels for core SDSE60, and their extension to core SDSE58.

The Swedish Deep Sea Expedition cores have also been correlated by Emiliani (1967). He used the size distribution of C. nodulifer and found generally good agreement with Olausson between cores SDSE58, 59, and 60, but not between cores SDSE60 to 61 nor between cores SDSE58 to 62. According to Olausson's stratigraphy for core SDSE61, Emiliani's second datum should be at approximately 625 cm in this core and at approximately 1400 cm in core SDSE62. Funnell's (1970) placement of the Plio-Pleistocene boundary at or just below 1170 cm in core SDSE62 (M12) is in general agreement with my correlation. M12 occurs just at the top of the Olduvai event in core V24-58. The Plio-Pleistocene boundary in deep-sea cores is commonly thought to occur within this event (Funnell, 1970). Funnell (1970) also published a comparison of Arrhenius' and Olausson's stratigraphic nomenclature for core SDSE58, but this correlation is not coincident with my analysis (Table 12).

The correlations are considered firm for the Brunhes epoch and somewhat questionable below the Brunhes-Matuyama boundary. In many of the cores, the oscillating parameter ceases its regularity below this horizon and distinctions of significant fluctuations become difficult. Hays et al. (1969) illustrated sparse stratigraphy below this boundary, and my additional specific correlations are conjecture based on numbers of cycles alone.

The fact that climatically related fluctuations in sedimentary parameters can be correlated oceanwide in the equatorial Pacific supports Arrhenius' (1952) theory of global atmospheric and oceanic circulation effects of glacial oscillations. Although comparative intensities of glacials and interglacials are not clearly discernible, especially in the SDSE cores, the correlation establishes eight major perturbations in the equatorial pelagic sedimentary record in the last 7×10^5 years and a general increase in curve amplitude in the vicinity of the Brunhes-Matuyama boundary. Oscillations in the parameters continue into the Matuyama and for that matter into the Tertiary (Hays et al., 1969), but are not to be considered *prima facie* evidence of glacial effects. Hays et al. (1969) reported eleven carbonate peaks (glacial stages) from the bottom of the Brunhes to the top of the Olduvai and prominent troughs at the top of the Gauss (cores V24-59 and V24-62). Two peaks appear in the upper Gauss, but below

the middle of the Gauss the carbonate decreases to its lowest level and remains generally low into the upper Gilbert, although core V24-59 exhibits a rise below the Gilbert "a" event.

An apparent cooling prior to the Brunhes-Matuyama boundary is indicated by a general increase in carbonate content and sedimentation rate between the Jaramillo and Olduvai events (Hays et al., 1969). Olausson (1961) recognizes his horizon 1 (M4) as a boundary of a great climatic change with declining temperatures above. The climatic stratigraphy from the western equatorial Pacific appears to indicate a warming trend across the Brunhes-Matuyama boundary by decreases in the frequency of the G. cultrata complex. Unfortunately, the cores are not temporally long enough to provide a sufficient comparative record below the Brunhes-Matuyama boundary and this anomalous result is speculative only. It is possible that the concentration of the G. cultrata complex is dependent on production-solution relations in such a manner as to only appear to indicate a warming. Actually, an increased production rate above any hypothetical level may produce reduced frequencies of the G. cultrata complex by dilution with other, proportionately more productive, species. Kennett (1966) also observed that climates were cooler between 1.2×10^6 and 5×10^6 yrs. B.P. than later in the Brunhes. Certainly there is a warming trend for the western

equatorial Pacific indicated within the Brunhes itself by many parameters.

A half-cycle, climatic-stage transition midpoint to transition midpoint chronology has been determined for equatorial Pacific Pleistocene events by averaging the chronologies of the continuous cores (Table 13). In cores lacking independent absolute age control, the Brunhes-Matuyama boundary was determined by its established coincidence with the interglacial B17. All the chronologies are based on extrapolated sedimentation rates calculated from this datum. The half- and whole-cycle durations recorded in the correlated equatorial Pacific cores agree with the average for the western equatorial Pacific (Table 8) for the Brunhes epoch. The half-cycle durations in the late Matuyama are about 20×10^3 years longer than those of the Brunhes.

Pacific-wide correlations

A number of marine paleoclimatic stratigraphies have been published for the Pacific Ocean. Kennett (1970) reported six climatically induced alterations in planktonic foraminiferal fauna in 7×10^5 years for subantarctic water and a total of eight in the last $1.2\text{-}1.3 \times 10^6$ years. The magnitude of the warmings was greater during the last 5×10^5 years B.P. than from 5×10^5 to $1.2\text{-}1.3 \times 10^6$ years B.P. Warmer waters than present existed 4 to 5×10^4 years B.P.

Table 13

Equatorial Pacific Pleistocene Chronostratigraphies
(Cores 68PC12, SDSE58, 59, 62, 74, V24-58, RC11-209)

Unit	$t_1 - t_2$ ($\times 10^3$ yrs.)	Midpoint ($\times 10^3$ yrs.)	t Half Cycle ($\times 10^3$ yrs.)	t Full Cycle ($\times 10^3$ yrs.)	
B 2	11- 12*- 92	51			longest cold
			62		
3	92- 133	113		110	
			48		
4	133- 189	161			
			45		
5	189- 222	206		76	
			31		
6	222- 251	237			shortest cold
			36		
7	251- 295	273		78	
			42		
8	295- 334	315			
			38		
9	334- 371	353		71	
			43		

Table 13. (Continued) Equatorial Pacific Pleistocene Chronostratigraphies

(Cores 68PC12, SDSE58, 59, 62, 74, V24-58, RC11-209)

Unit	$t_1 - t_2$ ($x10^3$ yrs.)	Midpoint ($x10^3$ yrs.)	t Half Cycle ($x10^3$ yrs.)	t Full Cycle ($x10^3$ yrs.)	
10	371- 421	396			
			36		
11	421- 442	432		69	shortest warm
			33		
12	442- 488	465			
			49		
13	488- 540	514		97	longest warm
			48		
14	540- 584	562			
			46		
15	584- 632	608		89	
			43		
16	632- 669	651			
			40		
17	669- 712	691		76	
			36		
18	712- 742	727			

Brunhes Average

t Half Cycle ($x10^3$ yrs.)	t Full Cycle ($x10^3$ yrs.)
42	83

Table 13. (Continued) Equatorial Pacific Pleistocene Chronostratigraphies

(Cores 68PC12, SDSE58, 59, 62, 74, V24-58, RC11-209)

Unit	$t_1 - t_2$ ($\times 10^3$ yrs.)	Midpoint ($\times 10^3$ yrs.)	t Half Cycle ($\times 10^3$ yrs.)	t Full Cycle ($\times 10^3$ yrs.)
M 1	742- 774	758		73
			42	
2	774- 826	800		
			52	
3	826- 878	852		129
			77	
4	878- 979	929		
			97	
5	979-1072	1026		183
			86	
6	1072-1151	1112		
			56	
7	1151-1186	1168		

Matuyama Average

t Half Cycle ($\times 10^3$ yrs.)	t Full Cycle ($\times 10^3$ yrs.)
68	128

*Accepted date of end of last glacial.

Blackman and Somayajulu (1966) divided core DWBG114 from the southeastern Pacific (18°20'S, 79°21'W; 3090 m) into five faunal intervals with the aid of vector analysis. Three warmings are evident in little more than 2×10^5 years. Hays et al.'s (1969) findings of eight major climatic oscillations in the eastern equatorial Pacific during the last 7×10^5 years have been discussed as have the similar results from the western equatorial Pacific.

Variations in ice-rafted debris (weight percent of the grain size fraction greater than 250 μ) revealed eleven periods of increased ice rafting in the North Pacific during the last 1.2×10^6 years (Kent et al., 1971). Only four cooler periods are recognized between 1.2 and 2.5×10^6 yrs. B.P. with a general cooling trend beginning about 1.2×10^6 yrs. B.P. and becoming markedly intense between 8.7 and 7×10^5 yrs. B.P. Eight to nine zones of increased ice-rafted sediment during the Brunhes normal are apparent from their general curve (Figure 27). A marked interglacial stage occurred between 4.6 to 5.3×10^5 yrs. B.P.

Herman (1970) illustrated an Arctic core (T3-67-11, 79°34.9', 172°30') with seven to possibly eight periods of very low faunal content (interglacial stages) in 7×10^5 yrs. B.P. Her cores demonstrate an Arctic Ocean free of permanent pack-ice up to 7×10^5 years ago and subsequent development of alternating ice-covered and ice-free conditions. She hypothesized that the "cold" peaks

Figure 27. Pacific-wide Pleistocene stratigraphic correlations and comparison with North American terrestrial and equatorial Atlantic and Caribbean stratigraphies. Stratigraphic nomenclature after Hays et al., 1969. Even numbers denote glacial stages.

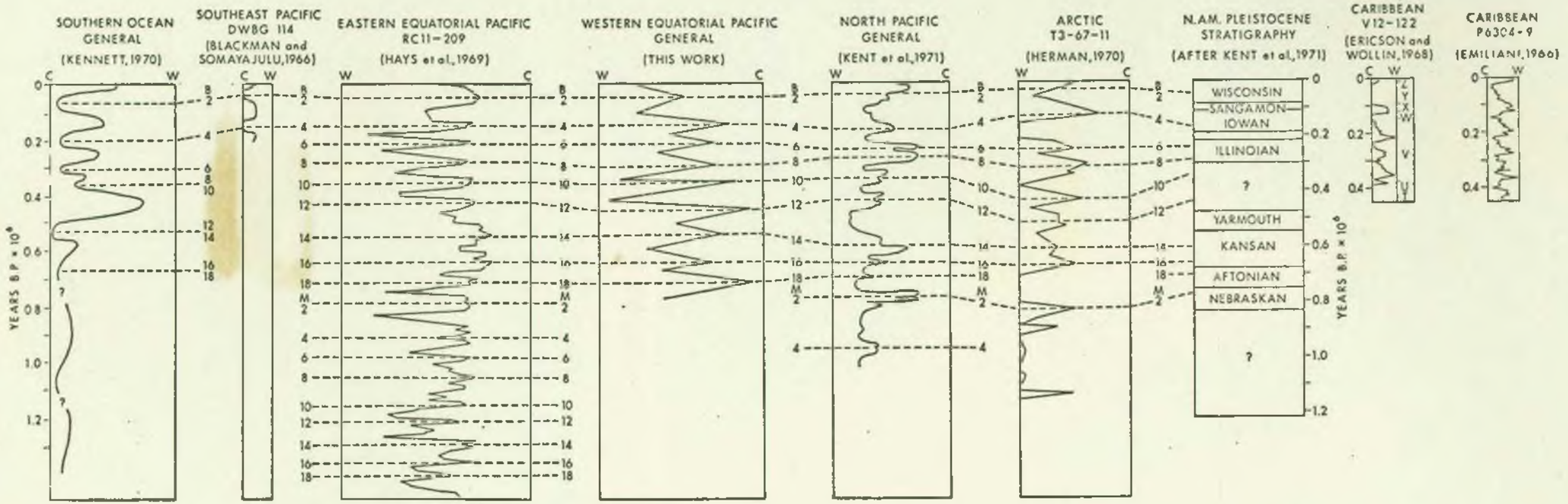
SOUTHERN OCEAN
GENERAL
(KENNETT, 1970)
SOUTHEAST PACIFIC
DWBG 114
(BLACKMAN and
SOMAYAJULU, 1966)
EASTERN EQUATORIAL PACIFIC
RC11-209
(HAYS et al., 1969)
WESTERN EQUATORIAL PACIFIC
GENERAL
(THIS WORK)
NORTH PACIFIC
GENERAL
(KENT et al, 1971)
ARCTIC
T3-67-11
(HERMAN, 1970)
N.AM. PLEISTOCENE
STRATIGRAPHY
(AFTER KENT et al, 1971)
WISCONSIN
SANGAMON
IOWAN
ILLINOIAN
?
YARMOUTH
KANSAN
AFTONIAN
NEBRASKAN
?
CARIBBEAN
V12-122
(ERICSON and
WOLLIN, 1968)
CARIBBEAN
P6304-9
(EMILIANI, 1966)
YEARS B.P. × 10⁶

(foraminifera-rich zones) actually represent mild glacials, i.e., conditions similar to present, because no sediment record would be left during complete cover with pack-ice. Thus this core represents an extreme example of the danger in applying average sedimentation rates to sections including glacial-interglacial oscillations (Broecker et al., 1958).

Absolute dating, especially paleomagnetic stratigraphy, allows the tentative correlation of these stratigraphies (Figure 27). The chronostratigraphy of the western equatorial Pacific agrees well with the interpretation of vector faunal analysis in the southeastern Pacific (Blackman and Somayajulu, 1966), carbonate cycles in the eastern equatorial Pacific (Hays et al., 1969) and cycles of ice-rafted debris in the North Pacific (Kent et al., 1971) (Table 14). The latter two schemes and this work exhibit five cold periods in the last 400 x 10^3 years. Atlantic G. cultrata complex (core V12-122, Ericson and Wollin, 1968) and O^{18}/O^{16} (P6304-9, Emiliani, 1966b) paleoclimatic stratigraphies also show five temperature minima in 400 x 10^3 yrs. (Figure 27). These specific cores were chosen for comparison with Pacific chronostratigraphies instead of the general schemes of the cited authors because of recent reevaluation of the chronology of core V12-122 and a previous paleoclimatic correlation of this core with core P6304-9 (Hays et al., 1969). It is remarkable that the

Table 14

Pacific Pleistocene Chronostratigraphies

Unit	Southern Ocean	Southeastern Pacific	Eastern Equatorial Pacific	Western Equatorial Pacific	North Pacific	Arctic
B 2	102*	68	85	84	80	25-70**
3	160	125	130	124	140	80
4	235	150	165	163	185	130
5	275		200	199	220	220
6	320		230	234	241	245
7	345		260	261	258	280
8	?		300	327	281	340
9	?		345	358	320	400
10	390?		380	396	360	440
11	475		410	436	400	480
12	?		445	478	440	525
13	?		505	529	540	595
14	565?		565	559	600	620

Table 14. (Continued) Pacific Pleistocene Chronostratigraphies

Unit	Southern Ocean	Southeastern Pacific	Eastern Equatorial Pacific	Western Equatorial Pacific	North Pacific	Arctic
15	610		620	627	638	645
16			660	656	660	685
17			700	688	685	
18			735	751	710	
M 1			765		760	
2			815		820?	
3			870			
4			930			
5			975			
6			1000			
7			1035			
8			1100			
9			1140			

*Beginning of unit from midpoint of climatic transition, x 10^3 yrs.
**Range of extrapolated sedimentation rate age to absolute age in other Arctic cores.

same conclusion was reached for different geographic areas using different techniques. Moreover, Hays et al. (1969) claims synchroneity of climatic change in the eastern equatorial Pacific and the Atlantic for the last 400 x 10^3 yrs. B.P. although Kent et al., 1971) emphasize the lack of agreement between their scheme and Ericson and Wollin's (1968) prior to this time. This work also supports interocean low-latitude synchroneity of climatic change during the last 400 x 10^3 yrs. B.P.

The north Pacific stratigraphy has been correlated to North American terrestrial stratigraphy by three tie-in points (Figure 27). Following this reasoning for the western equatorial Pacific general curve, the beginning of the Wisconsin at about 80 x 10^3 yrs. B.P. (Broecker and van Donk, 1970) is correlated to the beginning of the first high peak of the G. cultrata complex (84 x 10^3 yrs.). Another correlation is the low frequency just above the Brunhes-Matuyama boundary and a Cromerian (Mindel-Gunz) geomagnetic field reversal (van Montfrans and Hospers, 1969; Noltimier, 1967). The marked climatic change at about 7 x 10^5 yrs. B.P. may also correlate with the Sherwin Till underlying the 7 x 10^5 yrs. old Bishop Tuff in the Sierra Nevada (Dalrymple et al., 1965) and the Gokenya cold period in Japan (Ishida et al., 1969; Kent et al., 1971). The third tie-in is the extreme low frequency between 436 and 396 x 10^3 yrs. B.P. and the Mindel-Riss interglacial dated

at 430 x 10^3 yrs. B.P. (Evernden et al., 1964). The most intense interglacial is B11 in this work and B13 (460-530 x 10^3 yrs. B.P.) in the general curve of Kent et al. (1971), according to their correlation with Hays et al.'s (1969) core RC11-209. However, both units fall within the age range of the Mindel-Riss (Great Interglacial) of Zeuner (1959). Kennett (1970) also recognized a warmer-than-present interglacial in his Globorotalia inflata zone between 400-500 x 10^3 yrs. B.P.

Because the correlations are with European stratigraphies, "classical" European nomenclature is used in the discussion with the tentative North American classical equivalents given in parenthesis. It must be noted that the extrapolation of local terrestrial stratigraphic nomenclature to other terrestrial or marine sequences is, at present, speculative (Emiliani and Flint, 1963). The Cromerian (Aftonian) occurs between the Gunz (Nebraskan) and Mindel (Kansan) Glacials whereas the Great Interglacial (Yarmouth) occurs between the Mindel (Kansan) and Riss (Illinoian). Correlations between the Riss and the Wurm (Wisconsin) are difficult since terrestrial sequences show three glaciations whereas five cooler periods are indicated by the frequency of the G. cultrata complex.

An interesting Czechoslovakian loess sequence exhibits seven to eight complete cycles in the Brunhes geomagnetic epoch (Bucha et al., 1969; Kukla, 1969; Hays et al., 1969).

Similarly, the "classical" sequence in the Alps exhibits at least nine temperature minima from the Gunz through the Wurm (summary in Emiliani and Flint, 1963). Certainly, the application of the concept of four classic glaciations to Pleistocene theory must be reconsidered in the light of growing marine and terrestrial evidence of about eight climatic cycles in the last 7×10^5 years.

An intense climatic deterioration is recorded at 7 to 8.7×10^5 yrs. B.P. in the north Pacific and at 6.8×10^5 yrs. B.P. in the eastern equatorial Pacific. A climatic amelioration beginning approximately 7×10^5 yrs. B.P. is indicated for the western equatorial Pacific. The trend of climatic change was initiated greater than 1.2×10^6 yrs. B.P. in the North Pacific. Evidence for a marked climatic change in the period from 0.7 to 1.2×10^6 yrs. B.P. is widespread in the oceanic record (Berggren et al., 1969; Hays, 1965; Hays and Opdyke, 1967). The oceanic record combined with terrestrial evidence (Selli, 1967; Sharp, 1968) indicates the advent of continental glaciation in temperate latitudes at 0.7 to 1.2×10^6 yrs. B.P. (Hays and Berggren, 1970) and supports the concept of a Pleistocene division into pre-glacial and glacial portions.

Of three high stands of the sea isotopically dated in Alaska at 78-100, 170-175, and $210\text{-}224 \times 10^3$ yrs. B.P. (Karlstrom, 1965), the first two fall within the ranges of the last two interglacials as recorded in the western

equatorial Pacific. There is less agreement between Th^{230}/U^{234} dated terrace levels on Barbados (Mesollella et al., 1969) and this work. High sea-stands (interglacials) are reported at 82, 105, 125, and 175-230 x 10^3 yrs. B.P. and a low stand at 130-170 x 10^3 yrs. B.P. The first and the second high stands approximate B3 (84-124 x 10^3 yrs. B.P.); the third interglacial is partially equivalent to B5 (163-199 x 10^3 yrs. B.P.), and the glacial is chronologically equivalent to B4 (124-163 x 10^3 yrs. B.P.). Mesollella et al. (1969) cite these terrace dates as supporting evidence of the astronomical theory of climatic change--if Broecker's (1966) curve emphasizing precession over tilt is used.

In the western equatorial Pacific, the average duration for both warm and cold stages (calculated between climatic transition midpoints) is about 42 x 10^3 yrs., and the average complete cycle duration is about 84 x 10^3 years. The latter figure approximates the 75 x 10^3 yrs. reported for the last five cycles in the eastern equatorial Pacific (Hays et al., 1969), although specific differences in cycle durations are not coincident with the author's data. The half- and whole-cycle period durations also correspond to those reported by Ericson and Wollin (1968) and Emiliani (1966b) (Hays et al., 1969). Emiliani (1966b) considers the coincidence of 40-50 x 10^3 yrs. climatic half-cycles and the half-period of theoretical insolation variations in

the northern hemisphere to be evidence of a causal relationship. However, Broecker's (1966) modified Milankovitch curve emphasizing tilt relative to precession reduces the half-cycle period to about 20×10^3 years.

The fact that none of the investigated climatic schemes yields apparent durational differences of cold and warm periods is surprising. The extrapolated sedimentation rate chronology should show longer periods for glacials because the presumed greater sedimentation rates accompanying intensified biogenic production or ice-rafting are not considered. Either depositional rates were not significantly dependent on climate--contrary to Arrhenius' (1950; 1952; 1963) findings--or the glacials were generally shorter than the interglacials. It is possible, however, that increased bottom current velocities during glacials modified the expected increase in sedimentation rate.

A detailed comparison of the extrapolated sedimentation rate chronology of the Pacific curves (Table 14) produces a strong argument against high- and low-latitude synchroneity of the published record of Pacific glacial-interglacial fluctuations. Although the previously discussed low-latitude records are approximately equivalent in cycle number and timing, the Southern Ocean stratigraphy exhibits fewer and consistently older cycles. Arctic climatic change also consistently preceded that at lower latitudes prior to unit B6.

The question of synchroneity and number of Pacific Pleistocene events is made complex by the necessary use of different analytical techniques in different environments. Besides probable resolution differences, the response--e.g., of planktonic foraminiferal populations to upwelling intensity transformations at low latitudes--might not be expected to be synchronous with foraminiferal abundance variations in the Arctic sediments although actual global climatic change may have been simultaneous. As long as glaciers existed from Alaska to Greenland, melting ice in interglacial periods probably maintained "mild" glacial conditions in Arctic surface waters producing a time lag between sedimentary events there and elsewhere.

A time progression or lack of synchroneity of Pleistocene climatic events between high and low latitudes is not inconsistent with modified "Milankovitch" hypotheses. Wilson's (1964) treatment of Antarctic ice-sheet instability implies a time progression from the southern to the northern hemispheres both in climatic amelioration and in deterioration. As the ice shelf expanded, the earth's albedo would increase and earth temperature would be depressed resulting in worldwide glacial conditions. As the ice shelf waned, previously reflected solar energy would warm the Southern Ocean. This heat would eventually be transferred to northern hemisphere oceans and ultimately to the land. Although these ice-shelf pulsations may be

triggered by insolation variations, the theory accounts for apparent climatic time-lags between southern high and low latitudes.

According to the model preferred by Crowell and Frakes (1970), glaciers grew and diminished from the poles due to cyclic meridional perturbations of storm tracks (cf. Lamb, 1971). Expanding glacial centers displaced storm belts equatorward until the latitudinal tracks became unstable. Principal accretion of the ice cap during its growth occurred under the equatorward storm track. When the tail of the ice sheet had moved sufficiently equatorward from its place of origin, system instability resulted in more and more poleward storm tracks, thus completing the cycle. However, without the impetus of insolation variations, this autovariation model lacks a consistent imbalance and would probably result in equilibrium conditions. The modified Simpson (1940) hypothesis (Ericson and Wollin, 1970) discussed previously as an explanation of possible achronous climatic events also relies on changes in the sun's energy to supply increased precipitation for ice formation.

Pre-Quaternary sedimentation in the western equatorial Pacific

The great thickness of Cenozoic calcareous ooze on the Plateau and the distribution of oldest microfossils and sediment thicknesses appears to support the concept of the

general stability of the equatorial depositional system during the Cenozoic Era as inferred by Riedel (1971) and Ewing et al. (1968). These observations may also imply that from Cretaceous to the present, the western equatorial Pacific crust has moved in a direction consistently parallel to the equator. This, of course, contradicts the DSDP Legs 17 and 20 conclusions of a 1.5 cm to 5 cm/yr northward Cenozoic movement of the western Pacific crust (Scientific staff, 1971; 1972). These data may be reconciled by explaining the bilatitudinal oldest microfossil distribution as a product of continuous northward crustal drift. Cretaceous microfossils would occur within reach of the piston core north of the equatorial zone due to reduced sedimentation subsequent to the passage of the crust under the equator. Fossils of similar age may be collected south of the high productivity zone because sedimentation rates have been continuously low. It would also be necessary to assume that the bilatitudinal pattern of calcareous Cenozoic sediment thickness on the Plateau results from increased solution with increasing basement depth, rather than a meridional decrease in biogenic productivity. The great Cenozoic sediment thickness of the central Plateau could result simply from permanent position of the basement surface above the carbonate compensation depth. However, simultaneous northward crustal drift and documented subduction in the trenches of the western Pacific rim

require an additional spreading center to replace the northward-moving crust.

Alternatively, northward crustal drift may be a misinterpretation of a past greater latitudinal extent of the zone of calcareous sedimentation due to reduced dissolution intensities with higher bottom-water temperatures (Arrhenius, 1963), or to stimulated interocean circulation before the late Pliocene uplift of the Isthmus of Panama (Hays et al., 1969). An equatorial current system with much greater pre-late Tertiary bilatitudinal extent is consistent with the results of a cross section of eastern equatorial drill sites on DSDP Leg 8 (Scientific staff, 1970). Polar wandering in the earth's axial plane and accompanying latitudinal displacement of the equatorial current system relative to its present position is also feasible.

The pre-Tertiary flood basalt foundation of the Plateau probably originated in the eastern Pacific and moved westward parallel to the equator with its central surface above the compensation depth from late Eocene to late Miocene time. During this period, the central Plateau received a thick sequence of calcareous pelagic ooze from a gradually shrinking zone of high biogenic productivity associated with the equatorial current system. Denudation of the Plateau margins accompanied and followed the late Miocene tectonism associated with the collision of the

Plateau and the Australian plate. Perhaps with the late Pliocene blockage of a Pacific-Atlantic equatorial connection, upwelling and high productivity diminished or ceased in the western equatorial Pacific. Pleistocene climatic oscillations caused waxing and waning of oceanwide equatorial-upwelling intensity producing sedimentary sequences discernible only by subtle parameter variations in western Pacific sediments.

CONCLUSIONS

I. Surface sediment analysis

A. Subaerial volcanics reduce surface sediment calcium carbonate content on the western margin of the Ontong Java Plateau.

B. Two artificially generated sediment calcium carbonate solution boundaries, the sedimentary lysocline, and the slope break in the carbonate percent profile, are equivalent in the investigation region.

C. The lysocline depth in the western equatorial Pacific is shallower (3500 m) than in the eastern equatorial Pacific (3800 m).

D. The western equatorial Pacific compensation depth occurs at 5250 m, and establishes a greater interval between this level and the lysocline in the western as opposed to the eastern equatorial Pacific.

E. Both the less than 44 μ and the greater than 246 μ weight percents exhibit highly significant correlations with depth, and may be useful as solution indicators or delineators of displaced surface sediment.

II. Pleistocene paleoclimatic analysis and correlations

A. The western equatorial Pacific Pleistocene

paleoclimatic stratigraphy exhibits eight upwelling cycles in the Brunhes epoch, and indicates a general climatic amelioration continuing to the Recent from the Brunhes-Matuyama boundary.

B. This stratigraphy correlates well with previously published parameter fluctuations in equatorial cores across the entire Pacific Ocean.

C. The western equatorial Pacific chronostratigraphy also compares favorably with published paleoclimatic schemes from the southeastern, eastern, and north Pacific Ocean.

D. The above chronostratigraphies disagree in cycle number and timing with climatic oscillations interpreted from marine sediments in the Southern and Arctic oceans. A time progression or lack of cycle synchroneity between high- and low-latitude climatic change can be explained by modified "Milankovitch" hypotheses such as Wilson's (1964) Antarctic ice-shelf theory.

III. Western equatorial current system history

A. The equatorial current system has been stable in geographic position but has diminished in bilatitudinal extent during Tertiary time. Climatic oscillations induced alternating periods of upwelling and quiescence in the western equatorial Pacific during the Pleistocene Epoch.

APPENDIX A

SURFACE SEDIMENT DATA

Table 15

Surface Sediment Sample Locations

Sample Name		Latitude	Longitude
67 FFC	1	4°27. 4'N	169°43. 7'E
	2	2°56. 5'S	163°22. 3'
	5	5° 5. 9'S	162° 7. 2'
	6	5° 5. 5'S	162° 7. 3'
	7	5° 4. 3'S	162° 7. 8'
	8	4°45. 5'S	162°20. 4'
	9	4°46. 1'S	162°20. 0'
	11	5°20. 5'S	161°52. 2'
	12	5°19. 6'S	161°51. 8'
	14	3°29. 6'S	162° 8. 0'
	15	1°44. 6'S	162°44. 5'
	16	3°17. 1'S	161°10. 0'
	18	4°40. 9'S	160°13. 5'
	20	7°39. 3'S	160°18. 8'
	22	4°54. 0'S	158°34. 2'
	24	4°35. 3'S	154°38. 2'
	25	3°19. 8'S	155°30. 0'
	26	2° 4. 5'S	157°22. 2'
	27	0°52. 0'S	159°16. 5'
	28	2° 4. 3'N	163°23. 0'
	30	3°24. 9'N	164°59. 0'
	31	5° 3. 5'N	166°56. 2'

Table 15. (Continued) Surface Sediment Sample Locations

Sample Name	Latitude	Longitude
68 PC 3	7° 5. 5'S	179°50. 0'
4	9° 6. 7'S	173°50. 3'
7	7° 2. 0'S	159°49. 8'
9	6° 8. 0'S	158° 9. 0'
11	0°50. 8'S	162° 1. 5'
12	0°52. 1'S	161°13. 3'
14	6°20. 5'S	156°36. 9'
15	1° 0. 0'S	160° 3. 6'
16	1°36. 0'S	158°46. 0'
18	4°13. 0'S	155°36. 0'
20	4°54. 6'S	165°40. 5'
23	4°19. 5'S	172° 3. 9'
68 FFC 4	7°39. 0'S	159°59. 5'
10	6°55. 0'S	160° 9. 0'
15	7° 0. 0'S	158°11. 0'
21	5°56. 0'S	156° 1. 0'
70 PC 72	0°30. 8'S	161°49. 3'
78	8°42.54'N	154°34.32'
62	0°34.44'S	154°51. 6'
63	3°19.97'S	155°29.98'
64	3°19.97'S	155°29.98'
70 FFC 59	3°45.57'N	171°19. 9'

Table 15. (Continued) Surface Sediment Sample Locations

Sample Name		Latitude	Longitude
70 TC	1	6°45.25'S	171°40.15'
	2	10° 6.42'S	163°45. 5'

Table 16

Surface Sediment Size Fraction and Calcium Carbonate Data

Station	Depth (m)	Weight Percent: Size Fraction			Weight Percent: Calcium Carbonate			Total
		<44 μ	44-246 μ	>246 μ	<44 μ	44-246 μ	>246 μ	
67FC12	1586	41.5	30.5	27.9	78.8	93.0	49.3	47.9
67FC26	1606	41.5	28.8	29.7	69.6	91.7	100.0	84.4
*67FC11	1650	5.5	39.9	54.6	45.2	49.6	49.3	47.9
*67FC22	1720	68.2	21.0	10.8	64.2	85.1	88.8	78.9
67FC18	1746	53.9	28.5	17.6	75.4	93.4	94.0	87.3
*67FC25	1886	22.0	25.6	52.4	57.9	89.6	91.5	79.7
*70PC63	1915	49.1	28.2	22.6	53.4	86.4	91.5	77.7
*70PC64	1990	56.4	21.4	22.2	47.3	85.9	82.6	71.3
*67FC24	1996	40.1	41.4	18.5	28.5	41.6	36.6	35.4
68PC16	2020	18.7	45.6	35.7	84.7	95.6	94.6	91.9
67FC7	2178	55.8	25.9	18.3	77.1	94.4	92.5	88.4
67FC6	2232	50.9	27.9	21.1	77.8	93.3	92.3	87.8
68PC20	2250	33.6	40.0	26.3	95.1	94.4	90.5	90.0
67FC27	2254	51.8	24.4	23.8	79.9	93.2	96.8	90.1
67FC5	2256	52.2	28.2	19.6	77.7	94.2	93.9	88.6
67FC16	2340	43.8	32.9	23.3	85.0	93.7	95.2	91.2
*68FC15	2475	68.4	20.6	10.9	49.4	73.4	85.3	70.1

Table 16. (Continued) Surface Sediment Size Fraction and Calcium Carbonate Data

Station	Depth (m)	Weight Percent: Size Fraction			Weight Percent: Calcium Carbonate			Total
		<44 μ	44-246 μ	>246 μ	<44 μ	44-246 μ	>246 μ	
68PC15	2535	43.3	35.3	21.4	82.1	88.3	90.8	87.0
*68PC18	2580	60.1	29.2	10.7	23.2	37.5	60.9	40.5
*68PC9	2605	61.8	13.6	24.6	47.6	62.8	79.1	63.9
67FC9	2670	56.7	23.6	19.7	80.4	93.9	93.2	89.3
67FC8	2688	54.7	25.1	20.2	80.0	94.4	96.2	90.2
*68FC4	2707	52.3	28.3	19.4	43.5	52.2	67.6	54.9
67FC14	2820	59.6	22.0	18.4	80.6	92.0	94.0	89.0
70PC62	2910	54.3	19.1	26.6	69.8	91.4	92.6	84.9
*68PC8	2930	53.0	30.4	16.6	50.7	57.5	74.5	61.7
*68PC14	2965	40.7	36.0	23.3	18.0	26.0	34.6	26.2
*70TC2	3120	70.5	22.3	7.2	25.1	37.2	100.0	33.2
*67FC20	3196	83.7	12.4	3.9	42.0	41.1	48.5	43.7
67FC2	3360	63.3	19.3	17.4	83.0	90.3	95.9	89.9
68PC12	3430	67.0	14.9	18.1	80.1	92.1	94.9	89.0
*68FC10	3475	62.6	29.0	8.4	42.3	46.0	73.4	53.0
*68PC7	3850	71.6	17.1	11.3	33.9	37.5	43.4	38.5
*68FC21	3875	31.7	34.3	33.9	39.3	38.0	43.8	40.4

Table 16. (Continued) Surface Sediment Size Fraction and Calcium Carbonate Data

Station	Depth (m)	Weight Percent: Size Fraction			Weight Percent: Calcium Carbonate			Total
		<44 μ	44-246 μ	>246 μ	<44 μ	44-246 μ	>246 μ	
68PC11	3900	69.2	18.0	12.8	76.5	82.3	89.7	82.8
68PC23	3940	82.9	8.7	8.4	88.9	91.0	88.9	89.6
67FC30	4216	78.2	15.0	6.9	75.6	84.9	93.8	84.6
67FC15	4232	82.1	11.5	6.3	75.7	79.3	89.2	81.6
70PC72	4255	82.0	10.6	7.4	72.9	79.2	92.6	81.7
70FC59	4280	73.2	13.6	13.2	82.4	82.4	73.9	80.0
67FC1	4312	80.7	12.7	6.6	81.6	78.5	87.7	82.6
67FC28	4312	78.6	14.6	6.8	68.8	64.6	90.8	74.9
67FC31	4795	88.0	10.7	1.3	32.8	43.2	81.7	47.8
68PC4	5250	95.2	4.3	0.5	4.4	14.1	4.2	7.3
70TC1	5250	87.7	10.4	1.9	3.7	5.3	7.4	5.0
70PC78	5300	89.1	10.1	0.8	5.7	5.0	5.7	5.4

*Samples excluded from further analysis due to volcanic dilution.

Table 17

Foraminiferal Species Counts in Surface Sediment Samples

	67	67	68	67	67	68	67	67	67	70	67	68	68	68	67	67	70	70	67	67
Core	PC7	PC6	PC20	PC27	PC5	PC15	PC9	PC8	PC14	PC62	PC2	PC12	PC11	PC23	PC30	PC15	PC72	FFC59	PC28	PC1
Depth (meters)	2178	2232	2250	2254	2256	2535	2670	2688	2830	2910	3360	3430	3900	3940	4216	4232	4255	4280	4312	4312
Total No. Foraminifera (Whole Tests)	517	369	543	390	827	360	481	314	393	453	450	432	377	335	298	338	414	223	246	287
Total Weight (grams)	.03251	.0145	.0335	.0135	.04061	.0293	.02004	.01135	.03255	.03895	.038	.04339	.03258	.04194	.03069	.0419	.0374	.03224	.02855	.02821
Species																				
Globorotalia crassiformis	0	0	5	0	2	4	0	0	1	2	0	0	0	0	0	0	0	1	0	0
Globigerina calida	6	7	7	6	0	0	3	2	0	0	0	0	0	0	0	0	0	0	0	0
Globorotalia cultrata	14	11	21	5	18	30	8	9	7	32	8	2	13	15	15	4	24	13	5	14
Globorotalia tumida	0	0	0	3	0	2	3	0	4	8	5	2	10	9	4	0	2	3	4	5
Sphaeroidinella dehiscens	1	1	1	1	2	0	2	1	1	1	3	2	6	0	1	1	0	2	2	4
Globigerinoides conglobatus	23	15	22	7	75	10	31	20	17	6	14	7	5	18	5	6	4	1	2	3
Globigerinoides sacculifer	109	74	114	79	167	64	122	76	91	81	99	136	32	62	29	60	52	13	22	15
Globigerinoides ruber	169	104	148	112	238	36	123	81	97	78	31	38	10	19	2	23	7	6	9	5
Globigerina conglomerata	3	1	10	1	4	3	4	1	4	8	14	7	6	9	3	2	10	0	2	3
Globoquadrina dutertrei	62	37	50	25	78	37	37	36	18	44	37	16	22	16	15	41	43	5	27	11
Globorotalia scitula	0	1	0	1	0	0	1	0	0	1	0	0	0	1	0	0	0	0	0	0
Globigerinella siphonifera	67	39	70	57	86	42	61	40	64	70	72	80	27	50	9	17	21	6	16	13
Candeina nitida	4	4	8	3	6	1	4	4	0	1	0	0	0	2	0	0	0	0	0	0
Orbulina universa	5	2	5	0	2	2	4	2	1	1	1	0	0	1	0	0	1	0	0	0
Pulleniatina obliquiloculata	45	57	52	79	88	123	59	32	66	120	114	122	246	120	213	164	238	170	154	182
Globigerinoides quadrilobatus	64	58	78	54	108	53	94	46	66	58	70	87	19	49	21	50	36	8	18	10

APPENDIX B

SUMMARY DESCRIPTIONS OF PLEISTOCENE CORES

68PC11 (Tables 18, 19; Figure 15)

Location: 0°50.8'S, 162°01.5'E

Depth: 3900 m

Topography: This core was retrieved from the central outer floor of a large erosional submarine valley which strikes southwest deep into the Plateau (Figure 5).

Lithology:

0-1 111 cm: light gray (2.5Y7/2) and light brownish gray (2.5Y6/2) to pale yellowish brown (5Y7/3 and 10YR6.5/3) to white (10YR8/1.5 and N9/0) nannofossil chalk ooze; 10-25% foraminifera, decreasing to 1-3% foraminifera from 25-1 111 cm; 1-25% Radiolaria; 4-25% discoasters from 914-1 111 cm; 5-25% minerals

Chronology:

Paleomagnetic stratigraphy:

Brunhes-Matuyama boundary: 858 cm; sedimentation rate: 1.2 cm/10^3 yrs.

Micropaleontology and continuity:

68PC11 is composed of 918 cm of apparently continuous Quaternary sediment overlying 193 cm of late Miocene (Buyannanonth, 1971; Figure 15). From 968 to 977 cm, evidence of reworked N22 with admixed Miocene-Pliocene nannofossils is present indicating slumping or turbidity flows during the Quaternary in this erosional environment. Fluctuations of faunal parameters were

not investigated in this core due to the likelihood of extreme solution influence at the sublysocline collection site. Buyannanonth (1971) observed marked solution effects below 918 cm.

Table 18

Chronostratigraphy and Characteristics of the <44 μ Weight Fraction Profile for Core 68PC11

Unit B	$t_1 - t_2$ ($\times 10^3$ yrs.)	t ($\times 10^3$ yrs.)	Remarks*
2**	10- 19	9	warmest cold, shortest cold
3	19- 54	35	
4	54-112	58	
5	112-154	42	
6	154-204	50	
7	204-237	33	
8	237-262	25	
9	262-287	25	shortest warm
10	287-387	100	longest cold
11	387-412	25	shortest warm --lowest fluctuation
12	412-480	68	
13	480-521	41	coldest warm--lowest fluctuation
14	521-552	31	coldest cold --greatest fluctuation
15	552-652	100	longest warm
16	652-710	58	--greatest fluctuation
17	710- ?	---	warmest warm

*Surface value: warm warm surpassed or equalled only by B15 and 17.

**Wisconsin (B2): may be two cold peaks, i.e., may include B4; B2 is warmest cold; may record Wisconsin maximum at ca. 18 x 10^3 yrs. B.P. (Mesolella et al., 1969).

Table 19

Descriptive Statistics for Parameters
Measured in Core 68PC11

Parameter*	Mean	Standard Deviation	Range
P1	76.3	7.7	60. 7- 88. 5
P2	4.0	4.3	1. 8- 22. 6
P3	6.3	2.5	3. 5- 14. 1
P4	6.1	3.8	3. 0- 21. 4
P5	7.3	5.1	. 3- 26. 4
R1	27.8	58.7	2. 4-326. 5
R2	0.2	0.1	.03- .43
C44	23.7	7.7	11. 5- 40. 7
C61	19.7	7.5	9. 1- 37. 1
C124	13.4	6.3	3. 3- 29. 9
PC	79.9	11.3	46. 0-100. 0
P	510.0	121.3	287. 3-762. 1

*Key:

P1 : weight percent <44 μ
P2 : 44-61 μ
P3 : 61-124 μ
P4 : 124-246 μ
P5 : >246 μ
R1 : <44 μ/>246 μ
R2 : <124 μ/>124 μ
C44 : weight percent >44 μ
C61 : >61 μ
C124: >124 μ
PC : weight percent $CaCO_3$ in total sample
P : phosphorus in ppm

68PC12 (Tables 20 and 21; Figure 16)

Location: 0°52.1'S, 161°13.3'E

Depth: 3430 m

Topography: This core was taken from the northwestern slope of the large erosional submarine reentrant described under core 68PC11 (Figure 5).

Lithology:

0-145 cm: light gray (2.5Y7.5/2) nannofossil-foram chalk ooze; 17-34% foraminifera, 5% radiolarians and diatoms

145-535 cm: light to very light gray (10YR7.5/1 and N8/0) nannofossil chalk ooze; 6-17% foraminifera, 5-12% radiolaria

535-619 cm: light gray (N7.5/0) nannofossil-foram chalk ooze; 20-26% foraminifera, 12% radiolaria

619-991 cm: light gray (5Y7/1) nannofossil chalk ooze; 6-15% foraminifera, 3-11% radiolarians, 1-3% discoasters

Chronology:

C^{14}: 40-43 cm = 30,660 $^{+3080}_{-2220}$ yrs. B.P.; sedimentation rate = 1.3 cm/10^3 yrs.

Paleomagnetic stratigraphy:

Brunhes-Matuyama boundary: 606 cm; sedimentation rate: 0.9 cm/10^3 yrs.;

Jaramillo event: 776 cm; sedimentation rate: 0.9 cm/10^3 yrs. for sediment from the surface and from

the Brunhes-Matuyama boundary to the top of the Jaramillo

Micropaleontology and continuity:

The core is entirely Quaternary and appears to represent rare continuous deposition. However, the combination of the core's superlysocline position and low sedimentation rate may indicate winnowing. Occasional zones of extremely poorly preserved assemblages probably denote fluctuations in the production-solution relations discussed in the text.

Comments:

The chronology indicates that B2 through B4 may represent the Wisconsin in this core and that B2 may coincide with the maximum extent of glaciation previously dated by Broecker et al. (1968) at ca. 18×10^3 yrs. B.P.

Table 20

Chronostratigraphy of the G. cultrata Complex Frequency Profile for Core 68PC12 and Summary Characteristics of Figure 16 Profiles

Unit	$t_1 - t_2$ ($\times 10^3$ yrs.)	t ($\times 10^3$ yrs.)	Remarks*
B 2	? - 106	---	warmest cold
3	106- 151	45	
4	151- 207	56	
5	207- 240	33	
6	240- 273	33	
7	273- 298	25	
8	298- 359	61	
9	359- 381	22	shortest warm
10	381- 414	33	shortest cold
11	414- 448	24	
12	448- 482	34	
13	482- 517	35	lowest fluctuation
14	517- 550	33	lowest fluctuation
15	550- 528	78	
16	628- 673	45	longest cold
17	673- 718	45	longest warm, --highest fluctuation
18	718- 751	33	coldest cold, --highest fluctuation
M 1	751- 898	157	
2	898- 931	33	
3	931-1031	100	

*Surface value: warm warm nearly equal to previous intense warms. Wisconsin: warmest cold.

Table 21

Descriptive Statistics for Parameters
Measured in Core 68PC12

Parameter*	Mean	Standard Deviation	Range
P1	46.6	9.3	30.3- 68.1
P2	8.4	2.9	2.5- 13.7
P3	14.5	3.8	8.7- 21.5
P4	14.4	5.4	6.2- 33.9
P5	16.1	7.3	5.1- 36.8
R1	3.7	2.4	0.9- 12.6
R2	0.5	0.2	0.1- 1.0
C44	53.4	9.3	31.9- 69.7
C61	45.0	9.3	23.4- 61.0
C124	30.5	9.4	13.4- 48.8
PC	83.7	10.3	71.0- 100.0
P	506.2	65.3	417.0- 686.0
XPC	89.0	7.5	47.8- 96.3
SV	1521.8	13.6	1500.0-1550.0
SS	1.3	0.7	0.5- 3.7
WC	46.0	2.4	42.3- 52.9
Q	71.5	2.6	66.4- 77.6
GD	2.8	0.3	2.2- 3.5
BD	1.5	0.1	1.4- 1.6
VR	2.5	0.4	2.0- 3.5
GCC	1665.8	900.1	207.0-4450.0

Table 21. (Continued) Descriptive Statistics for Parameters Measured in Core 68PC12

Parameter*	Mean	Standard Deviation	Range
GT	392.9	505.2	16.0-2100.0
GC	172.6	182.5	17.6- 872.0
GS	467.0	566.0	4.4-2130.0
GCC/GS	20.3	32.6	0.2- 77.0
GS/GC	4.0	4.6	0.1- 17.0
GT/GC	5.7	12.2	0.1- 68.0
GCC/GT	11.7	13.6	0.2- 76.0

*Key:

XPC: weight percent $CaCO_3$ >61 μ
SV : sound velocity (m/sec)
SS : shear strength (tons/m^2)
WC : water content (% wet weight)
Q : porosity (%)
GD : grain density
BD : bulk density
VR : void ratio
GCC: G. cultrata complex per gram of sediment greater than 246 μ
GT : G. truncatulinoides
GC : G. conglomerata
GS : G. sacculifer

68PC15 (Tables 22 and 23, Figure 17)

Location: 01°00.0'S, 160°03.6'E

Depth: 2535 m

Topography: Core 68PC15 was collected near the crest of an east-west trending ridge which separates the previously described erosional valley to the southeast from a smaller reentrant to the northwest (Figure 5).

Lithology:

0-204 cm: light gray (2.5Y7/2 and 5Y7/1) and pale yellowish brown (10YR5.5/3/5) foram chalk ooze; 24-40% nannofossils

204-296 cm: light gray (7.5Y7/0 and 5Y7/1) nannofossil-foram chalk ooze: 30-40% foraminifera

296-303 cm: light gray (2.5YR7/0) foram chalk ooze; 25% nannofossils

303-560 cm: light gray (5Y6.5/1) to white (7.4YR8/0 and N9/0) and yellowish gray (GSA5Y8/1) nannofossil-foram chalk ooze; 20-40% foraminifera

560-767 cm: white (5Y8/1) to light gray (5Y7/1) nannofossil chalk ooze; 2-20% foraminifera

Chronology:

C^{14}: 4-7 cm = 8,780 ± 175 yrs. B.P.; sedimentation rate = 0.6 cm/10^3 yrs.

Paleomagnetic stratigraphy:

Brunhes-Matuyama boundary: 343 cm; sedimentation rate: 0.5 cm/10^3 yrs.

Jaramillo event: 548 cm; sedimentation rate: 0.6 cm/10^3 yrs. from the surface to the top of the Jaramillo and 1.1 cm/10^3 yrs. between the Brunhes-Matuyama boundary and the top of the Jaramillo

Micropaleontology and continuity:

No pre-Quaternary foraminifera were observed in this core. The higher, although still somewhat low, sedimentation rate between the Brunhes-Matuyama boundary and the top of the Jaramillo is in sharp contrast to depositional rates during the Brunhes. Sediment removal at the core top and during the Brunhes is indicated. Durations for the tentatively identifiable stages were calculated but qualitative comparisons are omitted due to the insufficient record length.

Comments:

Although the top few centimeters are apparently in situ a hiatus exists above 150 cm extending from units B12 through B2. This interpretation is supported by the abnormally low Brunhes sedimentation rate and the disturbed character of the parameter profiles above unit B12. No consecutive chronology is calculated for this core although unit durations for the G. cultrata complex frequency curve and the average characteristics of the Figure 17 profiles are available.

Table 22

Unit Durations of the G. cultrata Complex Frequency Profile for Core 68PC15

Unit	t ($\times 10^3$ yrs.)	Remarks*
B13	55	
14	75	
15	60	
16	80	
17	43	
18	83	
M 1	29	
2	43	
3	50	
4	39	

*Surface value: cold cold.

Table 23

Descriptive Statistics for
Parameters Measured in Core 68PC15

Parameter*	Mean	Standard Deviation	Range
P1	44.2	13.1	22.6- 68.4
P2	9.2	2.9	5.3- 18.6
P3	11.3	3.0	5.2- 17.6
P4	11.8	3.6	5.9- 18.8
P5	23.6	8.5	13.2- 47.2
R1	2.3	1.3	.5- 5.0
R124	0.6	0.3	.2- 1.4
PC44	55.8	13.1	31.6- 77.4
CPC61	46.7	12.6	26.3- 70.8
CPC124	35.4	11.1	19.2- 58.9
PC	86.7	6.2	68.4- 155.0
SV	1545.2	14.4	1520.0-1570.0
SC	44.6	2.4	40.0- 49.0
Q	69.8	2.9	62.9- 73.6
GD	2.8	0.3	2.3- 3.5
BD	1.6	0.1	1.4- 1.7
VR	2.3	0.3	1.7- 2.9
XPC	95.3	9.2	61.0- 100.0
GCC	1680.4	780.9	184.0-2840.0
GT	173.8	185.1	15.4- 857.0
GC	500.2	393.3	24.3-1790.0
GS	654.0	390.6	80.6-1910.0
GCC/GS	3.4	2.3	.3- 10.0
GS/GC	2.8	4.9	.4- 28.0
GT/GC	0.5	0.5	.1- 7.0
GCC/GT	16.7	12.4	3.6- 49.0

*Key: see key to Tables 19 and 21 for parameter identifications.

68PC16 (Tables 24 and 25; Figure 18)

Location: 01°36.0'S, 158°46.0'E

Depth: 2020 m

Topography: This core was collected from the flat eastern-central portion of the Plateau (Figure 5).

Lithology:

0-23 cm: light brownish gray (2.5Y6.5/2) to pale brown (10YR6.5/3) foram chalk ooze; 7-15% nannofossils, 0-7% Radiolaria and diatoms, 10% minerals

23-216 cm: light gray (2.5Y7/2 and 5Y7/1) nannofossil-foram chalk ooze; 16-38% foraminifera, 2-4% Radiolaria, 12-32% minerals

216-603 cm: greenish gray (5GY6/1) to white (GSA N9/0) and light gray (10YR7/2 and 5Y7/1) nannofossil chalk ooze; 10-20% foraminifera, 1-4% Radiolaria, 6-22% minerals

603-642 cm: white (5Y8/1) and light gray (5Y7/1) nannofossil-foram chalk ooze; 38% foraminifera, 9% minerals

642-782 cm: white (5Y8/1) and light gray (5Y7/1) nannofossil chalk ooze; 13-20% foraminifera, 8-18% minerals

Chronology:

C^{14}: 4-7 cm = 17,440 ± 430 yrs. B.P.; sedimentation rate = 0.3 cm/10^3 yrs.

Paleomagnetic stratigraphy:

Brunhes-Matuyama boundary: 730 cm; sedimentation rate: 1.1 cm/10^3 yrs.

Micropaleontology and continuity:

No pre-Quaternary microfossils were observed in this core and no evidence of hiatuses or extensive reworking was revealed by the fossil fauna. The paleomagnetically determined sedimentation rate is considered reasonable for the core location. However, about 10 cm representing all of the post-glacial and some of the late Wisconsin are missing or disturbed, as evidenced by the low C^{14} based sedimentation rate and the abnormality of the surface values in comparison to their vertical distribution.

Table 24

Chronostratigraphy of the G. cultrata Complex Frequency Profile for Core 68PC16 and Summary Characteristics of Figure 18 Profiles

Unit B	$t_1 - t_2$ ($\times 10^3$ yrs.)	t ($\times 10^3$ yrs.)	Remarks*
2	40?- 79	39	warmest cold
3	79-102	23	
4	102-125	23	shortest cold
5	125-171	46	
6	171-225	54	
7	225-257	32	
8	257-302	45	
9	302-348	46	longest warm
10	348-394	46	coldest cold, longest cold
11	394-451	57	
12	451-484	33	--least fluctuation
13	484-507	23	shortest warm
14	507-530	23	--greatest fluctuation
15	530-632	102	
16	632-652	20	
17	652- ?	---	coldest warm

Table 25

Descriptive Statistics for
Parameters Measured in Core 68PC16

Parameter	Mean	Standard Deviation	Range
P1	49.0	8.9	31.3- 63.3
P2	7.9	1.6	5.5- 11.0
P3	10.7	2.0	7.9- 17.7
P4	10.4	2.0	7.2- 14.3
P5	22.1	6.1	12.6- 38.9
R1	2.5	1.1	.9- 5.0
R124	0.5	0.2	0.3- .9
CPC44	51.0	8.9	36.7- 68.7
CPC61	43.1	8.3	29.6- 57.7
CPC124	32.5	7.3	20.4- 48.0
PC	94.1	2.8	88.3- 100.0
SV	1562.9	15.2	1540.0-1600.0
SS	1.1	0.2	.7- 1.8
WC	43.3	2.5	39.7- 49.8
Q	69.4	2.8	63.2- 75.8
GD	2.9	0.2	2.4- 3.6
BD	1.6	0.1	1.5- 1.7
VR	2.3	0.3	1.7- 3.1
XPC	95.1	4.6	82.1- 100.0
GCC	2336.8	851.1	735.0-4210.0
GT	646.5	739.1	46.1-2400.0
GC	488.0	224.2	171.0-1040.0
GS	1073.3	490.3	213.0-2650.0
GCC/GS	2.8	2.1	.4- 11.0
GS/GC	2.5	1.4	.9- 7.0
GT/GC	1.6	1.8	.1- 9.0
GCC/GT	13.1	14.8	1.1- 53.0

70PC62 (Tables 26 and 27; Figure 19)

Location: 00°34.44'S, 154°51.62'E

Depth: 2910 m

Topography: This core was taken near the western margin of the Plateau in an area of large valleys incised in flat-lying sediments.

Lithology:

0-519 cm: (5Y7/1-5Y6/1) nannofossil chalk ooze with 6-30% foraminifera, 0-37% discoasters, 1-6% minerals, 5-30% siliceous fragments

520-790 cm: (N7) nannofossil-foram chalk ooze with 35% foraminifera, 2-4% siliceous fragments, 1-4% minerals

791-1113 cm: (N7, 5Y7/1) nannofossil-chalk ooze with 8-24% foraminifera, 2-9% siliceous fragments, 1-6% minerals

Chronology:

Paleomagnetic stratigraphy:

Brunhes-Matuyama boundary: 694 cm; sedimentation rate: 1.0 cm/10^3 yrs.

Jaramillo event: 1015 cm; sedimentation rate: 1.1 cm/10^3 yrs. from surface to top of Jaramillo and 1.9 cm/10^3 yrs. between the Brunhes-Matuyama boundary and the top of the Jaramillo

Micropaleontology and continuity:

The presence of abundant Globoratalia tosaensis and Globigerinoides fistulosus indicates considerable reworking of Banner and Blow's (1967) N21 zone (upper Pliocene). Material of this age appears to have trickled across the core site during much of the depositional history represented by the core. From 60 to 540 cm, the sedimentary parameters are generally disturbed. In fact, from 320-500 cm, the G. cultrata complex exhibits a steady frequency increase reminiscent of graded bedding and may indicate the effect of turbidity flow. Thus, there is certainly disruption of normal pelagic sedimentation in the mid and upper Brunhes in this core and any stratigraphic interpretations in this interval are speculative at best. No consecutive chronologies or comparative qualitative remarks are presented for this core, but unit durations for the G. cultrata complex profile are discernible.

Table 26

Durations of the G. cultrata Complex
Units in Core 70PC62

Unit	t ($\times 10^3$ yrs.)	Remarks*
B 2?	40	
3?	29	
4?	30	
5?	44	
6?	40	
7?	30	
8?	50	
15?	43	
16	115	
17	21	
18	47	
M 1	21	
2	26	
3	37	

*Surface value: warm warm. Wisconsin: warm cold.

Table 27

Descriptive Statistics of Faunal Parameters Measured in Core 70PC62

Parameter	Mean	Standard Deviation	Range
GCC	2676.6	972.4	671.0-5100.0
GT	692.8	761.6	0.0-2660.0
GC	143.9	154.6	14.0- 756.0
GS	764.7	654.6	41.8-4290.0
GCC/GS	6.5	6.5	.8- 28.0
GC/GS	0.3	0.4	.1- 9.0
GT/GC	11.0	14.1	0.0- 75.0
GT/GCC	0.3	0.2	0.0- 9.0
GT/GS	1.9	2.6	0.0- 9.7

70PC64 (Tables 28 and 29; Figure 20)

Location: 03°19.97'S, 155°29.98'E

Depth: 1990 m

Topography: A flat topped, northeast striking divide between east-northeast trending, shallow valleys is the collection site of this core (Figure 5).

Lithology:

0-1168 cm: pale brown (5GY6/1) nannofossil-foram chalk ooze; 5-18% siliceous fragments, 5% minerals

1168 cm: 22% bioclastics

Chronology:

C^{14}: 30-32 cm = 23,590 $\pm \frac{965}{860}$ yrs. B.P.; sedimentation rate = 1.3 cm/10^3 yrs.

Paleomagnetic stratigraphy:

The core has normal polarity throughout establishing a minimum sedimentation rate of 1.7 cm/10^3 years.

Micropaleontology and continuity:

No micropaleontologic evidence of discontinuities or reworking was observed. The low C^{14}-determined near-surface sedimentation rate indicates that the top few centimeters are missing or disturbed.

Table 28

Chronostratigraphy of the G. cultrata Complex Frequency Profile for Core 70PC64 and Summary Characteristics of Figure 20 Profiles

Unit B	$t_1 - t_2$ ($\times 10^3$yrs.)	t ($\times 10^3$yrs.)	Remarks*
2	38- 68**	30	warmest cold
3	68-121	53	
4	121-157	36	
5	157-185	28	
6	185-203	18	
7	203-227	24	
8	227-321	94	longest cold
9	321-344	23	
10	344-379	35	
11	379-409	30	longest warm
12	409-468	59	coldest cold
13	468-562	94	
14	562-597	35	shortest cold } --least fluctuation
15	597-620	23	} --greatest fluctuation
16	620-644	24	
17	644-668	24	coldest warm; shortest warm

*Surface value: mixed; cold warm. Wisconsin: mixed; average cold.

**Maximum ages.

Table 29

Descriptive Statistics of Faunal Parameters Measured in Core 70PC64

Parameter	Mean	Standard Deviation	Range
GCC	2238.9	825.6	136.0- 441.0
GT	159.8	168.3	0.0- 683.0
GC	356.1	237.1	36.8-1110.0
GS	849.1	356.0	300.0-2100.0
GCC/GS	3.1	1.8	0.7- 9.8
GC/GS	0.5	0.4	0.1- 9.0
GT/GC	0.6	0.6	0.0- 8.0
GT/GCC	0.1	0.1	0.0- 9.0
GT/GS	0.2	0.2	0.0- 9.0

71PC35 (Table 30; Figure 21)

Location: 03°08.30'N, 154°21.00'E

Depth: 3200 m

Topography: No detailed analysis of this region is available. The general area is the gentle northwest slope of the Plateau.

Lithology:

0-1187 cm: white to gray (2.5Y8/2-5Y7/1) nannofossil chalk ooze; 30-72% coccoliths; 5-30% calcareous bioclastic hash; 2-20% foraminifera; 4-35% Radiolaria and other siliceous fragments; 5% minerals

Chronology:

Paleomagnetic stratigraphy:

The preliminary results exhibit a peculiar gradual inclination reversal over the interval from 500 to 650 cm indicating reworking in this zone. The erratic inclination data below 975 cm also indicates disturbed sediment and obscures any polarity reversal. Specific chronologies and qualitative comparisons are therefore unavailable for this core.

Micropaleontology and continuity:

The section appears normal above 500 centimeters. In the interval from 500 to 650 cm considerable breakage and occasional specimens of G. fistulosus point to sediment reworking. From 825 cm, the assemblages

exhibit severe fragmentation and some evidence of reduction. G. fistulosus is occasionally present and G. tosaensis occurs consistently from 885 cm to the bottom of the core. The character and abruptness of the faunal changes support the paleomagnetic interpretations of sediment disturbance between 500 and 650 cm and from about 885 cm to the bottom of the core.

Table 30

Descriptive Statistics of Faunal Parameters Measured in Core 71PC35

Parameter	Mean	Standard Deviation	Range
GCC	3424.0	1175.9	993.0-7570.0
GT	325.0	567.0	0.0-3030.0
GC	251.8	229.6	28.9- 909.0
GS	717.7	543.2	42.2-2240.0
GCC/GS	13.3	23.2	0.7- 118.0
GC/GS	0.7	2.1	0.1- 16.0
GT/GC	5.8	12.0	0.0- 61.0
GT-GCC	0.1	0.2	0.0- 9.0
GT-GS	1.1	2.9	0.0- 16.5

APPENDIX C

FOSSIL CORE DESCRIPTIONS

68PC10

Location: 06°26'S, 158°17.0'E

Depth: 3350 m

Topography: This core was taken from the southwest slope of an elongate northwest trending depression situated on the southwestern margin of the Plateau (Figure 5). The region is dominated by an anticlinorium characterized by intense faulting and slumping (Kroenke, 1972).

Lithology:

0-493 cm: white (2.5Y8/2) to light gray (2.5Y7/1) with light brownish gray (2.5Y6/2) and gray (5Y5.5/1) intervals, nannofossil chalk ooze; 1-7% foraminifera; 2.5% discoasters, increasing to 25% discoasters from 360-493 cm; 1-10% Radiolaria; 15-20% minerals decreasing to 2-7% from 143-693 cm

Chronology:

Paleomagnetic stratigraphy:

The core appears to be disturbed and contains no interpretable polarity sequences.

Micropaleontology and continuity:

Buyannanonth (1971) investigated the faunal aspects of 68PC10 (Figure 28a). Approximately 200 to 280 m of sediment have been eroded from the core site exposing

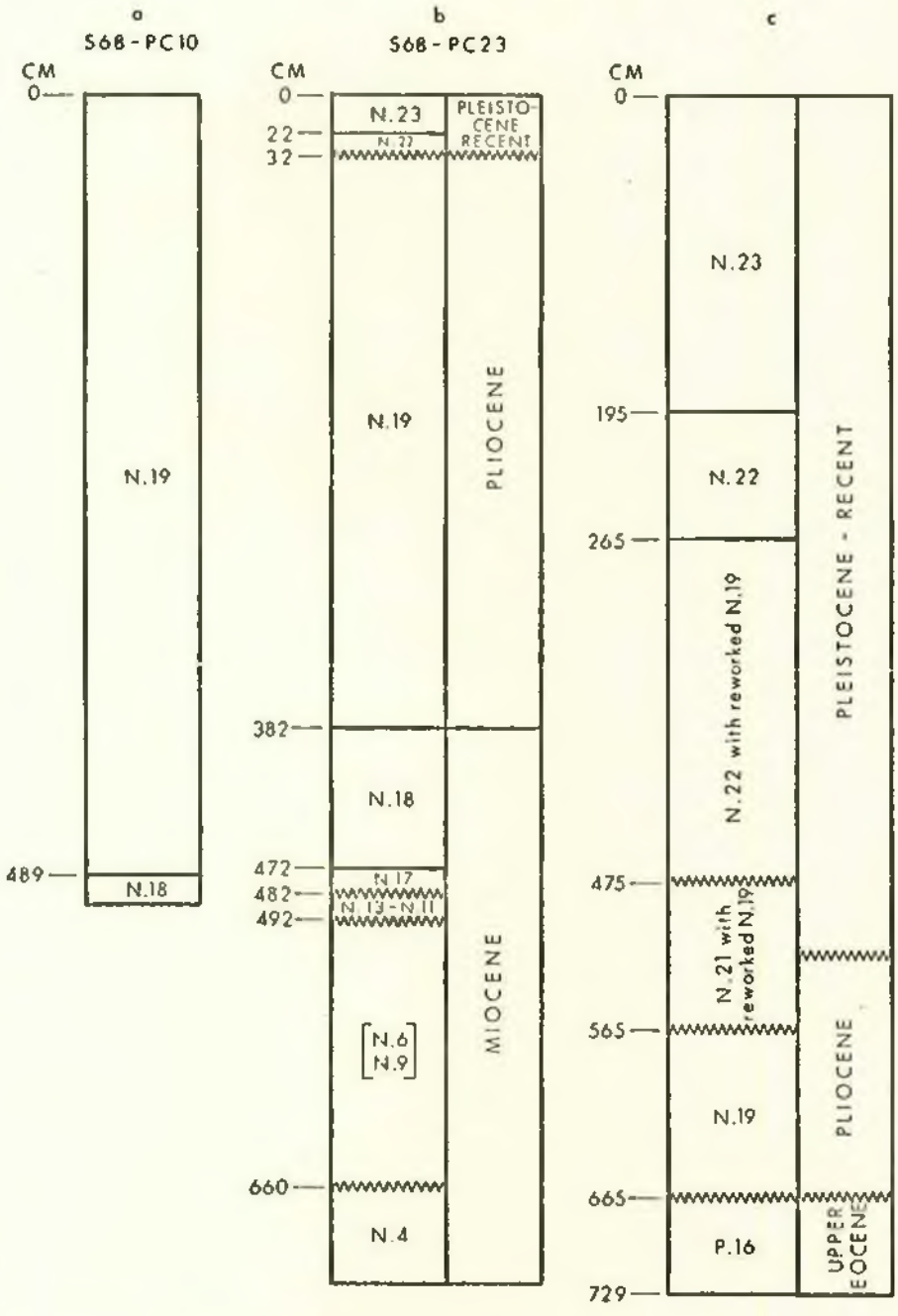

Figures 28a, b, c. Foraminiferal zonation of cores 68PC10 (a), 68PC21 (b) and 68PC23 (c) (after Buyannanonth, 1971).

an apparently continuous, late Miocene to middle Pliocene section to the piston core.

68PC20

Location: 04°54.6'S, 165°40.5'E

Depth: 2250 m

Topography: The large extension of the south-central Plateau characterized by horst and graben structure is the site of this core (Figure 5).

Lithology:

0-10 cm: very pale brown (10YR7/4) foram chalk ooze; 15% nannofossils; 15% minerals

10-161 cm: very pale brown (10YR7/4) to white (19YR8/2) nannofossil-foram chalk ooze; 20-38% foraminifera; 16-27% minerals

161-300 cm: white (N9) foram chalk ooze; 35% coccoliths; 12% discoasters; 5% minerals; 7% clay

300-349 cm: white (N9) nannofossil-foram chalk ooze; 25% foraminifera; 15% discoasters; 7% minerals; 7% clay

Chronology:

Paleomagnetic stratigraphy:

The core appears to be disturbed and contains no interpretable polarity sequences.

Micropaleontology and continuity:

Buyannanonth (1971) investigated the faunal aspects of 68PC10 (Figure 28a). Approximately 200 to 280 m of sediment have been eroded from the core site exposing

an apparently continuous, late Miocene to middle Pliocene section to the piston core.

68PC20

Location: 04°54.6'S, 165°40.5'E

Depth: 2250 m

Topography: The large extension of the south-central Plateau characterized by horst and graben structure is the site of this core (Figure 5).

Lithology:

0-10 cm: very pale brown (10YR7/4) foram chalk ooze; 15% nannofossils; 15% minerals

10-161 cm: very pale brown (10YR7/4) to white (19YR8/2) nannofossil-foram chalk ooze; 20-38% foraminifera; 16-27% minerals

161-300 cm: white (N9) foram chalk ooze; 35% coccoliths; 12% discoasters; 5% minerals; 7% clay

300-349 cm: white (N9) nannofossil-foram chalk ooze; 25% foraminifera; 15% discoasters; 7% minerals; 7% clay

Chronology:

Paleomagnetic stratigraphy:

The paleomagnetic data are not readily interpretable in this core.

Micropaleontology and continuity:

Landmesser (1971) reported that core 68PC20 consists of 160 cm of early Pleistocene overlying 210 cm of early Pliocene sediment. Thus there are erosional

unconformities at the surface and at about 160 cm in this core.

68PC21

Location: 04°19.5'S, 172°03.9'E

Depth: 3875 m

Topography: This and the next two cores (68PC22 and 23) were collected from the eastern tip of the structural crest of the eastward salient described under core 68PC20 (Figure 5).

Lithology:

0-744 cm: pale brownish gray (10YR7/2) to very pale brown (10YR8/3 and 10YR7.5/3) to pale brown (10YR6/4) and light gray (10YR7/1) to very pale brown (10YR7/3) and white (10YR8/2) nannofossil chalk ooze; 1-20% discoasters; 10-26% Radiolaria and diatoms; 5-25% clay

Chronology:

Paleomagnetic stratigraphy:

Brunhes-Matuyama boundary: 180 cm; sedimentation rate: 0.25 cm/10^3 yrs.

Jaramillo event: 280 cm; sedimentation rate: 0.3 cm/10^3 yrs. from surface to top of Jaramillo and 0.5 cm/10^3 yrs. from the Brunhes-Matuyama boundary to the top of the Jaramillo

Micropaleontology and continuity:

The faunal interpretation of this core is exhibited in Figure 28b (Buyannanonth, 1971). Extensive reworking is indicated between 265 and 565 cm along with several

erosional unconformities. However, apparently undisturbed although incomplete sections of Quaternary, Pliocene, and Eocene sediment are represented.

68PC23

Location: 04°19.5'S, 172°03.8'E

Depth: 3940 m

Lithology:

0-679 cm: dark yellowish brown (10YR3.5/7 and 10YR2.5/8) and very dark brown (10YR1.5/8) to white (10YR8/2) and light grayish yellow (2.5YR7.5/2) to light brownish gray (10YR6.5/3 and 10YR7/2.5) to pale brown (10YR8/1) with layers of white (N9/0) nannofossil chalk ooze; 15-80% discoasters; 1-35% siliceous bioclastics; 1-20% clay

Micropaleontology and continuity:

The foraminifera indicate a complex stratigraphy for this core (Buyannanonth, 1971) (Figure 28c). Although the zones increase normally in age, the Miocene, Pliocene and Pleistocene sections are laced with erosional unconformities and occurrences of sediment mixing.

68PC27

Location: 02°15.'N, 166°31.0'W

Depth: 5610 m

Topography: This core was taken off the Plateau in the middle of a great fault-controlled reentrant formed and maintained by sediment slumps and flows (Kroenke, 1972)

Lithology:

0-540 cm: white (10YR8/1.5 and 5Y8/2 and N9/0) nannofossil chalk ooze; 0-10% discoasters; 6-43% siliceous bioclastics; 1-10% Radiolaria; 1-10% diatoms; 1-15% clay decreasing with increasing depth

540-615 cm: gray and light olive gray (5Y6/1 and 5Y6/2) to brown (10YR5/3 and 10YR4/3) siliceous ooze; 10-20% Radiolaria; 10-14% diatoms; 1-5% calcareous bioclastics, 30-40% clay

615-670 cm: brown (10YR4/3) and white (10YR8/2 and 10YR8/1) nannofossil chalk ooze; 10% discoasters, 6-48% siliceous ooze; 5-10% Radiolaria; 15-20% diatoms; 1-5% calcareous bioclastics; 25-40% clay

720-744 cm: dark brown (10YR3/3) to white (10YR8/2) nannofossil chalk ooze; 7% discoasters; 23% Siliceous bioclastics; 5% Radiolaria; 8% diatoms; 5% clay

744-749 cm: brown (10YR4/3) siliceous ooze; 5% Radiolaria; 10% diatoms; 15% calcareous bioclastics; 20% clay

749-800 cm: white (N9/0) nannofossil chalk ooze; 5% discoasters; 5% foraminifera; 25% siliceous bioclastics; 10% diatoms; 5% Radiolaria; 10% manganese micronodules; 5% clay

800-817 cm: light olive gray (5Y6/2) to light yellowish brown (2.5Y6.4) to brown (10YR4/3) siliceous ooze; 2-20% Radiolaria; 5-20% diatoms; 1-8% calcareous bioclastics; 20-30% clay

Micropaleontology:

The core is Pliocene throughout (J. Resig, pers. commun.).

LITERATURE CITED

Arrhenius, G. O. 1950. Late Cenozoic Climatic Changes as Recorded by the Equatorial Current System. Tellus, v. 2, p. 83-88.

_____. 1952. Sediment Cores from the East Pacific. Sweden Deep-Sea Expedition Rept., v. 5, Fasc. 1, 89 p.

_____. 1963. Pelagic Sediments, In Hill, M. N., Ed., The Seas. New York, Interscience, v. 3, p. 655-727.

Andrews, J. and others. 1970. Sediment Core Descriptions: Solomon Islands, 1968-1969 and Murray Fracture Zone, 1967. Hawaii Inst. Geophys. Rept. HIG-70-25.

Banner, F. J. and W. H. Blow. 1967. Progress in the Planktonic Foraminiferal Biostratigraphy of the Neogene. Nature, v. 208, p. 1164-1166.

Berger, W. H. 1967. Foraminiferal Ooze: Solution at Depths. Science, v. 156, p. 383-385.

_____. 1968. Planktonic Foraminifera: Selective Solution and Paleoclimatic Interpretation. Deep-Sea Res., v. 15, p. 31-43.

_____. 1970. Planktonic Foraminifera: Selective Solution and the Lysocline. Marine Geology, v. 8, p. 111-138.

_____. 1971a. Sedimentation of Planktonic Foraminifera. Marine Geology, v. 11, p. 325-358.

_____. 1971b. Pleistocene Deep-Sea Stratigraphy: Statistical Study of Correlation by Faunal Variation. J. Foram. Res., v. 1, p. 178-186.

_____ and G. R. Heath. 1968. Vertical Mixing in Sediments. J. Marine Res., v. 26, p. 134-143.

Berggren, W. A. 1971. Tertiary Boundaries and Correlations, In Funnell, B. M. and Riedel, W. R., Eds., Micropaleontology of Oceans. Cambridge, University Press, p. 693-809.

LITERATURE CITED (Continued)

Berggren, W. A, J. D. Phillips, A. Bertels, and D. Wall. 1967. Late Pliocene-Pleistocene Stratigraphy in Deep-Sea Cores from the South-Central North Atlantic. Nature, v. 216, p. 253-254.

Blackman and B. L. K. Somayajulu. 1966. Pacific Pleistocene Cores: Faunal Analyses and Geochronology. Science, v. 154, p. 886-889.

Blow, W. H. 1969. Late Middle Eocene to Recent Planktonic Biostratigraphy In Bronniman, P. and Renz, H. H., Eds., Proc. First Internat. Conf. Plankt. Microfossils. Geneva, p. 199.

Bradshaw, J. S. 1959. Ecology of Living Planktonic Foraminifera in the North and Equatorial Pacific. Cushman Found. Foram. Res. Contr., v. 10, p. 25-64.

Bramlette, M. N. 1958. Significance of Coccolithophorids in Calcium Carbonate Deposition. Geol. Soc. Amer. Bull., v. 69, p. 121-126.

_____. 1961. Pelagic Sediments, In Sears, M., Ed., Oceanography. Washington, D. C., Amer. Assoc. Adv. Sci. Publ., p. 345-366.

Broecker, W. S. 1966. Absolute Dating and the Astronomical Theory of Glaciation. Science, v. 151, p. 299-304.

_____. 1971. Causes of Temporal Changes in the Carbonate Compensation Level. Amer. Assoc. Petrol. Geol., Program with Abs., 56th Ann. Mtg., p. 332.

_____ and others. 1968. Milankovitch Hypothesis Supported by Precise Dating of Coral Reefs and Deep-Sea Sediments. Science, v. 159, p. 297-300.

_____ and R. Horowitz, T. Takahashi, and Y.-H. Li. 1968. Factors Influencing the $CaCO_3$ Compensation Levels in the Ocean. Geol. Soc. America, Programs with Abs. for 1968, Ann. Mtg., p. 38.

_____, K. K. Turekian, and B. C. Heezen. 1958. The Relation of Deep Sea Sedimentation Rates to Variations in Climate. Amer. J. Sci., v. 256, 503-517.

_____ and J. van Donk. 1970. Insolation Changes, Ice Volumes and the O^{18} Record in Deep-Sea Cores. Geophysics Space Phys. Rev., v. 8, p. 196.

LITERATURE CITED (Continued)

Bronnimann, P. and J. Resig. 1971. A Neogene Globigerinacean Biochronologic Time-Scale of the Southwestern Pacific, In Winterer, E. L. and others, Initial Reports of the Deep Sea Drilling Project, v. 7. Washington, U. S. Government Printing Office, p. 1235-1469.

Bucha, V., J. Horacek, A. Koci, and J. Kukla. 1969. Die Paleomagnetische Messungen in dem Loss, In Demek, J, and Kukla, J., Eds., Perglazialzone-Loss und Paleolithikum in der Tsechechoslowakei. Geogr. Anstalt der Tsch. Akademie der Wiss., Brno.

Buddemeier, R. W. and T. H. Hufen. In press. Hawaii Inst. of Geophysics Radiocarbon dates I: Radiocarbon.

Buyannanonth, V. 1971. Biostratigraphic Correlation in the Area of the Ontong Java Plateau. Unpublished Master's Thesis, Univ. Hawaii, Honolulu.

Crowell, J. C. and L. A. Frakes. 1970. Phanerozoic Glaciations and the Causes of Ice Ages. Amer. J. Sci., v. 268, p. 193-224.

Dalrymple, G. B., A. Cox, and R. R. Doell. 1965. Potassium-Argon Age and Paleomagnetism of the Bishop Tuff, California. Geol. Soc. Amer. Bull., v. 76, p. 665-673.

Duncan, J. R., G. A. Fowler, and L. D. Kulm. 1970. Planktonic Foraminiferan-Radiolarian Ratios and Holocene-Late Pleistocene Deep-Sea Stratigraphy off Oregon. Geol. Soc. Amer. Bull., v. 81, p. 561-566.

Emiliani, C. 1966a. Isotopic Paleotemperatures. Science, v. 154, p. 851-856.

_____. 1966b. Paleotemperature Analysis of the Caribbean Cores P6304-8 and P6304-9 and a Generalized Temperature Curve for the Last 425,000 Years. J. Geology, v. 74, p. 109-126.

_____. 1967. The Pleistocene Record of the Atlantic and Pacific Oceanic Sediments; Correlation with the Alaskan Stages by Absolute Dating, and the Age of the Last Reversal of the Geomagnetic Field, In Sears, M., Ed., Progress in Oceanography, v. 4, The Quaternary History of the Ocean Basins. New York, Pergamon Press, p. 219-224.

LITERATURE CITED (Continued)

Emiliani, C. and R. F. Flint. 1963. The Pleistocene Record In Hill, M. N., Ed., The Sea, v. 3. New York, Interscience, p. 888-927.

_____ and J. Geiss. 1959. On Glaciations and Their Causes. Geol. Rundschau, v. 46 (1957), p. 576-601.

Ericson, D. B. and G. Wollin. 1968. Pleistocene Climates and Chronology in Deep-Sea Sediments. Science, v. 162, p. 1227-1234.

_____. 1970. Pleistocene Climates in the Atlantic and Pacific Oceans: A Comparison Based on Deep-Sea Sediments. Science, v. 167, p. 1483-1485.

Evernden, J. F., D. E. Savage, G. A. Curtis, and G. T. James. 1964. Potassium-Argon Dates and Cenozoic Mammalian Chronology of North America. Amer. J. Sci., v. 262, p. 145-198.

Ewing, J., M. Ewing, T. Aitken, and W. J. Ludwig. 1968. North Pacific Sediment Layers Measured by Seismic Profiling, In Knopoff, L., Drake, C. L. and Hart, P. J., Eds., The Crust and Upper Mantle of the Pacific Area; Geophysical Mongr. no. 12. Washington, Amer. Geophys. Union, p. 147-173.

Fairbridge, R. W. 1964. African Ice-Age Aridity, In Nairn, A. E. M., Ed., Problems in Paleoclimatology. New York, John Wiley and Sons, p. 356-360.

_____. 1965. Eiszeitklima in Nordafrika. Geol. Rundschau, v. 54, p. 399-414.

Fleming, R. H. 1957. General Features of the Oceans. Geol. Soc. Amer. Mem. 67, 1, p. 87-107.

Flint, R. F. 1947. Glacial Geology and the Pleistocene Epoch. New York, John Wiley and Sons, 589 p.

Funnell, B. 1970. Oceanic Micropaleontology of the South Pacific, In Wooster, W. S., Ed., Scientific Exploration of the South Pacific. Washington, National Acad. Sci., p. 133-151.

LITERATURE CITED (Continued)

Hays, J. D. 1965. Radiolaria and Late Tertiary and Quaternary History of Antarctic Seas, In Biology of the Antarctic Seas II. Antarctic Research ser. 5, Amer. Geophys. Union, p. 125-184.

_____ and W. A. Berggren. 1970. Quaternary Boundaries and Correlations, In Micropaleontology of Oceans. Cambridge, University Press, p. 669-692.

_____ and N. D. Opdyke. 1967. Antarctic Radiolaria, Magnetic Reversals and Climatic Change. Science, v. 158, p. 1001-1011.

_____ and T. Saito, N. D. Opdyke, and L. H. Burckle. 1969. Pliocene-Pleistocene Sediments of the Equatorial Pacific; Their Paleomagnetic, Biostratigraphic and Climatic Record. Geol. Soc. Amer. Bull., v. 80, p. 1481-1514.

Heath, G. R. 1968. Mineralogy of Cenozoic Deep-Sea Sediments from the Equatorial Pacific Ocean. Ph.D. dissertation, California Univ., San Diego, California, 168 p.

_____. 1969. Carbonate Sedimentation in the Abyssal Equatorial Pacific During the Past 50 Million Years. Geol. Soc. Amer. Bull., v. 80, p. 689-694.

_____ and C. Culberson. 1970. Calcite: Degree of Saturation, Rate of Dissolution and the Compensation Depth in the Deep Oceans. Geol. Soc. Amer. Bull., v. 81, p. 3157-3160.

Heezen, B. C. 1971. Deep Sea Drilling in the Pacific. 12th Pacific Science Congress, Canberra, Australia, Record of Proc., v. 1 (abstracts of papers), p. 346.

Herman, Y. 1968. Arctic Ocean Quaternary Microfauna and Its Relation to Paleoclimatology. Palaeogeogr. Palaeoclimatol. Palaeoecol., v. 6, p. 251-276.

_____. 1970. Arctic Paleo-Oceanography in Late Cenozoic Time. Science, v. 169, p. 474-477.

Hisard, P., Y. Magnier, and B. Wauthy. 1969. Comparison of the Hydrographic Structure of Equatorial Waters North of New Guinea and at 170°E. J. Marine Res., v. 27, no. 2, p. 191-205.

LITERATURE CITED (Continued)

Hulsemann, J. 1966. On the Routine Analysis of Carbonates in Unconsolidated Sediments. J. Sed. Petrol., v. 36, p. 622-625.

Ishida, S., K. Maenaka, and T. Tokoyama. 1969. Paleomagnetic Chronology of Volcanic Ash of the Plio-Pleistocene Series in Kinki District, Japan. Geol. Soc. Japan J., v. 75, p. 183-197.

Karlstrom, T. N. Y. 1965. Isotope-Dated Interglacial Marine Transgressions and the Cook Inlet Glacial Chronology. 8th INQUA Congress, Denver, Colorado, Abstracts, p. 258.

Kennett, J. P. 1966. Foraminiferal Evidence of a Shallow Calcium Carbonate Solution Boundary, Ross Sea, Antarctica. Science, v. 153, p. 191-193.

_____. 1968. Globoratalia truncatulinoides as a Paleo-Oceanographic Index. Science, v. 159, p. 1461-1462.

_____. 1970. Pleistocene Paleoclimates and Foraminiferal Biostratigraphy in Subantarctic Deep-Sea Cores. Deep-Sea Res., v. 17, p. 141-155.

Kent, D., N. D. Opdyke, and M. Ewing. 1971. Climatic Change in the North Pacific Using Ice-Rafted Detritus as a Climatic Indicator. Geol. Soc. Amer. Bull., v. 82, p. 2741-2754.

Knauss, J. A. 1962. On Some Aspects of the Deep Circulation of the Pacific. J. Geophys. Res., v. 67, p. 3943-3954.

Koblentz-Mishke, O. J., V. V. Volkovinsky, and J. G. Kabanova. 1970. Plankton Primary Production of the World Ocean, In Wooster, W. S., Ed., Scientific Exploration of the South Pacific. Washington, National Acad. Sci., p. 183-193.

Koppen, W. and A. Wegener. 1924. Die Klimate der Geologischen Vorzeit. Berlin.

Kroenke, L. W. 1972. Geology of the Ontong Java Plateau. Hawaii Inst. Geophys. Rept., HIG-72-5, 119 p.

LITERATURE CITED (Continued)

Kroopnick, P. M. 1971. Oxygen and Carbon in the Oceans and Atmosphere: Stable Isotopes as Tracers for Consumption, Production, and Circulation Models. Unpublished Ph.D. dissertation, California Univ., San Diego, 230 p.

Kukla, J. 1969. The Cause of the Holocene Climate Change. Geologie en Mijnbouw, v. 48.3, p. 307-334.

Kullenberg, B. 1947. The Piston Core Sampler. Svenska Hydrog.-biol. Komm. Skr. (ser. 3, Hydrog.) v. 1, no. 2, p. 1-46.

Lamb, H. H. 1971. Climates and Circulation Regimes Developed Over the Northern Hemisphere During and Since the Last Ice Age. Palaeogeogr. Palaeoclim. Palaeoecol., v. 10, p. 125-162.

_____ and A. Woodroffe. 1970. On the Atmospheric Circulation During the Last Ice Age. Quaternary Res., v. 1, p. 29-58.

Landmesser, C. W. 1971. The Distribution of Foraminifera and Other Microfossils in Late Tertiary-Recent Deep-Sea Sediments from the South Pacific. Unpublished Honors thesis, Amherst College.

Lisitzin, A. P. 1970. Sedimentation and Geochemical Considerations, In Wooster, W. S., Ed., Scientific Exploration of the South Pacific. Washington, National Acad. Sci., p. 89-132.

Lyakhin, Y. U. 1968. Calcium Carbonate Saturation of Pacific Water. Oceanology (English Trans.), v. 8, no. 1, p. 44-53.

Margolis, S. V. and J. P. Kennett. 1970. Antarctic Glaciation During the Tertiary Recorded in Sub-Antarctic Deep-Sea Cores. Science, v. 170, p. 1085-1087.

Mesollella, K. J., R. K. Matthews, W. S. Broecker, and D. L. Thurber. 1969. The Astronomical Theory of Climatic Change: Barbados Data. J. Geol., v. 77, p. 250-274.

Milankovitch, M. 1938. Mathematische Klimalehre und Astronomische Theorie der Kimaschwankungen. Handb. Geophys., v. 9, p. 593-698.

LITERATURE CITED (Continued)

Mitchell, J. M., Jr. 1965. Theoretical Paleoclimatology, In Wright, H. E., Jr. and Frey, D. G., Eds., The Quaternary of the United States. Princeton, N. J., Princeton Univ. Press, p. 881-901.

_____. 1968. Causes of Climatic Change. Amer. Meteorol. Soc. Meteorol. Mons., v. 8, no. 30, 159 p.

Morin, R. W., F. Theyer, and E. Vincent. 1970. Pleistocene Climates in the Atlantic and Pacific Oceans: A Reevaluated Comparison Based on Deep-Sea Sediments. Science, v. 169, p. 365-366.

Murray, J. and A. F. Renard. 1891. Deep-Sea Deposits Based on the Specimens Collected During the Voyage of H.M.S. Challenger in the Years 1872-1876, Report of the voyage of the Challenger. London, Longmans, 525 p. (Reprints from Johnson, London, 1965).

Needham, H. D., J. R. Conolly, F. A. Ruddiman, and F. A. Bowles. 1969. Continental Sediment in Equatorial Atlantic Ooze--a Climate Record of the Pleistocene. Geol. Soc. Amer., Abs. with Programs for 1969, Pt. 7. (Ann. Mtg.).

Nesterhoff, W. D. and C. C. von der Borch. 1971. J.O.I.D.E.S. Drilling in the Central Pacific. 12th Pacific Science Congress, Canberra, Australia, Record of Proc., v. 1, (Abstracts of papers), p. 358.

Noltimier, H. C. 1967. Impregnation of Weak Sediment for Paleomagnetic Measurements. Earth and Planetary Sci. Letters, v. 2, p. 177-178.

Okada, H. and S. Honjo. 1970. Coccolithophoridae Distributed in Southwest Pacific. Pacific Geology, v. 2, p. 11-21.

Olausson, E. 1960. Description of Sediment Cores from Central and Western Pacific with the Adjacent Indonesian Region. Swedish Deep-Sea Exped., v. 6, Fasc. 5.

_____. 1961. Remarks on Some Cenozoic Core Sequences from the Central Pacific with a Discussion of the Role of Coccolithophorids and Foraminifera in Carbonate Deposition. Goteborgs, K. Vetensk,-Vit. Samh. Handl., Sjatte Foljden, ser. B., v. 8, no. 10, 35 p.

LITERATURE CITED (Continued)

Olausson, E. 1967. Climatological, Geoeconomical, and Paleo-Oceanographical Aspects of Carbonate Deposition, In Sears, M., Ed., Progress Oceanogr., v. 4. London, Pergamon, p. 245-265.

_____. 1971. Quaternary Correlations and the Geochemistry of Oozes, In Funnell, B. M. and Riedel, W. R., Eds., The Micropaleontology of oceans. Cambridge, University Press, p. 375-398.

Parker, F. L. and W. H. Berger. 1971. Faunal and Solution Patterns of Planktonic Foraminifera in Surface Sediments of the South Pacific. Deep-Sea Res., v. 18, p. 73-107.

Peterson, M. N. A. 1966. Calcite: Rates of Dissolution in a Vertical Profile in the Central Pacific. Science, v. 154, p. 1524-1544.

Quinn, W. H. 1971. Late Quaternary Meteorological and Oceanographic Developments in the Equatorial Pacific. Nature, v. 229, p. 330-331.

Reid, J. L., Jr. 1962. On Circulation, Phosphate-Phosphorous Content and Zooplankton Volumes in the Upper Part of the Pacific Ocean. Limnol. Oceanogr., v. 7, p. 287-306.

Revelle, R. R. 1944. Marine Bottom Samples Collected in the Pacific Ocean by the Carnegie on Its Seventh Cruise. Carnegie Inst. Washington Publ. 556, Pt. I, 182 p.

Riedel, W. R. 1967. Radiolarian Evidence Consistent with Spreading of the Pacific Floor. Science, v. 157, p. 540-542.

_____. 1971. The Occurrence of Pre-Quaternary Radiolaria in Deep Sea Sediments, In Funnell, B. M. and W. R. Riedel, Eds., The Micropaleontology of Oceans. Cambridge, University Press, p. 567-594.

_____ and B. M. Funnell. 1964. Tertiary Sediment Cores and Microfossils from the Pacific Ocean Floor. Quat. Geol. Soc. London, v. 120, p. 305-368.

Ross, D. A. and W. R. Riedel. 1967. Comparison of Upper Parts of Some Piston Cores with Simultaneously Collected Open-Barrel Cores. Deep-Sea Res., v. 14, p. 285-294.

LITERATURE CITED (Continued)

Ruddiman, W. F. and B. C. Heezen. 1967. Differential Solution of Planktonic Foraminifera. Deep-Sea Res., v. 14, p. 801-808.

Saito, T., L. H. Burckle, and J. D. Hays. 1971. Catalogue of Pre-Quaternary Sediment Cores and Dredgings in the Lamont-Doherty Core Library. Unpublished manuscript.

Scientific staff. 1970. Deep Sea Drilling Project: Leg 8. Geotimes, v. 15, p. 14-15.

_____. 1971. Deep Sea Drilling Project: Leg 17. Geotimes, v. 16, p. 12-14.

_____. 1972. Deep Sea Drilling Project: Leg 20. Geotimes, v. 17, no. 4, p. 10-14.

Selli, R. 1967. The Pliocene-Pleistocene Boundary in Italian Marine Sections and Its Relationship to Continental Stratigraphies, In Sears, M., Ed., Progress Oceanogr., v. 4. London, Pergamon, p. 67-86.

Sharp, R. P. 1968. Sherwin Till-Bishop Tuff Geological Relationships, Sierra Nevada, California. Geol. Soc. Amer. Bull., v. 79, p. 351-363.

Sillen, L. G. 1967. The Ocean as a Chemical System. Science, v. 156, p. 1189-1197.

Simpson, G. C. 1940. Possible Causes of Change in Climate and Their Limitations. Linnaen Soc. Lond. Proc., v. 152, p. 190-219.

Southworth, J. H. 1971. Laboratory and in situ Measurement of Sound Velocity and Mass Physical Properties of some Unconsolidated Marine Sediment Cores. Unpublished Master's thesis, University of Hawaii, Honolulu, 132 p.

Stommel, H. 1958. The Abyssal Circulation: Deep-Sea Res., v. 5, p. 80-82.

_____ and A. B. Arons. 1960. On the Abyssal Circulation of the World Ocean--II. An idealized model of the circulation pattern and amplitude in oceanic basins. Deep-Sea Res., v. 6, p. 217-233.

LITERATURE CITED (Continued)

Sverdrup, H. V., M. W. Johnson, and R. H. Fleming. 1947. The Oceans: Their Physics, Chemistry, and General Biology. Englewood Cliffs, New Jersey, Prentice-Hall, Inc., 1087 p.

Tsuchiya, M. 1961. An Oceanographic Description of the Equatorial Current System of the Western Pacific. Oceanographical Mag., v. 13, no. 1, p. 1-30.

Turekian, K. K. 1964. The Geochemistry of the Atlantic Ocean Basin. New York Acad. Sci. Trans., ser. 2, v. 26, no. 3, p. 312-330.

_____. 1965. Some Aspects of the Geochemistry of Marine Sediments, In Riley, J. and Skirrow, G., Eds., Chemical Oceanography, v. 2. New York, Academic Press, p. 81-126.

U.N.E.S.C.O. 1963. Changes of Climate. Rome symposium 1961, organized by U.N. Educ. Sci. and Cultural Organization and the World Meteorol. Organization, Proc., 488 p.

van Andel, J. H., G. R. Heath, T. C. Moore, and D. F. R. McGeary. 1967. Late Quaternary History, Climate, and Oceanography of the Timor Sea, Northwestern Australia. Amer. J. Sci., v. 265, p. 737-758.

van Montfrans, H. M. and J. Hospers. 1969. A Preliminary Report on the Stratigraphical Position of the Matuyama-Brunhes Geomagnetic Reversal in the Quaternary Sediments of the Netherlands. Geologie en Mijnbouw, v. 48, p. 565-572.

Warren, B. A. and A. D. Voorhis. 1970. Velocity Measurements in the Deep Western Boundary Current of the South Pacific. Nature, v. 228, p. 849-850.

Wilson, A. T. 1964. Origin of Ice Ages: An ice shelf theory for Pleistocene glaciation. Nature, v. 201, p. 147-149.

Winterer, E. 1971. Sedimentary History of the Pacific Plate. 12th Pacific Science Congress, Canberra, Australia, Record of Proc., v. 1 (abstracts of papers), p. 349.

LITERATURE CITED (Continued)

Winterer, E. and others. 1971. Initial Reports of the Deep Sea Drilling Project, v. 7. Washington, U. S. Government Printing Office, p. 557-567.

Wooster, W. S. and G. G. Volkmann. 1960. Indications of Deep Pacific Circulation from the Distribution of Properties at Five Kilometers. Geophys., v. 65, p. 1239-1249.

Wyrtki, K. 1962. The Subsurface Water Masses in the Western South Pacific Ocean. Aust. J. Marine Freshwater Res., v. 13, no. 1, p. 18-47.

Zeuner, F. E. 1959. The Pleistocene Period. London, Hutchinson Scientific and Technical, 447 p.